Universidad Complutense Madrid

GRAN TELESCOPIO CANARIAS GTC

MEGARA Detailed Design:

Instrument Overview

GTC Code: TBD

Code: TEC/MEG/106

Issue: 1.A

Date: 05/04/13

Pages: 92

Authors:	Armando Gil de Paz Ana Pérez Calpena Ernesto Sanchez Blanco Manuel Maldonado Medina Simon Tulloch Daniel Ferrusca Xabier Arrillaga Marisa García Vargas
Revised by:	Marisa García Vargas
Approved by:	Marisa García Vargas Armando Gil de Paz

Distribution List:

Name	Affiliation	Date
Instrument Team		5/04/2012
Science Team		5/04/2012
GRANTECAN		5/04/2012

Acronyms:

ACS	Advanced Camera for Surveys
ADC	Atmospheric-Dispersion Corrector
AIV	Assembly, Integration and Verification
AOI	Angle of Incidence
AR	Anti-Reflection (coatings)
BCD	Blue Compact Dwarf galaxy
BH	Black Hole
CCD	Charge Coupled Device
CDR	Critical Design Review
CPU	Central Processing Unit
DAS	Data Acquisition System
DEEP	Deep Evolutionary Exploratory Probe
DRP	Data Reduction Pipeline
DSS	Digitized Sky Survey
EB	Error Budget
EED	Enclosed Energy Diameter
EER	Enclosed Energy Radius
F-C	Folded-Cassegrain
FOV	Field Of View
FRD	Focal Ratio Degradation
GOODS	Great Observatories Origins Deep Survey
GCS	GTC Control System
GTC	Gran Telescopio Canarias
HR	High-Resolution (VPHs)
HST	Hubble Space Telescope
IFU	Integral Field Unit
IGM	Inter-Galactic Medium

IRAC	InfraRed Array Camera
LCB	Large Compact Bundle
LCU	Local Control Unit
LDSS	Low Dispersion Survey Spectrograph
LR	Low-Resolution (VPHs)
MAD	Módulo de Arranque Distribuido (Distributed start-up module)
MEGARA	Multi Espectrógrafo en GTC de Alta Resolución para Astronomía
MHD	Magneto-HydroDynamics
MCS	MEGARA Control System
MCT	Módulo de Control de Temperatura (Temperature Control Module)
MDRP	MEGARA Data Reduction Pipeline
MICINN	Ministerio de Ciencia e Innovación
MINECO	Ministerio de Economía y Competitividad
MIP	MEGARA Inspector Panels
MOS	Multi-Object Spectrograph
MOPSS	MEGARA Observing Preparation Software Suite
MR	Mid-Resolution (VPHs)
MSP	MEGARA Sequencer Processes
NDWFS	NOAO Deep Wide-Field Survey
OS	Order-Sorting (filter)
PDR	Preliminary Design Review
PN	Planetary Nebula
PPN	Pre-Planetary Nebula
RGB	Red Giant Branch
RMS	Root Mean Square
ROC	Radius of Curvature
SCB	Small Compact Bundle
SSC	Super Stellar Cluster

SXDS	Subaru/XMM-Newton Deep Survey
TBA	To Be Assigned
TBC	To Be Confirmed
TBD	To Be Done
TBU	To Be Updated
UCM	Universidad Complutense de Madrid
UDF	(Hubble) Ultra-Deep Field
VPH	Volume Phase Holographic (grating)
WBS	Work Breakdown Structure
WP	Work Package

Change Control

Issue	Date	Section	Page	Change description
1.A	05/04/13	All	All	First Issue

Applicable (A) and Reference (R) Documents

Nº	Document Name	Code
R.1	Preliminary Design Science Case	TEC/MEG/024
R.2	MEGARA Conceptual Design. Science Case	TEC/MEG/010
R.3	MEGARA Detailed Design: Folded Cassegrain subsystems and pseudo-slit Optics and Opto-mechanics	TEC/MEG/112
R.4	Delta-PDR: MEGARA MOS positioner performance tests	TEC/MEG/093
R.5	MEGARA Detailed Design: SCB Optical Bundle	TEC/MEG/128
R.6	MEGARA Detailed Design: Spectrograph Optics	TEC/MEG/100
R.7	Sliced Pupil Grating prototype: verification report	VIENTOS/TEC/009
R.7	Spectrograph Mechanics: Design upgrades from conceptual design	TEC/MEG/043
R.8	Structure and Mechanism Preliminary Design	TEC/MEG/053
R.9	MEGARA Preliminary Design. Cryostat	TEC/MEG/028
R.10	Cryostat cooling system trade-off analysis	TEC/MEG/027
R.11	MEGARA Preliminary Design. Detector and DAS	TEC/MEG/051
R.12	MEGARA Detailed Design. System Engineering Plan	TEC/MEG/110
R.13	MEGARA Product Tree	TEC/MEG/008
R.14	MEGARA Detailed Design. Flux homogeneity	TEC/MEG/117
R.15	MEGARA Detailed Design. Mass and consumption budgets	TEC/MEG/061
R.16	MEGARA Detailed. Design RAMS Analysis	TEC/MEG/048
R.17	MEGARA. Integration and Verification Plan	TEC/MEG/045
R.18	MEGARA. Instrument Integration on site	TEC/MEG/046
R.19	MEGARA. PSF simulations: Spectral Resolution and Cross-talk effects	TEC/MEG/076
R.20	MEGARA. Alternatives Trade-off study	TEC/MEG/044
R.21	MEGARA Control System: Software Overview	TEC/MEG/075
R.22	MEGARA Control System. Stakeholders Needs (I). Mechanisms, devices and Sequencer	TEC/MEG/034
R.23	MEGARA Control System. Use Cases (I). Mechanisms, devices and Sequencer	TEC/MEG/038
R.24	MEGARA Control System: Hardware Architecture and Overview	TEC/MEG/042
R.25	MEGARA Control System. Stakeholders Needs (III). MOPSS – MEGARA Preparation Software Suite	TEC/MEG/036
R.26	MEGARA Control System. Stakeholders Needs (II). MOPSS – Data Factory (Pipeline)	TEC/MEG/035
R.27	MEGARA Control System. Use Cases (III). MOPSS – MEGARA Observing Preparation Software Suite	TEC/MEG/040
R.28	MEGARA Control System. Use Cases (II). MOPSS – Pipeline	TEC/MEG/039
R.29	MEGARA Preliminary Design. Project Management Plan	TEC/MEG/029
R.30	MEGARA Preliminary Design. Fiber MOS	TEC/MEG/025
R.31	MEGARA Functional Requirements	RQ/IN-MG/001
R.32	MEGARA Detailed Design: HR Sliced Pupil Elements Optics	TEC/MEG/120

Applicable (A) and Reference (R) Documents (GTC codes)

Nº	Document Name	Code
R.1	Preliminary Design Science Case	EXT/UCM/1715-R
R.2	MEGARA Conceptual Design. Science Case	No code
R.3	MEGARA Detailed Design: Folded Cassegrain subsystems and pseudo-slit Optics and Opto-mechanics	TBD
R.4	Delta-PDR: MEGARA MOS positioner performance tests	TBD
R.5	MEGARA Detailed Design: SCB Optical Bundle	TBD
R.6	MEGARA Detailed Design: Spectrograph Optics	TBD
R.7	Sliced Pupil Grating prototype: verification report	No code
R.7	Spectrograph Mechanics: Design upgrades from conceptual design	EXT/UCM/1733-R
R.8	Structure and Mechanism Preliminary Design	EXT/UCM/1739-R
R.9	MEGARA Preliminary Design. Cryostat	EXT/UCM/1744-R
R.10	Cryostat cooling system trade-off analysis	EXT/UCM/1743-R
R.11	MEGARA Preliminary Design. Detector and DAS	EXT/UCM/1737-R
R.12	MEGARA Detailed Design. System Engineering Plan	TBD
R.13	MEGARA Product Tree	No code
R.14	MEGARA Detailed Design. Flux homogeneity	TBD
R.15	MEGARA Detailed Design. Mass and consumption budgets	TBD
R.16	MEGARA Detailed. Design RAMS Analysis	TBD
R.17	MEGARA. Integration and Verification Plan	EXT/UCM/1721-R
R.18	MEGARA. Instrument Integration on site	EXT/UCM/1722-R
R.19	MEGARA. PSF simulations: Spectral Resolution and Cross-talk effects	TEC/MEG/076
R.20	MEGARA. Alternatives Trade-off study	EXT/UCM/1734-R
R.21	MEGARA Control System: Software Overview	EXT/UCM/1787-R
R.22	MEGARA Control System. Stakeholders Needs (I). Mechanisms, devices and Sequencer	EXT/UCM/1745-R
R.23	MEGARA Control System. Use Cases (I). Mechanisms, devices and Sequencer	EXT/UCM/1749-R
R.24	MEGARA Control System: Hardware Architecture and Overview	EXT/UCM/1753-R
R.25	MEGARA Control System. Stakeholders Needs (III). MOPSS – MEGARA Preparation Software Suite	EXT/UCM/1747-R
R.26	MEGARA Control System. Stakeholders Needs (II). MOPSS – Data Factory (Pipeline)	EXT/UCM/1746-R
R.27	MEGARA Control System. Use Cases (III). MOPSS – MEGARA Observing Preparation Software Suite	EXT/UCM/1751-R
R.28	MEGARA Control System. Use Cases (II). MOPSS – Pipeline	EXT/UCM/1750-R
R.29	MEGARA Preliminary Design. Project Management Plan	EXT/UCM/1716-R
R.30	MEGARA Preliminary Design. Fiber MOS	EXT/UCM/1725-R
R.31	MEGARA Functional Requirements	EXT/UCM/1711-R
R.32	MEGARA Detailed Design: HR Sliced Pupil Elements Optics	TBD

INDEX

1. SUMMARY

This document provides the overview of the Detailed Design of the MEGARA instrument. This Instrument Overview includes a general description of the instrument, summarizes the science case pursued by the MEGARA Science Team and identifies and briefly describes the current design of its main components.

2. INTRODUCTION

MEGARA (*Multi-Espectrógrafo en GTC de Alta Resolución para Astronomía*) is an optical Integral-Field Unit (IFU) and Multi-Object Spectrograph (MOS) designed for the GTC 10.4m telescope in La Palma. MEGARA offers two IFU-type modes with two different bundles, one covering 12.5 arcsec x 11.3 arcsec with a spaxel size of 0.62 arcsec (Large Compact Bundle; LCB, which makes use of 100μm-core optical fibers) and another one covering 8.5 arcsec x 6.7 arcsec with a spaxel size of 0.42 arcsec (Small Compact Bundle; SCB, with 70μm-core fibers). The MEGARA MOS mode will allow observing up to 100 objects in a region of 3.5 arcmin x 3.5 arcmin around the two IFU bundles. Eight of these bundles will be devoted to the determination of the sky during the observation with the LCB IFU, so only 92 of these positioners will be available for MOS observations. Both the LCB IFU and MOS capabilities of MEGARA will provide intermediate-to-high spectral resolutions (the requirement is R_{FWHM} ~ 6,000, 12,000 and 18,700, respectively for the LR, MR and HR modes; current design values, error budget included, are better than these numbers). When the SCB is used the resolving powers to be provided by MEGARA should be R_{FWHM} ~ 7,000, 13,500 and 21,500, respectively. These spectral resolutions are derived from simulated extracted (1D) spectra and are expressed in terms of the FWHM[1] of unresolved spectral lines, while the image quality criterion is given in terms of the number of spectral pixels of the EED_{80} (see R.19 for more details on how these effective resolving powers are determined). In Table 1 we provide a summary of the characteristics of the three MEGARA modes (LCB, SCB and MOS) and the corresponding spectral resolutions required for each set of VPHs.

Regarding the sets of VPHs used by MEGARA, we have defined the wheel with 11 positions so that we would mount 6 LR gratings, 3 MR gratings (the most widely-used ones) and 2 HR gratings (LR+HR configuration). In an alternative configuration (MR+HR configuration) all 10 MR and 1 HR (e.g. the once centered at CaT) gratings could be mounted simultaneously yielding full optical coverage to MEGARA at R (EED80) = 10,000 – 17,000. Having the possibility of having two configurations is a requirement for the wheel design. The specific spectral resolution achieved for each configuration and each VPH set (LR, MR, HR) depends on whether the 100μm-fiber LCB IFU and MOS or the 70μm-fiber SCB IFU is used. We refer the reader to Table 1 for information on the spectral resolutions expected at the central wavelength

[1] *The MEGARA Resolving Power requirements for the LCB IFU and MOS are R_{EED80} = 5,500, 10,000 and 17,000, respectively, when expressed in terms of the number of spectral pixels enclosing 80% of the light, i.e. EED_{80} (see [R.19] for more details).*

(the variation of resolution across the detector is discussed in Section 5.2). The exchange between the two configurations, which means replacing the 6 LR VPHs (or a subset of these) by MR VPHs, should be performed as part of the observatory daytime activities. In the case of the LR+HR configuration one of the two largely overlapping VPHs situated at the red end of the optical spectrum are to be used (see Section 5.2). In the case of the MR+HR configuration we also assume that only one of the two VPHs centered on the Hα feature are to be used (i.e. either MR-R or HR-R).

		IFU Modes		**MOS Mode**
Parameter		**Large Compact Bundle**	**Small Compact Bundle**	**Dispersed Bundle**
Spaxel size		0.62 arcsec	0.42 arcsec	0.62 arcsec
Field of View		12.5 x 11.3 arcsec^2	8.5 x 6.7 arcsec^2	3.5 x 3.5 arcmin^2
Δλ (EED_{80})	*Requirement*	4 pix	3.48 pix	4 pix
Δλ (FWHM)	*Requirement*	3.6 pix	3.14 pix	3.6 pix
Resolving Power ($R_{FWHM}=\lambda/\Delta\lambda$) (*Requirement*)	LR VPHs	6,000	7,000	6,000
	MR VPHs	12,000	13,500	12,000
	HR VPHs	18,700	21,500	18,700

Table 1: *Main characteristics of the MEGARA LCB and SCB IFU modes and the MOS mode.*

From the Detailed Design phase thereon we are only considering the scope of having one single spectrograph on the Nasmyth platform of GTC (MEGARA-Basic) that can be fed by the fibers coming from either one of the IFUs or the MOS robotic positioners. MEGARA-Advanced, where two spectrographs would be available, one fed by one of the two IFU bundles and the other by the Dispersed bundle (MOS) is considered out of the scope of the project. The funds from GRANTECAN plus the in-kind contributions from the partners are expected to cover MEGARA-Basic only. Even although the MEGARA Science Case document (see R.1) describes the potential benefits of having two spectrographs simultaneously working within MEGARA, *our baseline for the CDR will be MEGARA-Basic, or simply MEGARA.*

The consortium responsible for the design and construction of the instrument includes the Universidad Complutense de Madrid (UCM, Spain) where the MEGARA Principal Investigator (Armando Gil de Paz) is located, the Instituto Nacional de Astrofísica, Óptica y Electrónica (INAOE, México), the Instituto de Astrofísica de Andalucía (IAA-CSIC, Spain), and the Universidad Politécnica de Madrid (UPM, Spain).

In the following sections we summarize the current MEGARA design and provide reference to other Detailed Design documents where each subject is described in more detail. Section 3 is devoted to identify the requirements that GRANTECAN and the MEGARA Science Team have imposed to the instrument. Section 4 summarizes the scientific objectives that have driven the design of MEGARA. Section 5 identifies the MEGARA main components and provides a brief description of each component. Section 6 summarizes the dependencies between the MEGARA main components and with GTC and other System Engineering issues that are being considered during the MEGARA Detailed Design.

3. REQUIREMENTS

In this section we summarize the requirements that come from GRANTECAN and from the MEGARA Science Team (validated through the instrument Consortium representatives).

Scientific/Performance requirements

- Wavelength range: 3700 Å – 9800 Å. Proposers may extend the wavelength coverage towards either end of the spectrum if the science case justifies it (*From GRANTECAN*).
- Spectral resolutions: Dispersion ranges centered on R~10,000 and ~20,000 (proposers may extend or add resolution ranges towards either lower and/or higher resolutions if the Science Case justifies the extension) (*From GRANTECAN*).

Note: As part of the Preliminary Design phase a discussion between GRANTECAN and the MEGARA team took place where both parts shared their views on the meaning and scope of these requirements as they were specified in the "*Announcement of Opportunity for new instrumentation for the Gran Telescopio Canarias*".

As a consequence of this discussion and of the feedback received from the PDR panel, the MEGARA team decided to incorporate a number of changes in the design of the MEGARA focal plane, pseudo-slit unit, and pupil elements compared to that presented in the Conceptual Design. These changes, discussed later in this document, are intended to ensure that the entire optical range is available (i.e. simultaneously mounted on the MEGARA spectrograph) at least at one resolution in the range R=10,000-20,000 both in IFU and MOS modes while maximizing the instrument throughput.

- Low-to-intermediate spectral resolution (R_{FWHM} ~ 6,000, i.e. $R_{\mathbf{EED80}}$~5,500) in the full range 370–950nm, with a resolution change on the detector not larger than 20% with respect to the central wavelength (*From the MEGARA Science Team*).
- High throughput, especially at $\lambda > 4000$ Å (*From the MEGARA Science Team*).

Managerial requirements

- Total cost envelope: 5 Million Euros (*From GRANTECAN*).

Note: As part of aforementioned discussions held during the Preliminary Design phase and at the beginning of this Detailed Design phase, GRANTECAN showed its willingness to raise extra funds to cover the costs associated to the changes implemented to the instrument Conceptual Design (which was limited to the *Total Cost envelope* of 4 Million Euros stated in the *Announcement of Opportunity*). These changes aim at improving the basic functionality and versatility of the instrument towards the community. In particular, these changes should provide MEGARA with full spectral coverage at resolutions R ≥ 10,000. According to the Management plan of the project an additional budget of 1 Million Euros was seen as needed to cover those extra costs. The complete scope described in this document (LCB, SCB and MOS, plus all LR, MR and HR VPHs described in the design) costs 5 Million Euros in money plus an in-kind manpower effort done by the MEGARA Partners of about 1.7 Million Euros. Nevertheless, several de-scoping options are considered in order to get this budget as close as possible to the amount originally stated in the *AoO*.

- Time envelope: 2015 (*From GRANTECAN*).

Design requirements

In addition to these requirements, the following design requirements have been applied during the MEGARA Detailed Design:

- MEGARA shall include IFU and MOS capabilities.
- Fiber units shall be installed in a GTC Folded-Cassegrain station. The MEGARA spectrograph shall be installed in one of the GTC Nasmyth platforms.
- The FOV of the LCB IFU should be ~ 12.5 x 11.3 arcsec^2 centered near the instrument optical axis.
- The FOV of the IFU SCB should be an area of roughly ~ 8.5 x 6.7 arcsec^2.
- The MOS FOV should occupy the region between the LCB and SCB IFUs and the maximum FOV of the instrument, i.e. 3.5 arcmin x 3.5 arcmin.
- Fiber core shall be 100 μm in diameter for the LCB IFU and MOS, which provides a spaxel (fiber) size of 0.62 arcsec on sky. The spaxel size chosen should provide a good compromise between point-source light gathering (and minimization of atmospheric refraction effects) for each individual MOS positioner and pupil-image oversizing and, therefore, pupil light losses.
- Fiber core shall be 70 μm in diameter for the SCB IFU, which provides a spaxel (fiber) size of 0.42 arcsec on sky.
- Spectrograph f input number shall be approximately f/3. Microlens arrays shall be used to provide the f/17 to f/3 coupling between GTC and the spectrograph.

- When the LCB IFU or the MOS are being used the spectral resolution element shall be kept in 4 pixels (in EED_{80}). In order to partly minimize cross-talk on the detector, a separation of approximately 2 pixels between adjacent fibers shall be kept.

- When the IFU SCB is being used the resolution element shall be 1.15 smaller than that of the LCB & MOS (i.e. 3.48 pixels in EED_{80}). In other words, the requirement of the LCB and MOS image quality is 15% more relaxed than for the SCB, i.e. the resolution element of the LCB and MOS should be at least 15% larger. The level of cross-talk on the detector in the SCB should be reduced by using 70µm-core fibers with a mechanical coating of 170 µm.

- The fibers of 8 positioners shall be evenly distributed along the pseudo-slit of the LCB IFU in order to provide a simultaneous measurement of the sky background when using this bundle.

- The pupil size shall be not larger than 170mm.

- The fcoll/fcam relation shall be kept to approximately 2 in order to guarantee the needed sampling at the detector focal plane and to make a doable camera.

- A single 4k x 4k detector shall be used with 15µm pixel size.

- The instrument should include the possibility of blocking the light from half of the MOS robotic positioners in order to be able to produce virtually null-cross-talk observations when needed. This will also require of a special arrangement of the fibers of MOS robotic positioners on the pseudo-slit.

- The instrument should include the possibility of blocking the light from half the spaxels in the LCB IFU in order to be able to produce virtually null-cross-talk observations when needed. This will also require of a special arrangement of the fibers from the LCB IFU on the pseudo-slit.

4. SCIENCE

In this section we briefly summarize the scientific objectives that have driven the Detailed Design of MEGARA, as put together and agreed by the MEGARA Science Team. The detailed MEGARA Science Case is exhaustively described in R.1.

The scientific interests of the MEGARA Science Team can be grouped in two categories, (1) the study of Galactic and extragalactic nebulae and (2) the study of point sources (or close to point sources) with intermediate-to-high surface densities. Among the former our interests include the study of Planetary Nebulae, nearby galaxies, and the high-redshift IGM and among the latter Galactic open stellar clusters, resolved stellar populations in Local Group galaxies, intermediate-redshift dwarf and starburst galaxies, and high-redshift cluster galaxies are the main subject of our research activities.

The MEGARA Science Team encompasses researchers with a broad range of scientific interests belonging to institutions of all members of the GTC community (Spain, Mexico and UF). This guarantees that, as a facility instrument, MEGARA will also successfully serve to the interests of the entire astronomical communities of the GTC Consortium members. In Figure 1 below we show a diagram that summarizes the main lines of research of the MEGARA Science Team and the corresponding team members with interest in each of these topics.

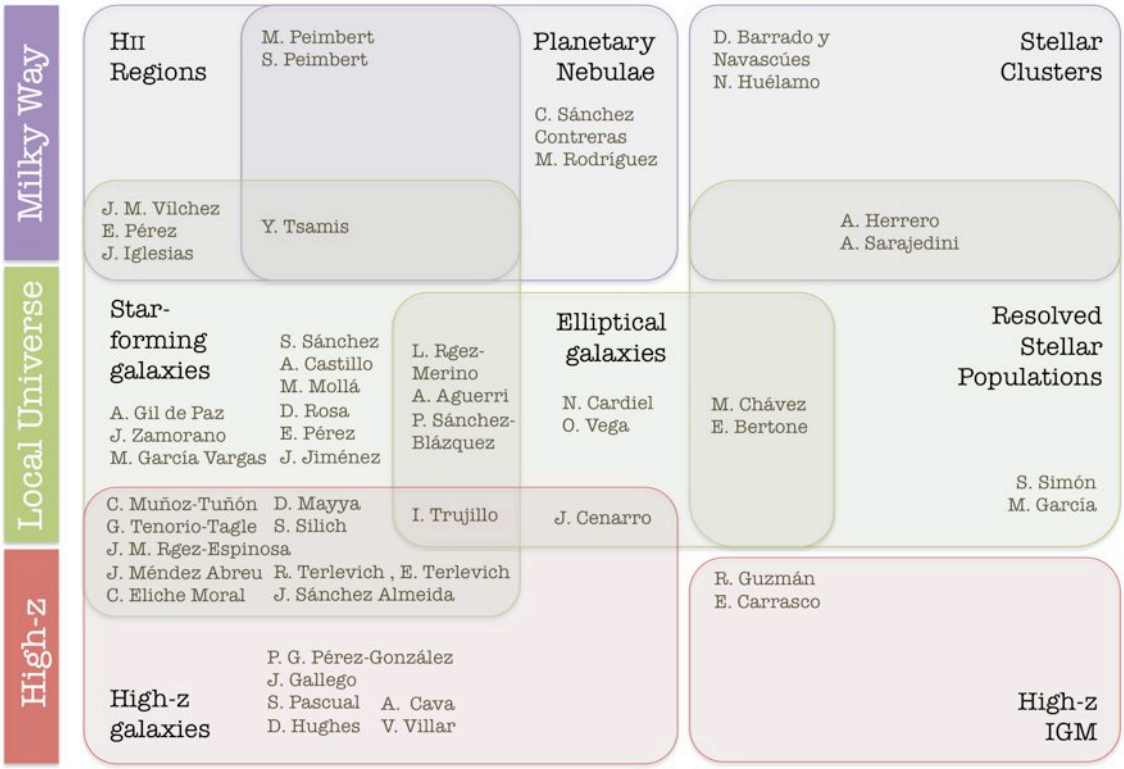

Figure 1: *Areas of main scientific interest of the MEGARA Science Team. We note that these include most of the areas of research in Astronomy (excluding the study of the Sun and the Solar System). The main interest of the UPM group (F.M. Sánchez Moreno, R. Cedazo, E. González, F. Serena) is e-Science with focus in Astronomy, which, as a general discipline, shares interests with all of the above.*

Except for the study of the Sun and the Solar System our team includes experts from most research areas in Astronomy, both Galactic and extragalactic.

What is common to all our scientific interests is the need for an intermediate-to-high spectral resolution, in the range R=6,000-20,000. In some of the cases above this need is a mere consequence of velocity resolution (kinematics) but in many cases is given by the need of reducing line blending, either directly when lines from different elements ought to be measured in stars or *via* a reduction in the degeneracy of the properties of composite stellar populations.

4.1 Galactic and extragalactic nebulae: The need for the MEGARA IFU

In the case of the study of nebulae, it has now become clear that the use of a bi-dimensional spectrometer is critical to obtain precise answers to the problems that these fields (either in its Galactic or extragalactic version) are facing. While the use of a Fabry-Pérot might be a good choice in this regard should someone be only interested in single emission-line kinematics *and* if a precise flux calibration across the line profile is not required, the use of a Integral Field Unit (IFU) has shown to be a more reliable approach, especially if one is interested on more than one single spectral feature or on absorption features (e.g. the SAURON or CALIFA projects).

It is because of this that early in the design process of MEGARA it became obvious the need for an IFU that would yield the required spectral resolution (R=6,000-20,000). Although some of the science cases originally planned by the MEGARA Science Team (see R.2) require of an IFU with a FOV significantly larger (~1x1 arcmin^2) than that included in the current MEGARA design (12.5x11.3 arcsec^2 in the case of the LCB), we still should be able to achieve our objectives by (1) targeting objects of smaller angular size (more distant and/or physically smaller) and (2) by fast-mapping extended targets. We note the reader that during the design process of MEGARA we have always prioritized throughput, which, along with the large light-gathering power of GTC and an optimized Control system should allow mapping relatively extended targets with high efficiency.

The main interests of the MEGARA Science Team regarding the study of nebular objects are:

4.1.1 Nearby galaxies (beyond the Local Group)

We aim to study the evolution of galaxy disks through the analysis of their velocity ellipsoids and the 2D spatial distribution of spectral indices and chemical abundances. This goal constitutes the core of MEGADES, the *MEGARA Galaxy Disks Evolution Survey*. This analysis is fundamental to disentangle the roles of the secular processes involved in the shaping the present-day properties of disks, i.e. in-situ star formation, stellar migration and satellite accretion and (minor-) merging among others. In addition to the study of the unresolved stellar populations in galaxy disks outlined here, MEGADES will also include the detailed single-star spectroscopic analysis of the Local Group galaxies M33 and IC 1613.

Furthermore, MEGADES will also be used to study the interplay between the massive-star formation and the interstellar medium and its consequences on the further evolution of actively star-forming galaxies (positive vs. negative star-formation feedback) through the analysis of galactic winds both in line emission (Hα primarily) and in absorption lines (NaI D, KI) arising from cool ISM associated to the galactic-wind material. We will make use of the observations proposed within MEGADES to address some of the most fundamental problems on the analysis of the chemical properties of galaxies, including the long-standing problem of the abundance discrepancies and the potential identification and analysis of chemo-dynamical phenomena (i.e. kinematical components of the ISM with distinct chemical enrichment).

In order to be as much efficient as possible and given the current budget constrains (which limit the number of MEGARA spectrographs to unity and, therefore, the FOV of the MEGARA IFU to 12.5x11.3 arcsec^2) we will target galaxies which can be scanned along the major and minor axes in just a few IFU pointings. These galaxies, with an apparent size comparable to the MEGARA MOS FOV, will be also observed (simultaneously in the case of the MEGARA-Advanced configuration) with the set of robotic positioners placed on individual HII regions with the objective of measuring metal-abundance radial and 2D distributions. Galaxies included in the S4G survey (Sheth et al. 2010, PASP, 122, 1397), a magnitude-, diameter- and volume-limited sample of galaxies within 40 Mpc, will be used as targets for this program.

With regard to the spatial resolution, a sampling close to that of the typical seeing in La Palma, as that provided by the LCB, is good enough for most scientific applications described above. However, in the case of the study galactic winds in relatively distant galaxies and also in both pre-Planetary Nebulae (pPN) and young Planetary Nebulae (PN) the improved spatial and spectral resolutions of the SCB is needed..

In terms of the resolving power, the study of the stellar velocity ellipsoid and ionized-gas kinematics (including chemo-dynamical phenomena) requires of resolutions in the range R=6,000-20,000 (depending on the properties -e.g. mass and inclination- of the target under analysis). The determination of the 2D spatial distribution of spectral indices and chemical abundances both require of a wide wavelength coverage (in the lower number of spectral setups possible) while a spectral resolution of R~5,000 would suffice. Such a spectral resolution would also take advantage of state-of-the-art spectral libraries (e.g. the X-shooter Stellar Library or XSL; Cheng et al. 2011, JPhCS, 328, 012023) when analyzing spectral indices throughout the disks of our targets.

4.1.2 Planetary Nebulae: from the Asymptotic Giant Brach to the Planetary Nebulae stage

The process (or processes) that lead to Planetary Nebula (PN) formation out of the winds of Asymptotic Giant Branch (AGB) stars is complex and poorly known. In this proposal, we focus on two of the biggest challenges in the study of these latest stages of the stellar evolution of intermediate mass (Sun-like) stars: understanding 1) nebular shaping and acceleration beyond the AGB and 2) chemical enrichment. Our twofold approach highlights the power of MEGARA to carry out different but complementary studies of nebular objects, on the one hand, characterization of the spatio-kinematic structure and, on the other hand, ionized-gas diagnostics with spatial resolution.

4.1.2.1 Nebular shaping and acceleration beyond the AGB: early evolution of PNe

One of the aims of our studies of PNs and pre-PNs (i.e. objects that have recently left the AGB phase) with MEGARA is to make progress in our understanding of the nebular shaping process, which is believed to be driven by the interaction between collimated, fast (i.e. jet-like) winds

ejected during the late-AGB or early post-AGB stages and the slow, largely spherical envelopes formed during the previous AGB phase as a result of a heavy mass-loss process. We will use MEGARA for a detailed characterization of the morphology and velocity structure of a sample of objects displaying diverse morphologies and spanning a range of evolutionary stages (from early post-AGBs, PPNs, and PNs). Special emphasis will be made on the study of sources with post-AGB ejections currently active and sculpting the AGB circumstellar envelopes (CSEs).

The FOV required for the MEGARA IFU is simply given by the size of the vast majority of young PN and PPNs known to date (5-20 arcsec, see e.g. Sahai et al. 2007, AJ, 134, 2200; Sahai et al. 2011, ApJ, 740, 39). We anticipate that no more than three pointings with the SCB mode (FOV=8.5"x6.7") are required and, in many cases, the targets can be accommodated in one pointing. Since both spatial and spectral resolution are required for a comprehensive study of the spatial-kinematic structure of the different nebular components typically present in these objects (such as shocked elongated lobes, axial knots, arc-like features, etc), the SCB will be the preferred observational configuration used. Resolving the kinematical structure imprinted by the interaction of the fast post-AGB wind on the AGB CSE requires high spectral resolutions; we will use the HR-R VPH for a resolution of R~20,000 around the Hα line, which is an excellent tracer of the atomic and ionized gas component in these objects. Also, full spectral coverage at lower resolutions (R~6,000-10,000, using the LR and MR VPHs) is desired for a proper characterization of the physical conditions in the nebulae derived from emission line diagnostic ratios.

The main features in the emission line profiles to be analyzed are the broad wings, observed to reach FWZIs~1,000-2,000 km/s in a number of PPNs/PNs, and the blue-shifted, absorption features observed in the HI Balmer profiles of some PPNs – the latter P-Cygni like profiles are probably produced by intervening cooler gas associated to pristine post-AGB winds. The simultaneous access to, e.g., Hα, [SII]λλ6717,6731ÅÅ and [NII]λλ6548,6584ÅÅ lines (with the LR, MR and even HR VPHs) is a clear benefit of the use of an IFU compared with what would be obtained from Fabry-Pérot observations alone.

4.1.2.2 Chemical abundances in PNs and HII regions

We aim at characterizing the emission-line spectra of evolved (fully photo-ionized) PN. Such a study would allow us not only to determine the chemical abundances of their envelopes but also to tackle fundamental open questions about the physical properties of the ionized gas. Major open questions include:

What is the origin of the discrepancy between the oxygen abundances implied by recombination lines and collisionally-excited lines?

As a related question, which lines provide the most reliable abundances and what method should be used to calculate the metallicity of the gas?

How do the best estimates of chemical abundances in PN compare with those derived for the present-day interstellar medium located in HII regions?; and how do they compare with those that have been derived for intermediate-mass stars?

The disagreement between the abundances implied by recombination lines and collisionally-excited transitions of heavy elements in HII regions and PNs is one of the main open questions in the study of ionized nebulae. This discrepancy not only introduces an uncertainty of at least a factor of 2 in our abundance determinations but also might provide clues on processes that are crucial to our understanding of galactic chemical evolution. A related issue on which we need more information concerns the temperature structure of real objects and whether it can be reproduced with photoionization models, since the assumed temperature structure affects significantly the abundances derived with collisionally-excited lines.

MEGARA on GTC can provide for nearby nebulae spectral maps with enough spectral resolution and wavelength coverage to address these topics by studying variations, both spatially and from object to object, in the abundance discrepancy and in the temperatures implied by different diagnostics. For some PNs, MEGARA will also provide integrated fluxes, which will allow a direct comparison with spectral diagnostics and emission lines from other wavelength regimes, such as the UV, radio, and the IR.

We intend to obtain deep spectra with spectral resolutions around or above R=5,000 of specific regions of a sample of nearby PNs. These observations will allow us to carry out a detailed analysis of the chemical abundances of most elements found in PNs using both temperature-sensitive collisionally-excited transitions and recombination lines. This study will be further extended by including the observation of specific individual Galactic HII regions.

4.1.3 Arcs and highly-magnified distant galaxies in clusters

In addition to the study of the high-redshift IGM another application of the MEGARA IFU for the study of the high-redshift Universe envisioned by our Science Team is the 2D spectroscopy of far-infrared (Herschel) selected sources in regions of high-magnification in intermediate-redshift clusters. These sources are being identified thanks to the *Herschel Lensing Survey* (PI: E. Egami), a *Herschel Open Time Key Programme* devoted to the observation with the PACS and SPIRE instruments that reaches 5 mJy at 100 μm and 10 mJy at 250 μm in a total of 40 clusters. The faint continuum emission and relatively large projected size in the sky of some of these sources (arclets in most cases) make necessary the use of an IFU in order to identify them and for spectroscopically measuring their redshifts. Indeed, in many cases the position of the optical counterpart of the IR-bright galaxy is not known (it is extremely faint in the continuum), so only using an IFU with an exceptional covering factor such as MEGARA we can target the area with high magnification and try to recover spectroscopic data from the arc. Moreover, the magnification produced by the cluster can be used to explore the faintest regime in all the science topics introduced in this section. For example, MEGARA observations of nearby clusters with known Herschel arcs could also target (with the positioners, taking advantage of the high multiplexing of MEGARA) candidates for faint green peas at intermediate- or even

high-z, since they may count with a significant magnification from the cluster (or weak-, medium-lensing from individual galaxies in the field).

4.1.4 UV resonant-line emission from the high-redshift IGM

According to state-of-the-art models of the evolution of the meta-galactic UV radiation field at high-redshift, an instrument such as MEGARA in combination with GTC could allow, for the first time, detecting emission from red-shifted UV resonant lines such as OVI 1033Å, CIV 1550Å, Lyα that arise in the high-z IGM. This is particularly feasible if we use statistical filament stacking techniques but even direct imaging detections are possible (depending on the model parameters adopted for the evolution of the radiation field at high redshift).

This kind of pioneering work requires of a FOV comparable to the extension of the features to be analyzed (filaments, Lyα-blobs). Thus, depending on the model parameters and the redshift range explored, maps of a few to tens of pointings should be needed to disentangle the 3D structure of the high-z IGM line emission. A good blue sensitivity at λ~5000 Å and spectral resolution (not worse than R~5,000) are a must in this case. This is due to the necessity of resolving the 3D structure of the IGM in velocity, to differentiate the effects of bulk motions from those of radiative transfer in these resonance lines and to improve sky subtraction (see e.g. Martin et al. 2010, SPIE, 7735, 21).

The detection of the high-redshift IGM emission would have a tremendous impact on the community and on the general public as it would allow tracing the cosmic web directly for the first time. GTC would break new ground here.

We are currently working on involving members of the GTC community with interest on this science topic in the MEGARA Science Team as this a topic where MEGARA and GTC combined could best show their power.

4.2 Point-source science

The other major area of scientific interest within our team refers to the study of point sources (or marginally-resolved sources from the ground). This includes the study of Galactic open clusters, individual stars in Local Group galaxies and very distant galaxies. Except in the case of the study of the RGB population in Local Group galaxies, where the use of a wide-field IFU could still provide a significant advantage at some galactocentric distances (<7 Mpc in the case of M33), in the remaining cases the surface densities range between a fraction to a few sources per arcmin^2. For such science applications the possibility of having a relatively high multiplexed (~100x) MOS mode within the unvignetted FOV of the Folded Cass focus of GTC is ideal. In ***Figure 2*** we show the maximum field density reachable with the Multi-Object Spectrograph (MOS) mode proposed for MEGARA compared with other instruments. Clearly, the MEGARA MOS is the best instrument for performing spectroscopic observations of moderate-to-highly crowded fields, such as Galactic stellar clusters, resolved stars in Local Group galaxies, ultra-deep cosmological fields (e.g. UDF) or distant galaxy clusters.

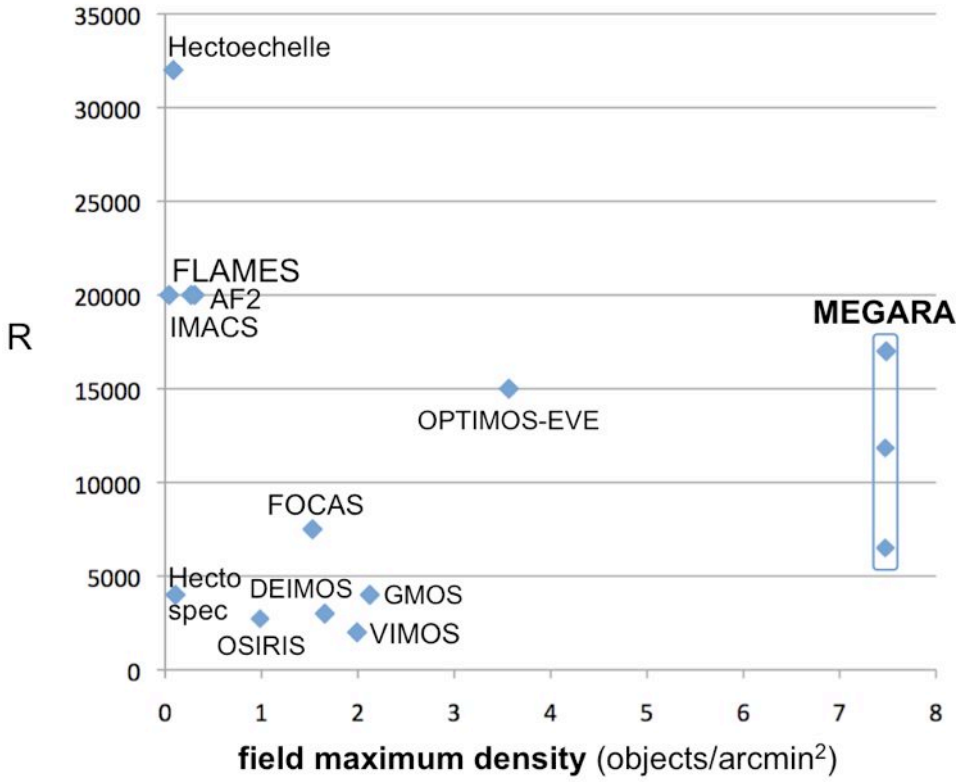

Figure 2: *Spectral resolution versus maximum density of objects for different multi-object spectrographs (MOS) already built or planned. For the sake of comparison we also show the different resolutions (in FWHM) and maximum density reachable with MEGARA.*[2]

Given the fact that GTC lacks an ADC at least a total field covered by each MOS positioner should be at least 1.5 arcsec. This is achieved in our case by using 7 hexagonally packed lenslets covering 0.62 arcsec each (~1.61 arcsec in diameter total). In order to highlight the need for having such configuration in the case of the MEGARA MOS mode we note that at R~12,000 in the blue the differential refraction across the entire wavelength range simultaneously covered at this resolution (~500 Å) at an airmass of 1.8 is ~0.7 arcsec, i.e. comparable to the size of each individual spaxel in the MEGARA MOS (0.62 arcsec), with effects being noticeable at an airmass of 1.30 already. Moreover, as the targets in the some of the studies described above are marginally resolved from the ground under good seeing conditions, the use of small mini-bundles of 7 spaxels each (instead of single fibers) provides a way to recover some (rather limited though) spatial information. The lenslets used for the robotic positioners that patrol the outer 3.5x3.5 arcmin^2 are identical to those used in the LCB IFU. Thus, we have devoted a set of eight positioners for simultaneous sky-background determination when observing with the LCB IFU. The fibers associated to these positioners will be evenly distributed along the LCB pseudo-slit for a further improvement in the sky-

[2] We refer the reader to the Exposure Time Calculator User Guide for a similar comparison in terms of throughput.

background determination. Note that although these eight fiber bundles do not need to move to a specific position within their patrol area we are using robotic positioners as this actually saves both design and manufacturing costs should a new frame and mechanical interface with the sky bundles be implemented in MEGARA.

Below we include a summary of the main interests of the MEGARA Science Team related to the study of (or close to) point sources:

4.2.1 Galactic stellar clusters

The characteristics of the MEGARA MOS are optimal for the analysis of the properties of stars in Galactic open clusters, especially at Galactocentric distances beyond which the apparent size of the clusters matches the MEGARA MOS field of view (at and beyond ~2 kpc). Among the MEGARA Science Team there is interest in two different aspects regarding the study of the stellar content of Galactic open clusters that refer to the characterization of (i) solar analogs and (ii) low-mass stars.

4.2.1.1 Solar analogous in Galactic open clusters

The objective of this study is to re-calibrate the activity-sensitive Ca H+K index with the stellar age for an extended sample of solar analogs in stellar open clusters. Once properly calibrated this relation could be applied to field stars and, in particular, to specific solar-type stars showing IR excesses or possibly hosting planetary systems. We will also make use of the measurements of spectral indices to be obtained from the MEGARA observations proposed for the determination of the effective temperature and gravity. This study is done in the context of the characterization of solar analogs candidates for the future search of Sun-Earth-like planetary systems.

4.2.1.2 Formation of low-mass stars in stellar clusters

This project intends to study of properties of very low mass stars (and brown dwarfs) in young stellar associations from a holistic perspective. First, within the Gould Belt (the Local Bubble, a structure few hundred parsec across), then, moving farther away, to the galactic anticenter and the Perseus Arm (beyond 2 kpc). The goal is to put star formation in a galactic perspective and to include the effects of both metallicity and environment.

Specifically, we will study the low-mass star formation in the Gould Belt by carrying out a complete census of three clusters in this region (NGC1333+IC348, NGC7160, IC4665). This study will also include the derivation of stellar properties such as accretion along with the characterization of the lowest (planetary-)mass objects. It will then be extended to a sample of a few clusters in the Perseus Arm (including the complex formed by W3-W4 and W5) with the aim of exploring these properties in a completely different environment within the Galaxy.

We will first characterize a sample of photometrically-selected stars in all these clusters using medium-resolution spectroscopy (R~6,000) covering Hα, Li λ6708Å, NaI λ8200Å, CaT (LR-R and LR-I) and then, once their membership is confirmed and their spectral types derived, we will obtain high-resolution spectroscopy (R~19,000) in the Hα (including also the Li λ6708Å line) and CaT regions to identify activity and accreting related phenomena along with accurate radial velocities.

This project is carried out in the context of the Gaia mission and its supporting (and follow-up) observing programs, including the ESO-Gaia (FLAMES) ESO Large Programme. In this regard, MEGARA will provide the needed multiplexing for observing some of the stellar clusters to be observed with Gaia but, where the high stellar density, prevents its observation with FLAMES at VLT and it allows to reach significantly fainter magnitudes thanks to both the larger collecting area of GTC compared to VLT and to the significantly better efficiency of MEGARA compared with FLAMES (see Figure 3) and comparable to those of MUSE and X-Shooter although these latter not reaching the working spectral resolutions of MEGARA.

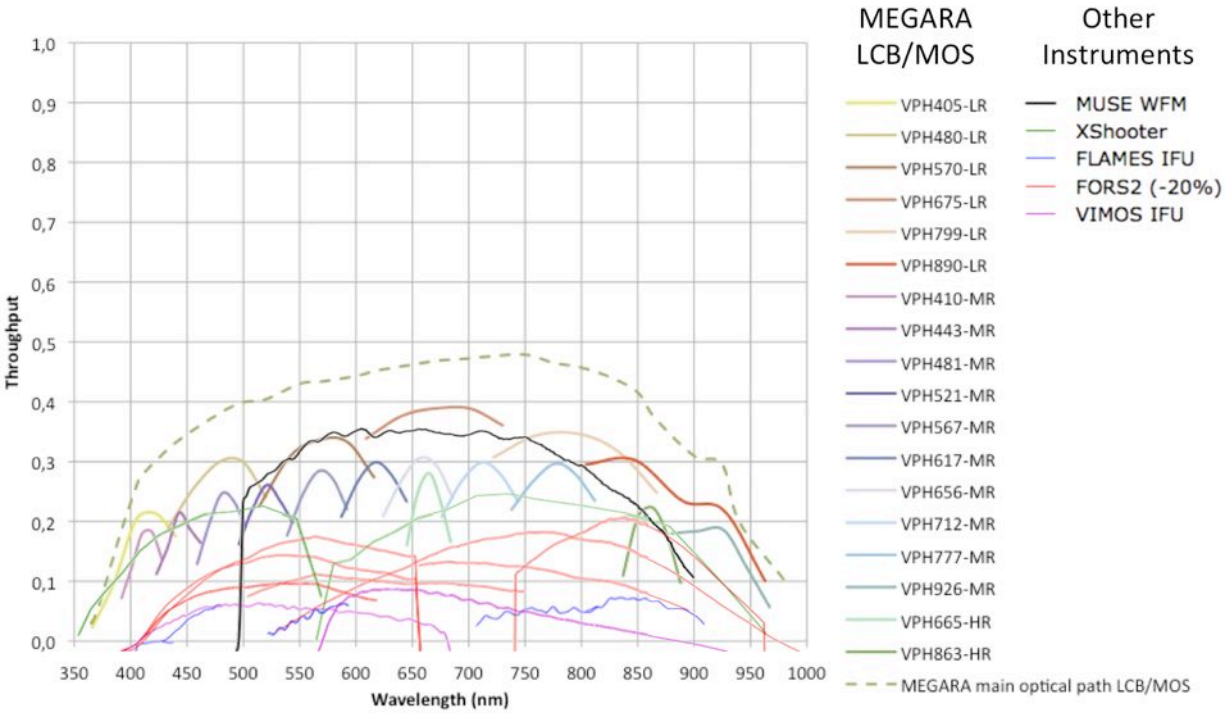

Figure 3: *Efficiency of MEGARA compared with that of the VLT instruments in their different spectral configurations. VLT instruments efficiency curves courtesy of L. Wisotzki.*

4.2.2 Local Group galaxies

Two are the objectives of the spectroscopic characterization of the resolved stellar population in star-forming Local Group galaxies.

First, we aim at characterizing the massive blue star population in the late-type Local Group star-forming galaxies M33 (the Triangulum galaxy) and IC1613 from intermediate-to-high-

resolution spectroscopy in the blue range of the optical spectrum (R~11,000) and in the Hα region (R~19,000). These observations will allow us to study of the role played by stellar rotation in the surface abundance enrichment of massive stars and characterize their mass loss rates at a wider range of metal abundances than previously accomplished, from $1.3Z_{\odot}$ (in the central parts of M33) to $0.04Z_{\odot}$ (IC1613).

Secondly, we will study the RGB population in the disk of M33 using intermediate spectral resolution (R~6,000) in the CaT region. From there measurements we will derive both the single-star velocity ellipsoid and the disk metal-abundance gradient. Observations in the CaT at high-resolution (R~19,000) will be also performed in order to self-calibrate the low-resolution metal-abundance estimates and in cases where the velocity dispersion (σ) is expected to be low. This study will be done as a function of galactocentric distance, which, again, should allow us to disentangle among others the effects in-situ star formation, stellar migration, and satellite accretion on the evolution of disks, as these various mechanisms leave a distinct imprint in the velocity pattern of individual stars at different radii.

The fact that both objectives can be accomplished using common targets ensures an optimal use of the MEGARA MOS mode. Since both M33 and IC1613 are far more extended than the flat, non-vignetted Folded-Cass focal plane of GTC a series of a few MOS pointings will be obtained. In the case of the M33 these will be arranged along both the major and minor axes (see Figure 3).

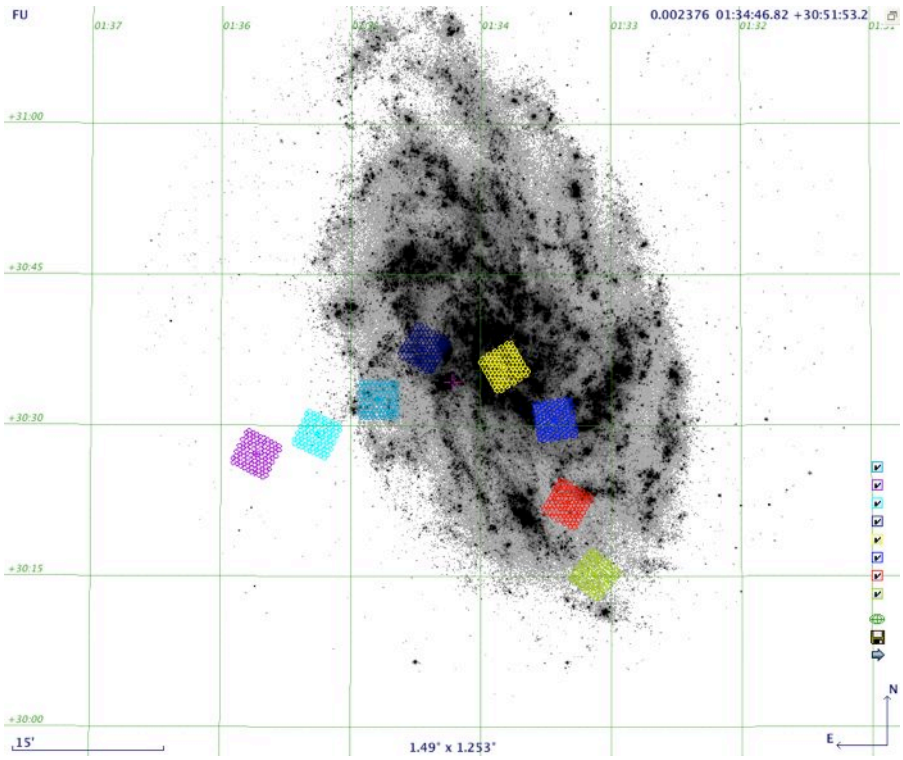

Figure 3: *Layout of the proposed MEGARA MOS fields on the disk of M33. All except one pointing (in cyan) coincide in position, field-of-view (FOV) and orientation with observations obtained with ACS/HST in at least two bands, F606W and F814W. These will be used to identify potential spectroscopic blends.*

4.2.3 Distant galaxies

There are multiple interests within the MEGARA Science Team regarding the study of high-redshift galaxies: Intermediate-redshift Blue Compact Dwarf (BCD), clump-cluster, peas and starburst galaxies and high-redshift proto-clusters. In order to address all these topics with maximum efficiency a MOS with the capability of observing a relatively large number of objects within a small patch of the sky (density ≥ 1 arcmin^{-2}) is required. The high number densities of sources accessible with the MEGARA MOS will allow pursuing many of these goals as part of a common observing program.

4.2.3.1 Intermediate-redshift BCDs:

Very little is known on the properties of distant dwarf galaxies. This situation is particularly critical in the range $0.4 < z < 1.3$ since this is the epoch (1) when cosmic SFR density started to decline, (2) the overall galaxy population moved from highly active systems to the current Hubble sequence; and (3) when expansion accelerates. Our main goal here is to take advantage of the good multiplexing (~100x) and optimization for high-number density fields of the MEGARA MOS to carry out an extensive spectroscopic survey of these numerous, but faint dwarf systems between $0.4 < z < 1.3$. In addition to the population of star-forming dwarf galaxies in general we will specifically target BCD candidates as these are expected to show high equivalent widths in emission and central surface brightnesses (Gil de Paz et al. 2003, ApJS, 147, 29; see Figure 4).

The goals are to (1) confirm their nature as intermediate-redshift BCDs, (2) determine their dynamical masses (from their emission-line widths), (3) identify those galaxies with galactic winds and (4) analyze their physical properties when possible.

This study requires of intermediate spectral resolutions (R~6,000) in order to properly determine dynamical masses for such low-mass systems. Significantly higher resolutions are not advisable as they will imply a large number of spectral setups to cover the emission from the [OII]λλ3726,3729ÅÅ doublet in the entire redshift range of exploration ($0.4 < z < 1.3$).

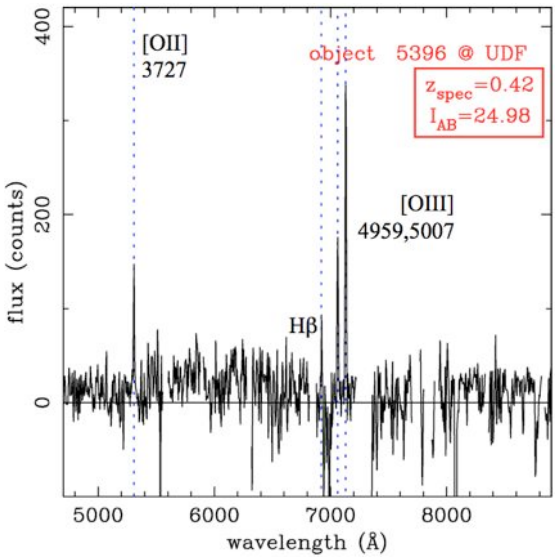

Figure 4: *Optical spectrum of one of the UDF intermediate-redshift BCD candidates obtained with LDSS-3 at the Magellan 6.5m telescope (Rodríguez et al. 2013, in preparation). This very faint (I~25mag) object has a rest-frame B-band luminosity of M_B=-16.1 and a redshift of z=0.42.*

4.2.3.2 Clump-cluster, peas and starburst galaxies:

Large and massive clumps of star formation have been detected in more than half of the resolved z>1 galaxies in the Hubble UDF (see Elmegreen et al. 2005, ApJ, 631, 85). These star-forming entities are found in galaxies at all distances in the range 0.07<z<5. They have sizes of about 2 kpc and masses often larger than 10^8 M⊙. They are so luminous that dominate the appearance of their host galaxies at optical wavelengths. Massive clumps like these are found in galaxies with a variety of different morphologies, from somewhat normal compact galaxies (ellipticals?), spirals, and irregulars, to types not observed locally, including chain galaxies and their face-on counterparts, clump-cluster galaxies (see Elmegreen et al. 2005; see Figure 5).

These observations have an interpretation within the framework of the evolution of galaxies, where clump-cluster galaxies are considered as examples of star-forming disks at their earliest stage, and maybe also initial seeds for spiral galaxies and, through mergers, spheroids as well (Bournaud, Elmegreen, & Elmegreen 2007, ApJ, 670, 237). In order to model and understand the various feedback mechanisms at these early stages of galaxy disks evolution (see e.g. Tenorio-Tagle et al. 2010, ApJ, 708, 1621; Silich et al. 2010, ApJ, 711, 25 and references therein), it is important to determine the kinematics and physical state of the gas in the clumps.

The basic questions to answer here are: do the clumps show ionized-gas features? Do they show signs of negative feedback (e.g., shells, chimneys, winds)? Are they coeval star formation events or the result of continuous star formation? Are there cases of positive star-formation feedback? The main goal of this program is to determine the physical properties of star-forming clumps for galaxies at different redshifts selected from a Cosmological field such as COSMOS.

We plan to obtain spectroscopy for a large subsample of a few hundreds (~300-400) candidate clump cluster galaxies using MEGARA at GTC. We will use the LR VPHs with R=6,000 in order to detect one or several of the most relevant emission lines expected to be present in these galaxies so to perform a basic spectral analysis.

In addition, for a small subsample (half dozen at different redshifts) of well positioned objects in redshift space (as confirmed by the LR observations described above), we aim at obtaining integral-field high-resolution spectroscopy in order to resolve spectroscopically (σ~5-7 km/s) and spatially (~1 kpc/resolution element) the line emission for the most massive clumps present in the galaxies of the sample. The resolved emission line profiles of the star-forming clumps in this galaxy will be analyzed looking for the presence of a single or a double component in the velocity space that will give us important insights on the hydrodynamical state of this object. In addition, by spatially resolving the different clumps using integral field spectroscopy we will obtain information on possible spatial differences where positive/negative feedback takes place. We will use the MEGARA SCB IFU (8.5 x 6.7 arcsec^2) with either the HR-R *or* HR-I VPHs depending on redshift, in this case.

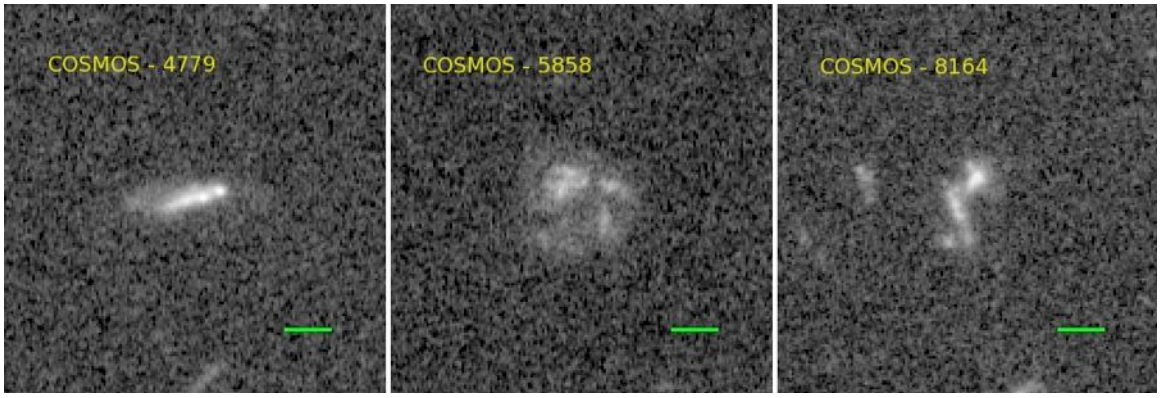

Figure 5: *HST images of the proposed galaxies obtained from the COSMOS cutout tool. Images have a spatial resolution of 0.05", the yellow line indicates an angular separation of 1".*

High-redshift proto-clusters:

Another objective for which the high number density of objects simultaneously observable with MEGARA MOS is best suited is the identification and characterization of high-redshift proto-clusters of galaxies. Recent studies on the evolution of the properties of galaxies in clusters at z~1 have shown (1) that red galaxies still prefer denser environments up to this redshift (Elbaz et al. 2007, A&A, 468, 33) and (2) that there are also more bright blue galaxies in over-densities than in the Local Universe (Cooper et al. 2008, MNRAS, 383, 1058). However, this has been limited to z~1 due to the lack until quite recently of photometric surveys that would allow covering fields large enough to identify the sparse population of high-redshift over-densities (<10 deg^{-2}; Eisenhardt et al. 2008, ApJ, 684, 905) with enough depth. Thanks to the new generation of photometric surveys (e.g. COSMOS, NDWFS, SXDS) some high-redshift over-densities (or proto-clusters) are now being found (see Figure 6).

The objective of this program is to spectroscopically confirm high-redshift (z>1) over-density candidates extracted from our own photometric database (RAINBOW; Pérez-González et al. 2008, ApJ, 675, 234; Barro et al. 2011, ApJS, 193, 13). The proto-cluster candidates will be observed in the red for z<1.5 and in the blue for z>1.5, both at intermediate spectral resolutions (R~6,000). This intermediate spectral resolution, similar to that of DEEP2 but higher than most spectroscopic surveys, will allow (1) optimizing the detection of the [OII]λλ3726,3729ÅÅ doublet in between the OH forest and (2) measuring velocity widths down to Δv~50 km s^{-1}.

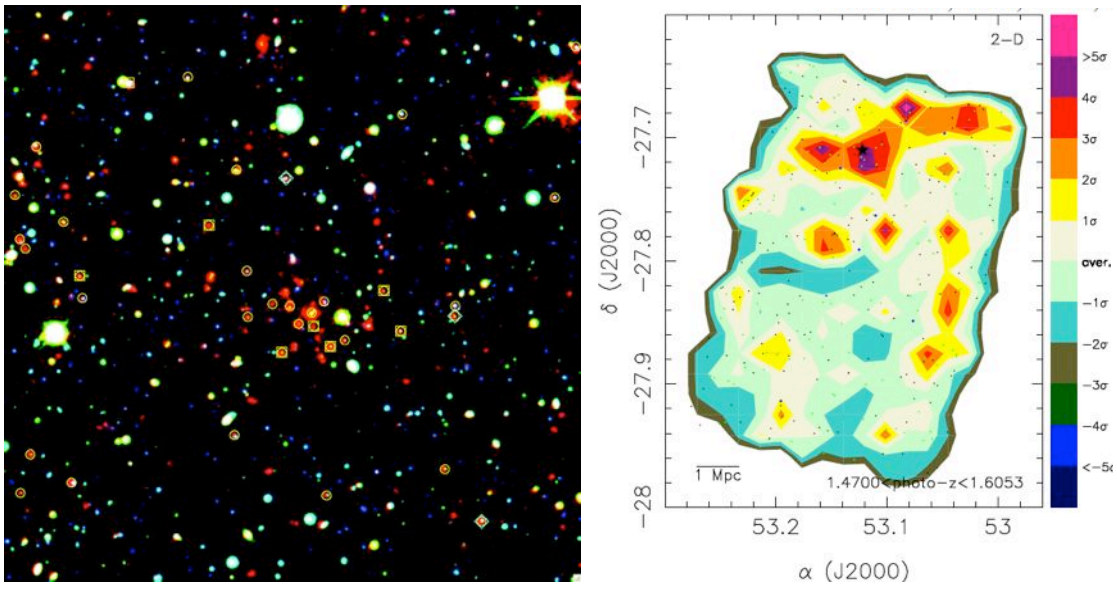

Figure 6: Left: *Cluster (or proto-cluster) candidate at z~1.3 detected by Eisenhardt et al. (2008) in the NDWFS field using photometric redshifts. The image is an RGB composite using the Bw, I and IRAC 4.5μm bands. Galaxies tentatively belonging to the over-density are marked with circles. Cluster members marked with squares have been confirmed spectroscopically. The image is 5x5 arcmin^2 in size.* ***Right:*** *Density map of the GOODS-S region built by our group. Magenta regions present surface densities more than 4σ above the average (shown in gray and light green) for the quoted redshift interval. We mark the higher density peak detected by Castellano et al. (2007, ApJ 671, 1497) with a cyan filled star. We demonstrate that our algorithm is able to recover the position of the proto-cluster.*

5. MEGARA SUBSYSTEMS DETAILED DESIGN

This section is devoted to briefly describe the design of the main MEGARA subsystems. We are grouping the subsystems in two main areas: the Folded Cassegrain subsystems (Section 5.1) and the Spectrograph (Section 5.2). Additionally, the MEGARA Control System, which provides the monitoring and control of all MEGARA subsystems, is described in Section 5.3.

5.1 Folded-Cassegrain Subsystems

MEGARA Folded Cassegrain subsystems include all components that collect and conduct the light from the Folded Cassegrain focal plane to the spectrograph entrance. Those elements are basically: (a) a Field Lens to correct from lack of telecentricity providing a telecentric focal plane for the microlens arrays, (b) the cover that allows obtaining very low cross-talk observations with half the FOV and multiplexing of the MEGARA default mode, (c) the microlenses that change the focal number of the telescope allowing a good coupling with fibers, (d) the fiber bundles, (e) the Fiber MOS that allows to position 92 minibundles in a dedicated area of the focal plane, (f) the interface plate that supports the LCB and SBC IFUs in the central area of the focal plane, (g) the Folded-Cassegrain Rotator Adapter that provides the interface with the F-C rotator at GTC and (h) the pseudo-slit plate that positions fibers at the Spectrograph entrance.

In the following subsections we briefly describe how the fiber units are arranged at the GTC F-C focal plane and, then each F-C subsystem design, providing the reference documents where the current detailed design of these subsystems is described in more detail.

5.1.1 Fiber Units at the GTC Focal Plane

The MEGARA Instrument is composed of three modes, two IFUs and the multi-object spectrograph (MOS) mode, that correspond to the three fiber bundles available: the Large Compact Bundle (LCB), the Small Compact Bundle (SCB) and the Dispersed Bundle (see Figure 7).

The fibers that constitute the **Large Compact Bundle (LCB)** (100 μm in size) are arranged on a square area of 12.5 arcsec x 11.3 arcsec near the optical axis of the instrument, the fibers that constitutes the **Small Compact Bundle (SCB)** (70 μm in size) are distributed in a square image area of. 8.5 arcsec x 6.7 arcsec, whose center is offset ~19 arcsec from the center of the LCB. The fibers belonging to the dispersed bundle **(MOS mode)** (also 100 μm in core diameter) can be positioned anywhere in the central 3.5 arcmin x 3.5 arcmin around the two IFU bundles thanks to the positioner robots (or simply positioners).

Note that a total of 8 robotic positioners (orange hexagons in Figure 7) out of those located in the outer edge of the instrument FOV are kept fixed in order to be used for measuring the sky background simultaneously with the observations with the LCB. The layout of the hexagonally-packed (and shaped) microlens arrays of the LCB and SCB IFUs is also shown.

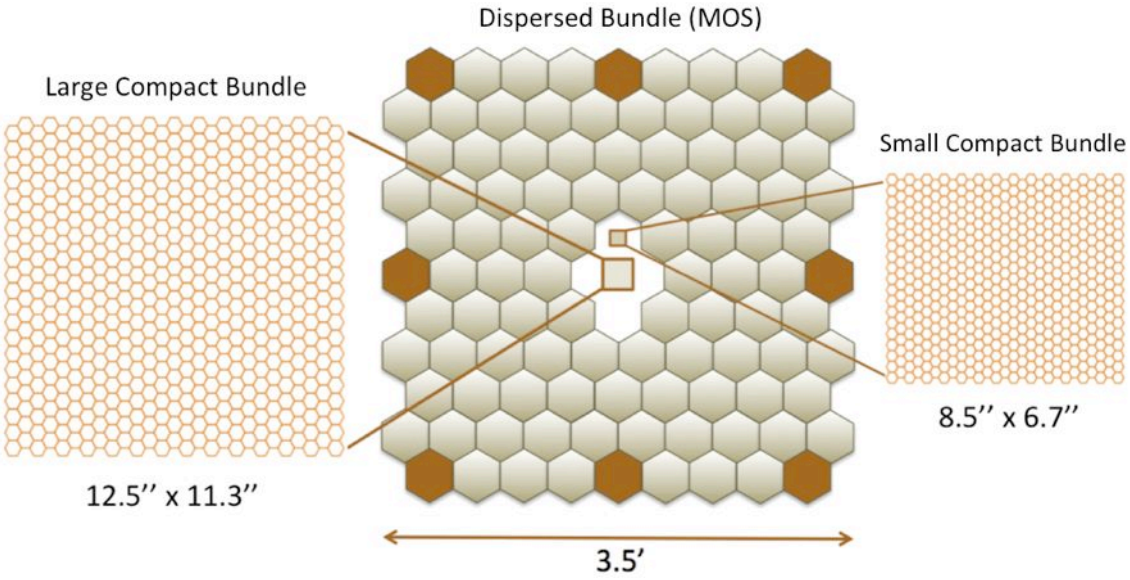

Figure 7: *Layout of the Large and Small Compact (LCB and SCB, respectively) and Dispersed fiber bundles of MEGARA.*

Large Compact Bundle IFU

The requirement for this IFU bundle is to place its 100μm-core fibers in the most optimum way possible to minimize pitch and provide maximum compactness (maximum filling factor[3]). This naturally leads to either (i) a honeycomb arrangement of hexagon-shaped lenslets for the fibers or (ii) a Cartesian distribution of square-shaped lenslets. The former arrangement is preferred as, according to the microlens-array manufacturer, it is expected to deliver a better image quality.

The LCB bundle shall have 567 fibers (see Figure 7) that, along with the 8 seven-fiber sky bundles located at the edges of the instrument FOV, leads to a total of 567+(8x7)=623 fibers feeding one of the pseudo-slits of MEGARA-Basic (or one of the spectrographs in the case of MEGARA-Advanced). This allows a total FOV of 12.5 arcsec x 11.3 arcsec. This number takes already into account the detailed design of the pseudo-slit and it is restricted to the aperture along the pseudo-slit where the optical design has been optimized and is within the image-quality requirements. See Section 5.1.7 for a description of the pseudo-slit design. The conclusions from the cross-talk analysis (both with and without using the focal-plane cover) presented in R.19 have been also considered for the final design of the pseudo-slit.

The LCB IFU is ideally suited for the study of individual compact objects under average seeing conditions and for absolute flux-calibration purposes when the MOS mode is used. When the

[3] *A coverage of ~ 95% is reached taken into account the microlens manufacturing process requires a real boundary between two lens surface (the light losses due to bondary scattering that is estimated in a ~ 5% or less are considered).*

object under study is larger than ~8-10 arcsec the use of the LCB is preferred over the SCB given the improved sky subtraction yield by the former under those conditions.

Small Compact Bundle IFU

The Small Compact Bundle IFU also provides a very high filling factor but it makes use of optical fibers with a smaller core diameter (70μm compared to the 100μm-core fibers used in the LCB). This yields an improved spatial (a spaxel size of 0.42 arcsec) and spectral resolution (see R.19 and R.20) but more limited FOV, 8.5 arcsec x 6.7 arcsec. Given its better spatial resolution, poorer spectral sampling and in order not to lose any information in the vicinity of bright point sources this bundle has a more stringent requirement for the maximum cross-talk allowed on the detector. Thus, a gap of 170 μm is used in the pseudo-slit of the SCB, i.e. a factor ~2.5x the core size, compared to a gap of size 1.7x the core size used in the LCB.

The current estimate on the total number of 70μm-core fibers that can be placed along the MEGARA pseudo-slit is between 500-550 fibers, after taking into account the 170μm-gap in between two adjacent fibers (see Table 9 of R.20). The IFU SCB shown in Figure 7 is composed of 511 fibers that yield the 8.5 arcsec x 6.7 arcsec FOV quoted above. The SCB IFU will then make use of the part of the pseudo-slit that is expected to produce the best image quality, ensuring an improvement in the spectral resolution compared to the LCB IFU.

Note that the SCB is not a mode of the MEGARA instrument that is currently of interest to GRANTECAN. It is included in this document as its design was completed and documented well before the scope of the MEGARA Optics Detailed Design was defined. Moreover, the outcome of the SCB design provides relevant information on the actual image quality yield by spectrograph. We emphasize here and elsewhere throughout the text that the addition on the SCB would not jeopardize the performance and feasibility of any of the other MEGARA modes and subsystems under any circumstances.

Nevertheless, in order to facilitate the work of GRANTECAN in evaluating the MEGARA Optics Detailed Design documentation, the Detailed Design of the SCB fiber bundle is given in a separate –non-delivered– document (TEC/MEG/128; R.5), different from the one describing the "MEGARA Detailed Design: Folded Cassegrain subsystems and pseudo-slit Optics and opto-mechanics" (TEC/MEG/112; R.3).

MOS Mode (Dispersed bundle)

There will be a number of dispersed individual sets/mini-bundles of fibers (7 fibers each) that could be positioned anywhere in the central 3.5 arcmin x 3.5 arcmin around the two IFU bundles thanks to the use of a set of positioner robots (also referred here as robotic positioners). These fibers will go to a different and separate pseudo-slit. The current detailed-design configuration includes a total of 100 positioners, 92 of them dedicated to MOS observations, which yields a total of 644 fibers in the MOS pseudo-slit. The rest of positioners (8) would be evenly distributed along the pseudo-slit of the LCB IFU. Note that these 8 positioners, since are devoted to measuring the sky background, are not required to move, so they will be always kept

in parking position[4]. In Figure 8 we show the 3D view of the positioners system with the two IFU bundles in the center.

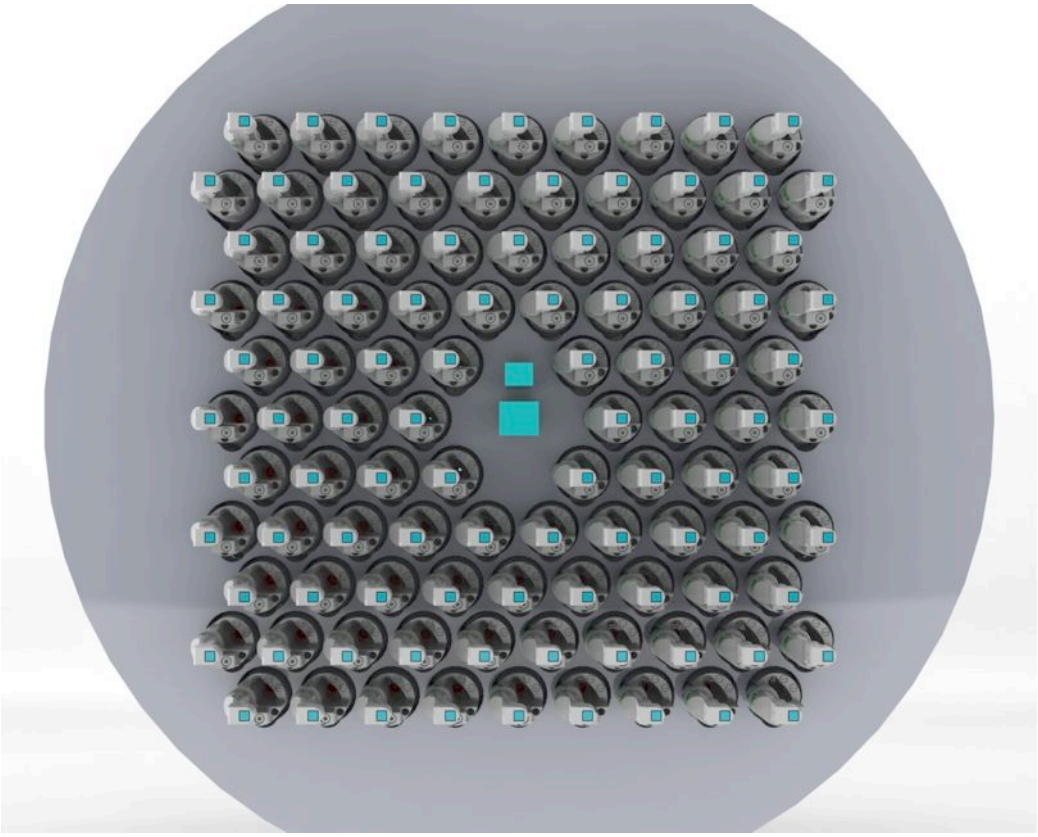

Figure 8: *3D view of the Fiber MOS system. The positions of the LCB and SCB IFUs are shown as two blue cubes near the center of the system. All positioners are identical.*

The fibers constituting the IFUs will be arranged in two pseudo-slits (one for LCB and another for SCB) with the fibers coming from the robotic positioners (MOS mode) arranged in a third additional pseudo-slit.

5.1.2 Field lens

A field lens has been designed to provide a telecentric field for MEGARA (see Figure 9). The GTC telescope has the aperture at the secondary mirror. Thus the exit pupil as seen from the telescope focal plane coincides with this position (-18mts from the focal plane), which implies that the FOV at the focal station is not telecentric.

[4] *Although it could be possible having these eight 7-fiber bundles mechanically attached (fixed) to the Folded-Cassegrain Rotator Adaptor frame, we estimate that, due to the associated increase in design costs, this would more expensive that having eight additional robotic positioners parked.*

With the field lens the opto-mechanical axes of all the fiber bundles will be parallel among them. Thus, the positioners move on a flat surface (the focal plane) with their opto-mechanical axis perpendicular to this surface. The field curvature has not disappeared (this would require at least 2 lenses to avoid changing the plate scale) but it is below 0.1arcsec in the whole FOV.

The lens is a fused silica meniscus (R1= -2147.6, R2= -1731.8 mm and CT=30mm). The aperture is 260mm in diameter.

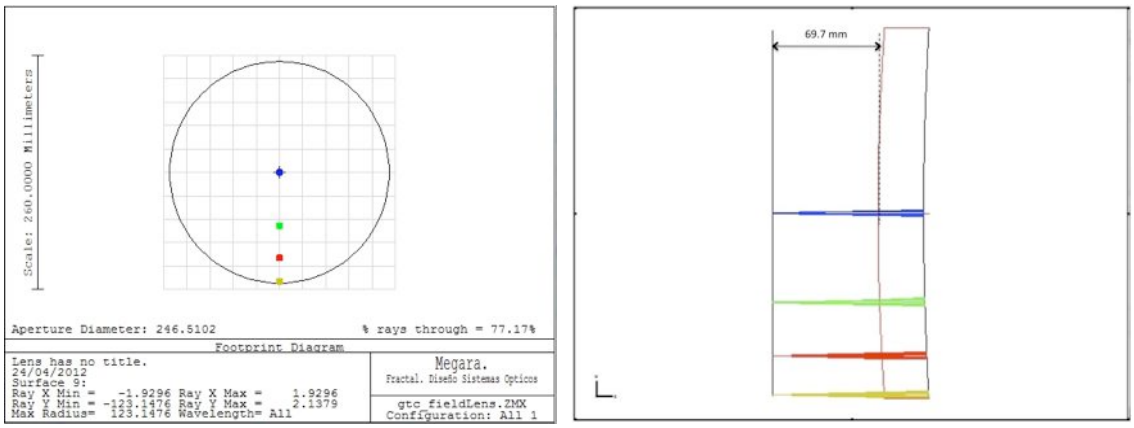

Figure 9: *Field lens layout for the entire MEGARA FOV corrected with the field lens (Left). Footprint diagram at the field lens surfaces (Right). The beam cross diameter for the different fields are under 6mm in diameter.*

The first surface of the lens is +69.7 mm in front of the focal plane in the F-C co-ordinate system.

As the lens is close to the focal plane it does not change the plate scale. The focal plane position is moved 13.5 mm from its nominal position (the distance between M2 – and therefore M3– and the focal plane is increased). Therefore, the position of the microlenses first surface shall be z = -13.5 ± 0.1mm in the GTC F-C co-ordinate system.

A detailed description of the field lens optical design is provided in R.3.

5.1.3 Focal-Plane Cover

As part of the delta-PDR phase we carried out a detailed evaluation of the effects of cross-talk on the CCD between the light coming from adjacent fibers on the pseudo-slit. The results of this analysis were presented to the MEGARA Science Team at the latest MEGARA Science Team Meeting held in Granada (Spain) in December 2012. Although the current level of cross-talk is not an issue for any of the science cases proposed, the team considered that it would be beneficial to the future community of users of MEGARA to provide a way to carry out null-cross-talk observations.

In order to perform such observations a Focal-Plane Cover would be used so to allow removing the light coming from one every two consecutive fibers (or sets of fibers) at the corresponding pseudo-slit. In the case of the LCB this implies arranging the fibers so two consecutive fibers will come from different halfs of the FOV. Regarding the MOS the decision was that all seven

fibers from each MOS would be placed together in the pseudo-slit (to minimize inter-positioner cross-talk between the central -brightest- fiber of each positioner) but that adjacent sets of 7-fiber would come, again, from different halfs of the FOV. In the case of the SCB, as the separation between adjancent fibers (170μm) at the pseudo-slit relative to the fiber-core size (70μm) is significantly larger than in the case of the LCB and MOS, we did not find necessary to include that funcionality.

This concept allows performing null-cross-talk observations without introducing any modification to the current optical design of the instrument. Only minor changes in the mechanical design, and only to the level of the Folded-Cassegrain subsystem, are being implemented. The layout of the optical fibers in the LCB and MOS pseudo-slits described in R.3 takes already into accounts the needs imposed by this Focal-Plane Cover when carrying out very demanding observations in terms of the level of cross-talk on the detector.

In Figure 10 we show the results of simulations of the spatial profiles obtained on the CCD with and without using the Focal-Plane cover in the case of the MOS. The same thing is shown for the LCB IFU in Figure 11.

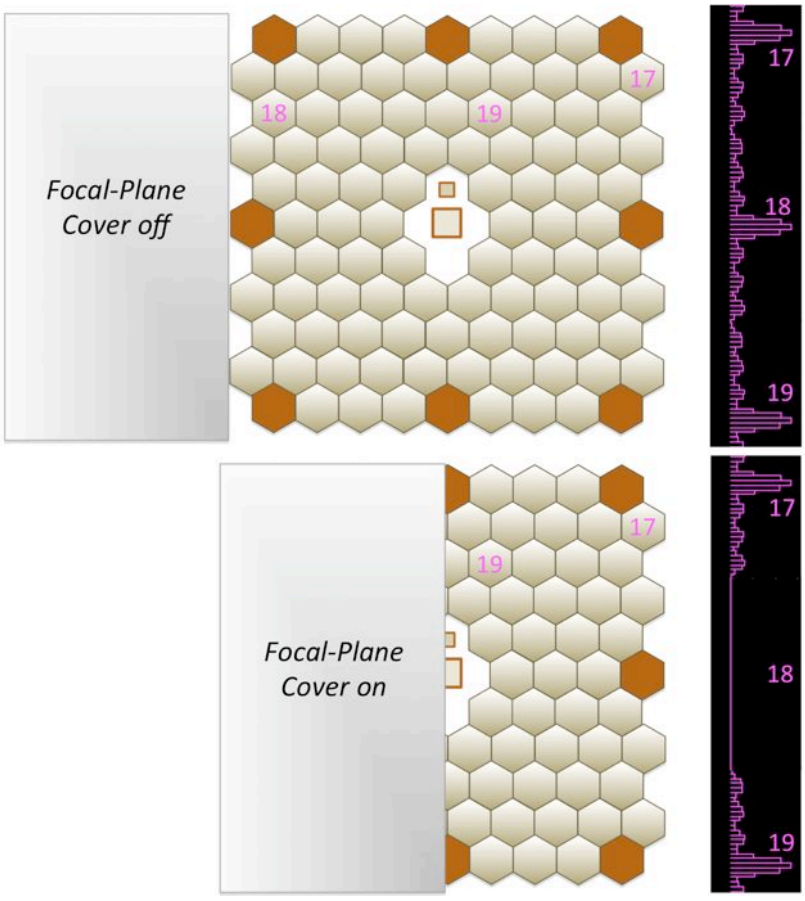

Figure 10: *MEGARA footprint with the Focal-Plane Cover off (default mode) and on (for demanding null-cross-talk obsevations). The corresponding simulated spatial profiles obtained in the CCD for three adjacent positioners on the pseudo-slit (numbers 17, 18, 19) are shown in the right.*

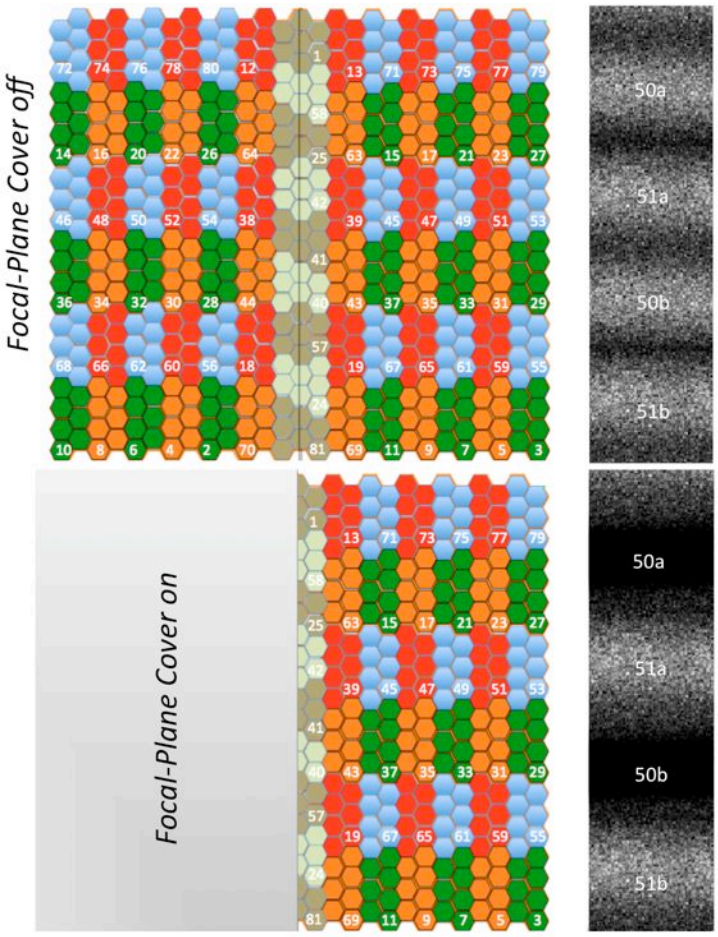

Figure 11: *MEGARA LCB footprint with the Focal-Plane Cover off (default mode) and on (for demanding null-cross-talk obsevations). The corresponding simulated CCD image sections for four consecutive fibers on the pseudo-slit (numbers 50a, 51a, 50b, 51b) are shown in the right. Note that in this simulation each pixel has been supersampled compared to the actual MEGARA CCD pixel size.*

We note the reader that the addition of the Focal-Plane Cover (or use) does not affect in any aspect to the MEGARA Optics Detailed Design being currently evaluated. Since there have been no funds allocated by GRANTECAN to the developement of any aspect of the mechanical detailed design of MEGARA since PDR, no progress could be made on the Focal-Plane Cover design.

5.1.4 Microlens array

A 2D microlens array is proposed to couple the science light at the telescope focal plane into the fibers. The microlens array main functions are to define the FOV that will be introduced in the fiber, adapt the telescope F# from f/17 to f/3 to minimize focal ratio degradation (FRD) effects during the beam transport and provide a telescope pupil image on the 100 μm fiber core (70 μm in the case of the SCB) for stray light control.

Refractive microlenses are manufactured using standard semiconductor technologies, like lithography, which allows very accurate shaping of the lens profile and precise positioning of the lenslets in the array.

The microlenses array will be placed at the telescope focal plane. In the case of the LCB and the Dispersed bundle, all the microlenses will have the same optical parameters although the arrays will be geometrically different (in terms of the number of lenslets used) for the LCB IFU and dispersed-bundle-fed MOS. Figure 12 shows the detail of one of these lenslets (left) along with the corresponding full-field diagram (right). This figure shows the design for the LCB or Dispersed-bundle (MOS) lenslets, both using 100µm-core fibers. A similar design shall be used for the SCB, where 70µm fibers are used instead, is shown in Figure 13.

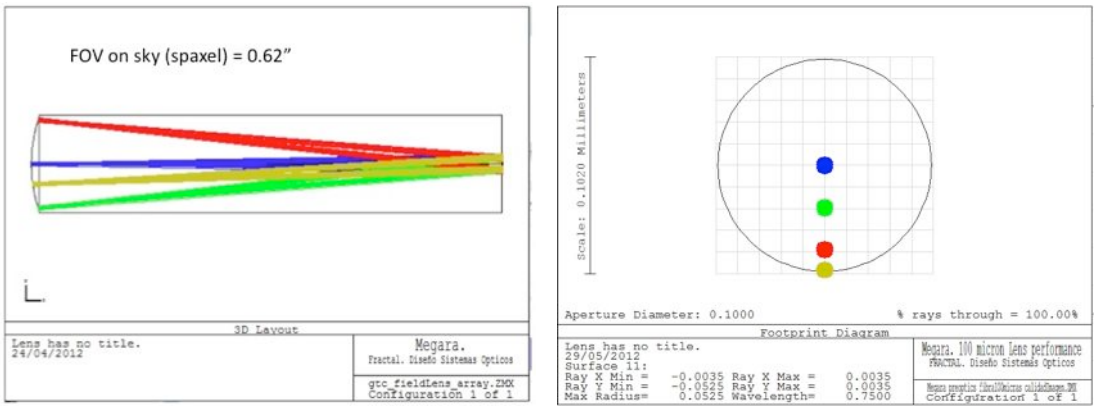

Figure 12: *Detailed design for one of the LCB and MOS lenslets (Left). Full-field diagram showing the four fields across the fiber core. Black circle is the fiber core of 100 µm (Right).*

In the case of the Dispersed bundle, the array aperture contains 7 lenslets to feed 7 fibers arranged in a hexagonal geometry covering 1.6" arcsec in the sky at the telescope focal plane.

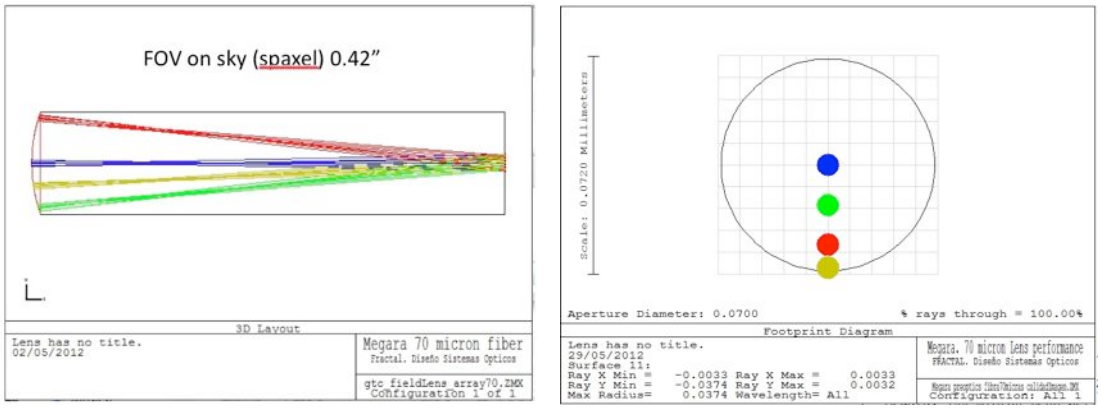

Figure 13: *Detailed design for one of the SCB lenslets (left) showing the telescope focal plane and the FOV aperture. Full-field diagram showing the four fields across the fiber core. Black circle is the fiber core of 70 µm (Right).*

The array is made in fused silica due to its good UV transmission. In the case of the LCB and MOS each lenslet is a plano-aspherical lens of ROC = 0.844mm, c= -0.9797 and aperture of 0.511 mm. For the SCB lenslet the design is also a plano-aspherical lens made in fused silica with ROC=0.563mm, c=-0.927 and aperture of 0.346mm. The Refraction Index vs. λ for Fused Silica is listed in Table 2 while the main optical parameters for the 100μm-core (left) and 70μm-core (right) fibers are given in Table 3.

Wavelength (μm)	Index
0.37000	1.4738257766
0.40000	1.4701161181
0.60000	1.4580377015
0.80000	1.4533172547
0.91000	1.4516122685

Table 2: *Refraction index vs. Wavelength for Fused Silica.*

Property	Aspherical microlens
ROC (mm)	0.844
Thickness (mm)	2.727
Aperture (μm)	511
Conic constant	c = -0.9797

Property	Aspherical microlens
ROC (mm)	0.563
Thickness (mm)	1.815
Aperture (μm)	346
Conic constant	c = -0.927

Table 3: *Left: LCB and MOS microlens array design parameters (100mm-core fibers). Right: SCB microlens array design parameters (70μm-core fibers).*

In the current design the pupil image, which is formed at the back surface of the array, is overfilling the fiber core (see Figure 14 and Figure 15). The purpose of this approach is two-fold:

- To provide an illumination condition as similar as possible to the one given by the spectral calibration system. That means to fully illuminate the fiber core. The spectral flux will be provided at f/16. We would need a simple system to project the calibration lamps of the Instrument Calibration Module on the fibers. The details will be a topic to be discussed with GRANTECAN once the final design of the ICM is provided to the MEGARA team.
- To minimize the impact of either mounting or assembly errors between fibers and microlenses. The use of an overfilled image ensures good flux homogeneity and a similar performance in between fibers. The maximum tolerance aceptable is 10 μm (LCB and MOS) and 8 μm (SCB) at the pupil image, which is doable.

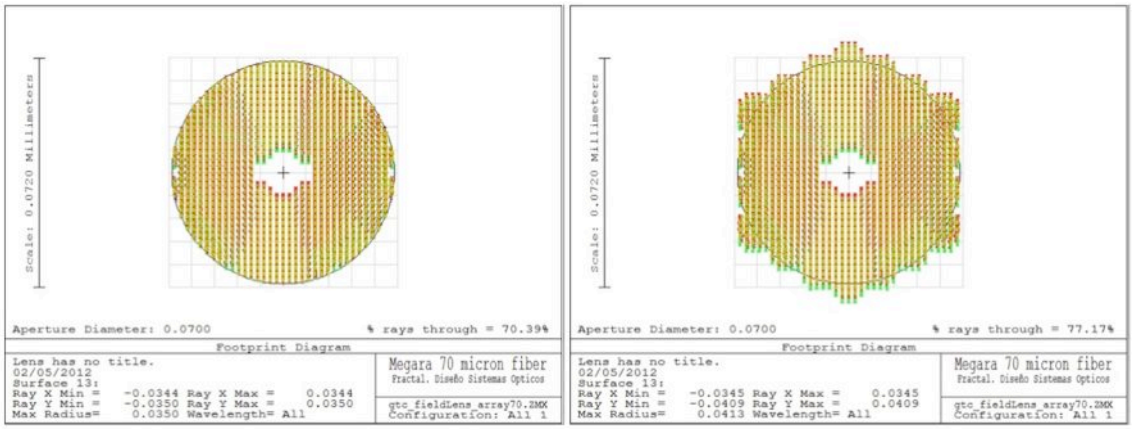

Figure 14: *GTC pupil image at the 100µm-core fiber entrance of LCB and MOS. On the left, the light entering in the fiber (a flux of 64.41%). On the right, the complete pupil, (a flux of 77.17%). This is the value corresponding to 100% of effectiveness. If we make the ratio between the two values, we have a transmission of 83.5% = 64.41/77.17).*

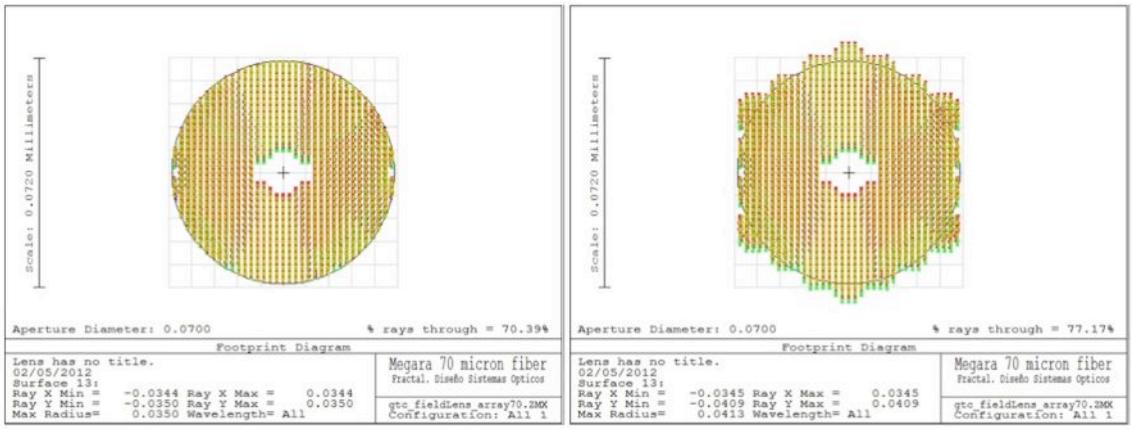

Figure 15**:** *GTC pupil image at the fiber entrance. On the left, the light entering in the fiber (a flux of 70.39%). On the right, the complete pupil, (a flux of 77.17%). This is the value that corresponds to 100% effectiveness. The ratio between the two values gives us an effective transmission of 91.2% (i.e. 70.39/77.17).*

In the current design the oversize of the pupil on the fiber core will decrease 16.5% (LCB and MOS) and 8.8% (SCB) the total flux of the maximum telescope aperture. The trade-off performed between FOV, flux homogeneity, flux losses at the pupil, and atmospheric refraction effects is discussed in detail in R.3.

Finally, the microlens array contains two fiduciary marks that are referenced to the lenses centers within 5µm in order to help for the alignment between the fiber and the array.

In Figure 16, Figure 17 and Figure 18 we show the design drawings for the LCB lens array, one individual MOS array of 7 lenslets and the SCB lens array, respectively. The manufacturing drawings proposed by the AMUS are shown in document R.3. A detailed description of the microlenses parameters and optical performance is also included in R.3.

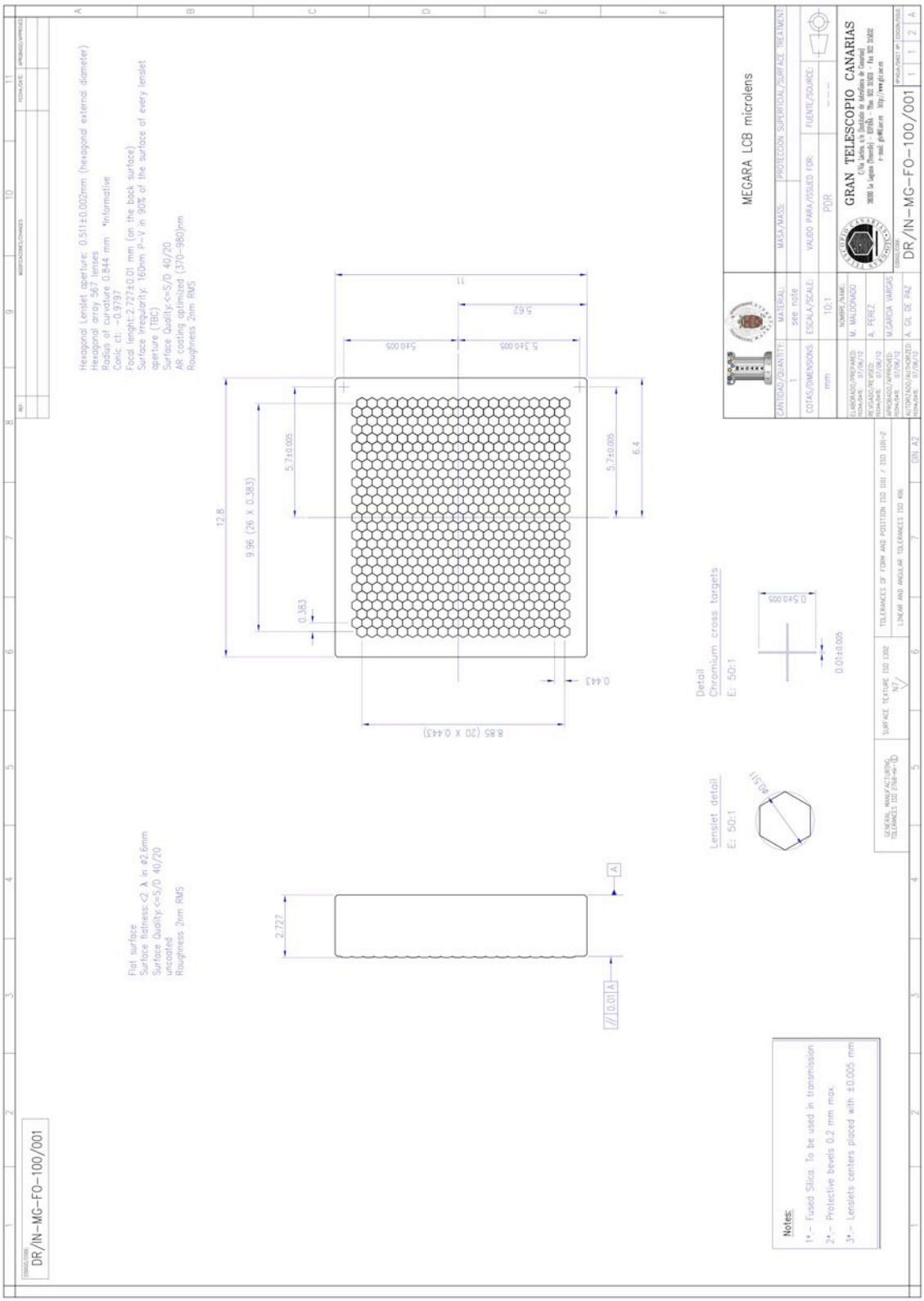

Figure 16: *LCB microlens array.*

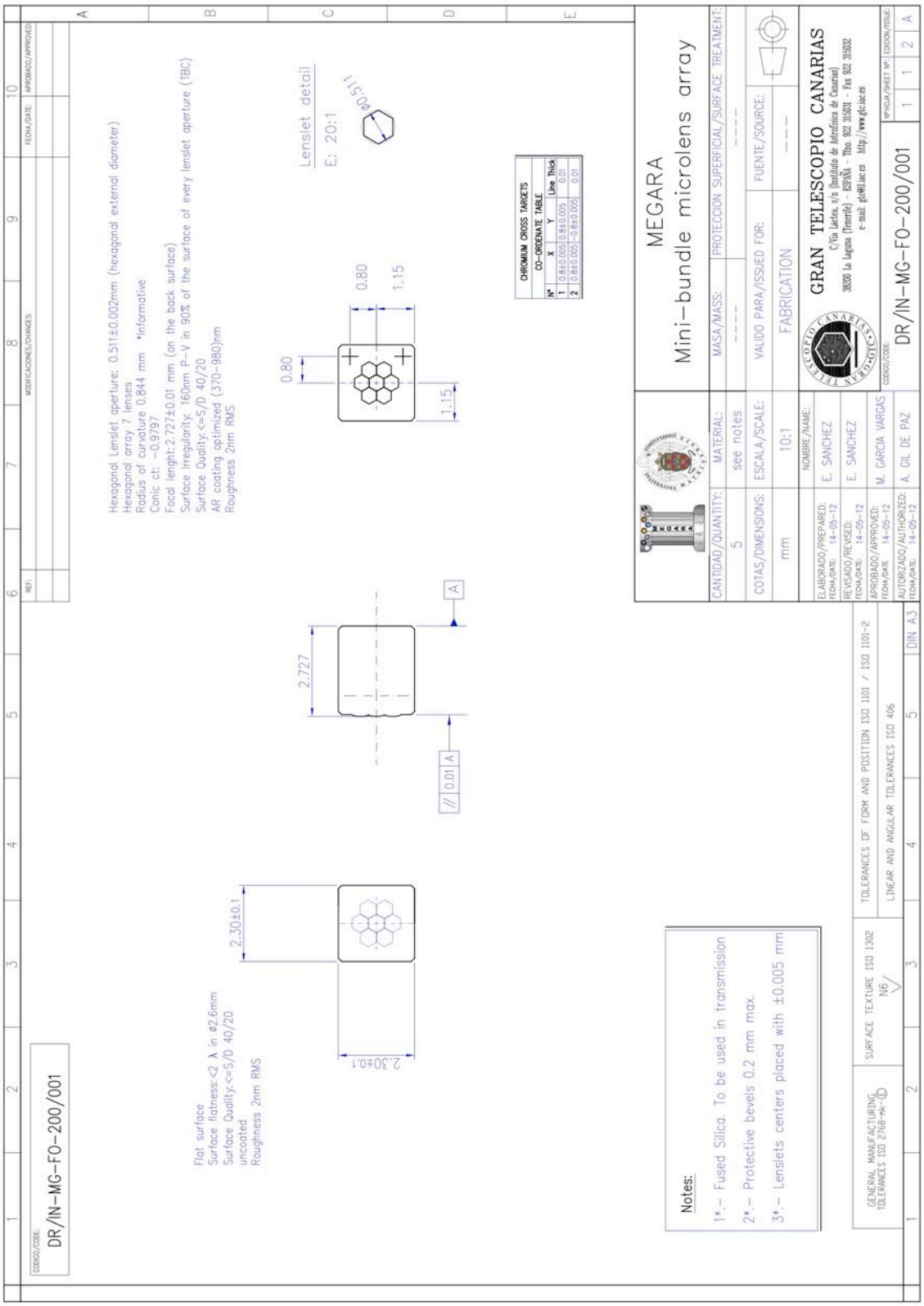

Figure 17: *MOS (7 fiber mini-bundle) microlens array.*

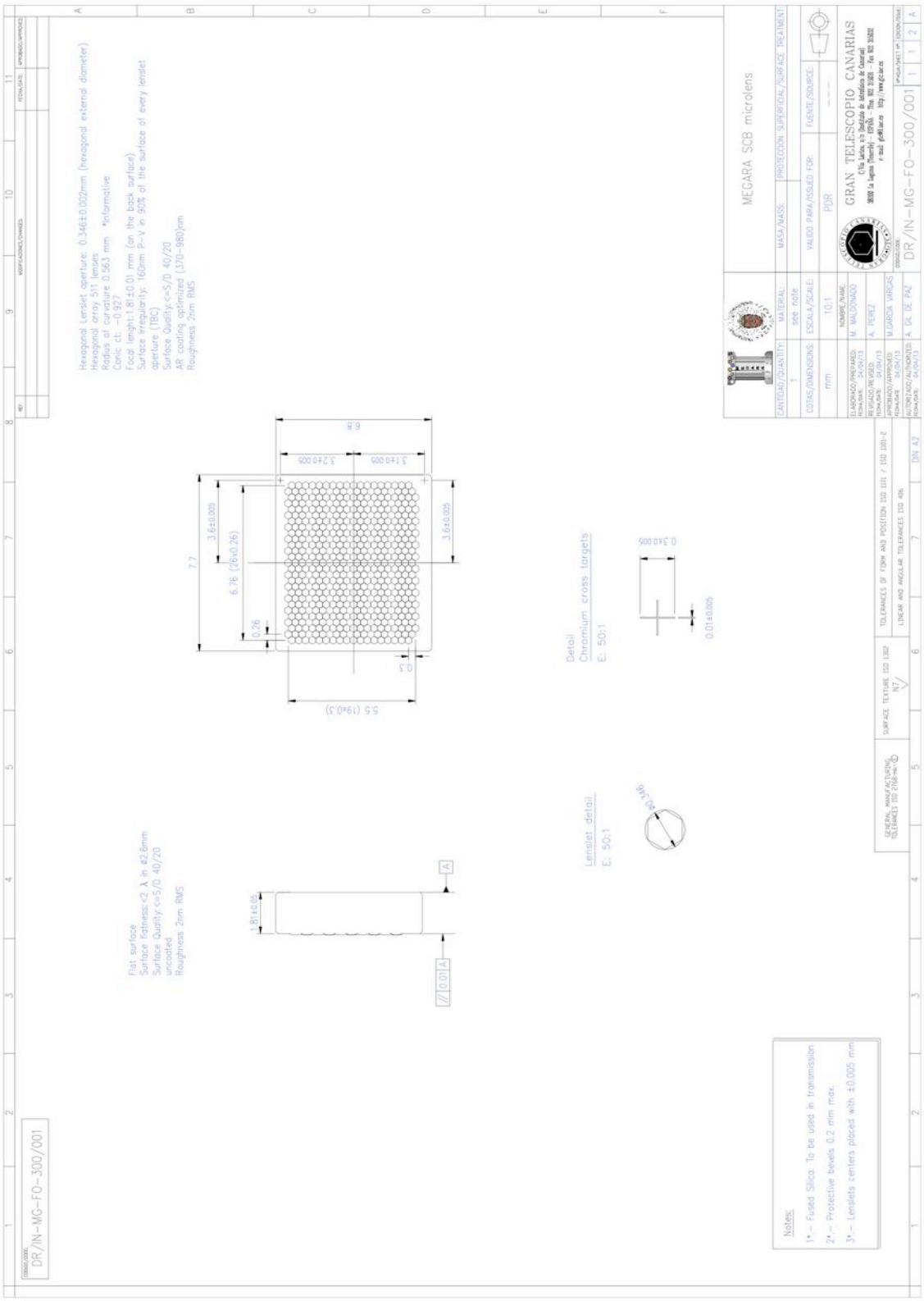

Figure 18: *SCB microlens array.*

5.1.5 Fibers

The fiber cables transport the light from the focal plane to the spectrographs at the pseudo-slit position. The characteristics of the fibers to be used for LCB/MOS and SCB are slightly different.

5.1.5.1 Large Compact Bundle & Dispersed bundle fibers

The fiber selected in this case is the one from Polymicro FBP 100/140/170; 100µm is the core, 140µm is the cladding and 170µm is the mechanical coating. This fiber has a numerical aperture of 0.2 ± 0.02 (optical angle acceptance and output light angle of the fiber, sin (12.71)). This is a wide broadband fiber and provides a good FRD. We shall use this fiber for both the LCB IFU and MOS modes.

Figure 19 shows the expected transmission for the fiber model Polymicro 100/140/170.

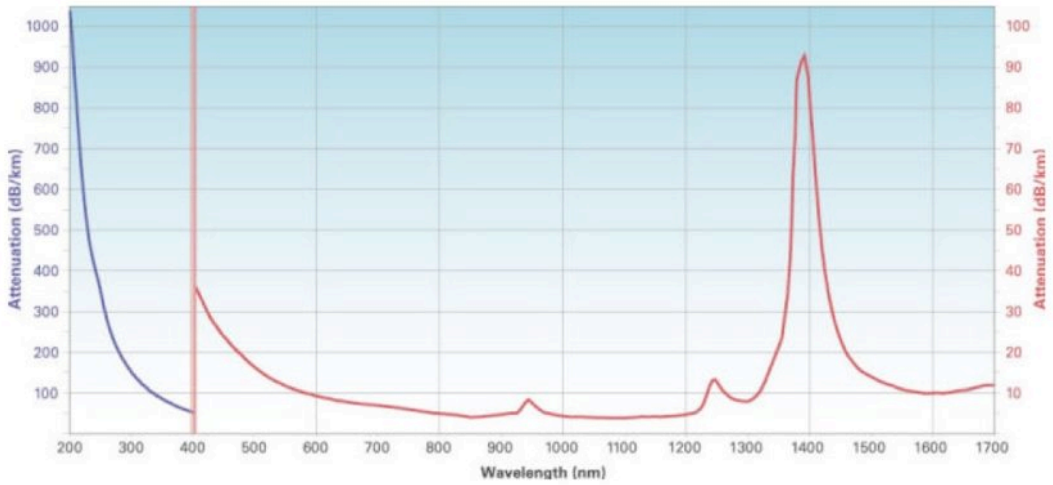

Figure 19: *Fiber model FBP 100/140/170 from Polymicro.*

Light is collected at the fiber exit at f/3 to minimize losses due to FDR.

The Dispersed-bundle fibers must be integrated in sub-units of 7 fibers. The LCB IFU fibers shall be also grouped in sub-units of 7 fibers. Then, both LCB sub-units (plus the 8 sub-units coming from the 8 positioners that shall be also attached the LCB pseudo-slit) and MOS sub-units shall be independently covered by two polyurethane loose tubing (not a tight jacket) with an external diameter lower than 40 mm.

The fibers (organized in cable bundles) will be supported on a mechanical interface plate and positioned at the center of the pupil images formed by the microlenses. The impact on the fiber-to-fiber flux homogeneity of the positioning tolerances of the fibers with respect to the images of the pupil is described in detail in R.14. The mechanical interface plate will be attached to the Folded Cassegrain Rotator Adapter, which will guarantee the position of the fibers in the focal plane. Then, the fibers will transport the science light coupled via the microlenses from this input plane to the spectrometer final position (estimated length of the fiber link is no more than 40 meters). The fibers at the fiber cable output will be arranged in a pseudo-slit configuration

and position in front of each spectrograph at the pseudo slit position. Each fiber will be clearly identified with the corresponding position within the bundle on the Folded-Cass placement to allow a perfect correspondence between positions in the pseudo-slit and positions on-sky. The detailed correspondence between pseudo-slit and on-sky positions is given in Section 5.1.9.

5.1.5.2 Small Compact Bundle fibers

The fibers to be used in the Small Compact Bundle (SCB) share the same manufacturer (Polymicro) and some basic properties with those used for the LCB IFU and MOS modes, such as the numerical aperture and expected transmittance. Besides the different core size previously mentioned other differences arise in terms of thickness of the silica cladding (70 μm in diameter) and the polymide coating (30 μm). For a 70 μm silica core this yields total fiber diameters of 70/140/170 μm. These fibers will then have the same external diameter as in the case of the LCB and MOS 100μm-core fibers.

The Focal Ratio Degradation (FRD) shall be the same applicable to the 100μm fiber used in the LCB and MOS modes. Thus, we foresee a loss below 5% of the beam introducing the light at f/17 and collecting it at f/3.

Fibers must be also arranged in as many units as boxes the pseudo-slit frame is composed of and these in sub-units of 7 fibers, as in the case of the LCB. Again, all sub-units will be covered by polyurethane loose tubing and not with a tight jacket. This protection tubing extends on the bundle length (telescope to spectrograph) to protect the fibers. Polyethylene (PE) is the standard jacket material for outdoor fiber optic cables. PE has excellent moisture and weather-resistance properties. Polyurethane material is also the best one used when a robot is moving. It has very stable dielectric properties over a wide temperature range. It is also abrasion-resistant.

More information about the fiber characteristics and other fiber issues related with assembly and manipulation are included in R.3.

5.1.6 Fiber MOS

The Fiber MOS subsystem holds the MEGARA dispersed mode and allows placing all 100 seven-fiber minibundles (92 in the MOS-dedicated pseudo-slit and 8 in the LCB pseudo-slit for sky background measurements) anywhere in the 3.5 x 3.5 arcmin^2 FOV, each within its circular patrol area. The Fiber MOS includes the following elements:

- The positioner system, which consists of 100 identical positioners, which integrates the positioner mechanism and fibers minibundle (7 fibers each).
- The positioners mechanism control software, which provide the low-level control of the positioner mechanism.
- The positioner control electronics or LCU, which include the positioner electronic cards and CPU board.
- The cabling between positioners and positioner control electronics.

The positioner system will consist of 100 identical positioners that will be distributed on the 3.5 x 3.5 arcmin^2 (on sky) area around the central LCB and SCB IFUs. The technological challenge associated to the development of the positioner system is due to the required reduced size and precision of each fiber positioner robot.

In Figure 8 we showed the distribution of the fiber positioners in the focal plane and the LCB and SCB IFUs in the center. The distance between centers of two adjacent positioners is 20.1mm. Each positioner covers a diameter of 23.1mm. We remind that the system is able to obtain spectra of up to 100 objects (92 on the MOS-dedicated pseudo-slit and 8 on the LCB pseudo-slit).

The positioning of the fiber minibundle is performed by combining the interpolation of two rotations, which allows covering a circle with a radius of 11.605mm from the centre of the positioner (this circle reaches the corners of the hexagon with an E/C of 20.1mm). Figure 20 shows the datasheet of the detailed design of the positioner robot.

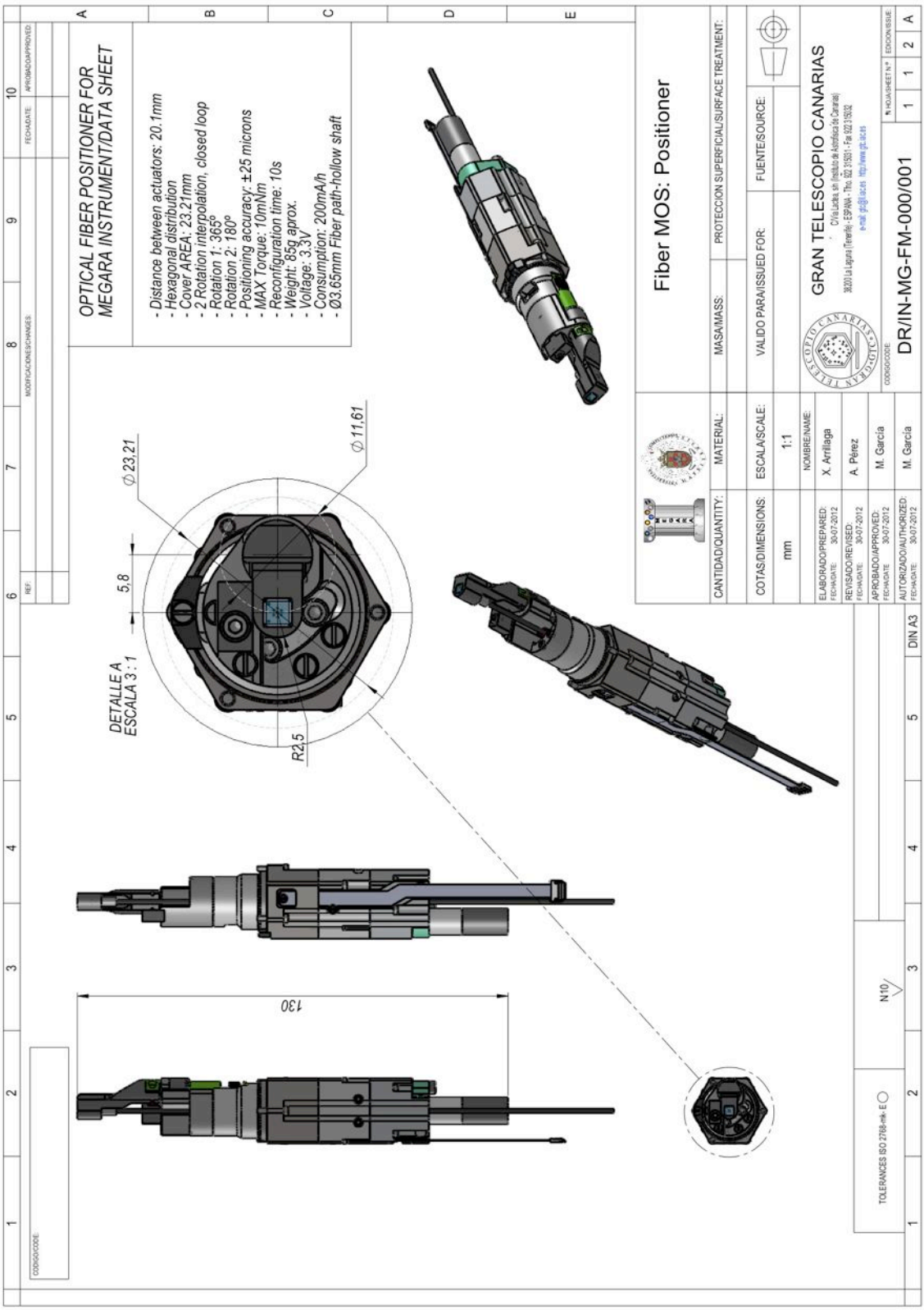

Figure 20: *Fiber MOS prototype positioner Data sheet.*

The button, which is the mechanical part where the fibers are attached, has been defined taking into account the assembly of the micro lenses and fibers, optical considerations and possible

micro machining issues. Lens assembly will have a square geometry, which includes 7 lens and a couple of reference marks to properly align the lens array with the micro fibers. However, a revolution shape for the button is used in order to adjust and assemble the microlens to the positioner arm. This geometry allows an exact X-Y positioning of the lenses and have also defined the position and tolerances of the micro-bores on the button and cross-shaped reference marks.

The fixing of the positioner button to the positioner, which shall be strong and repetitive, has been designed considering that it must be possible to disassembly it from its back in order to facilitate the maintenance of the mechanical and electronics parts. The length of the feeding and the signal cables and the fibers shall be also defined taking into account the need to assembly and disassembly each positioner independently.

Figure 21 shows a sketch of this component.

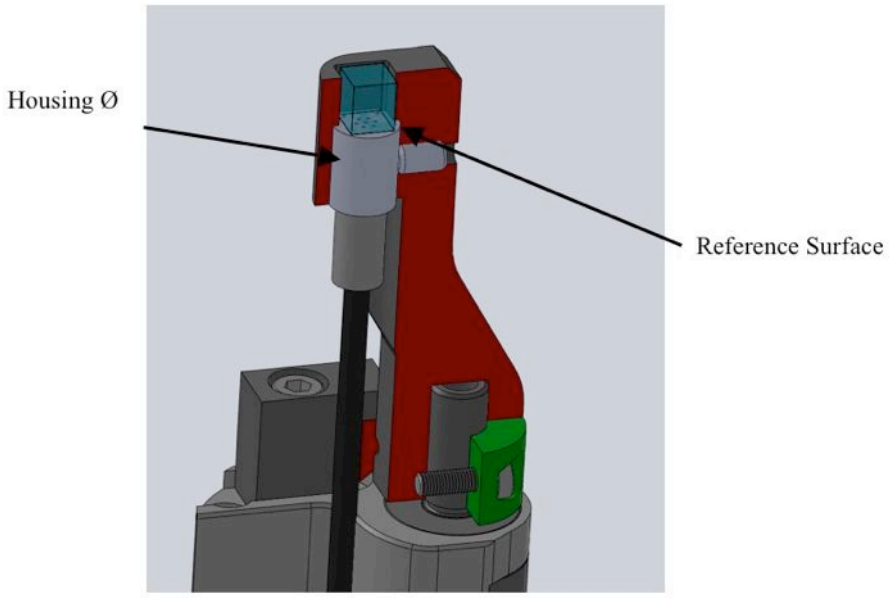

Figure 21: *Positioner button detailed design.*

Figure 22 shows the manufacturing drawing of the detailed design button.

A study of different coatings for the fiber bundle has been carried out in order to validate the system and the position of all the elements inside the positioner.

Regarding the positioner electronics, it has been decided to use a stepper motor with incremental encoders (as the initial choice of DC motors and absolute encoders is not yet available for the required size), which involves the addition of hard stops or Hall sensors in order to determine a zero position for the positioner.

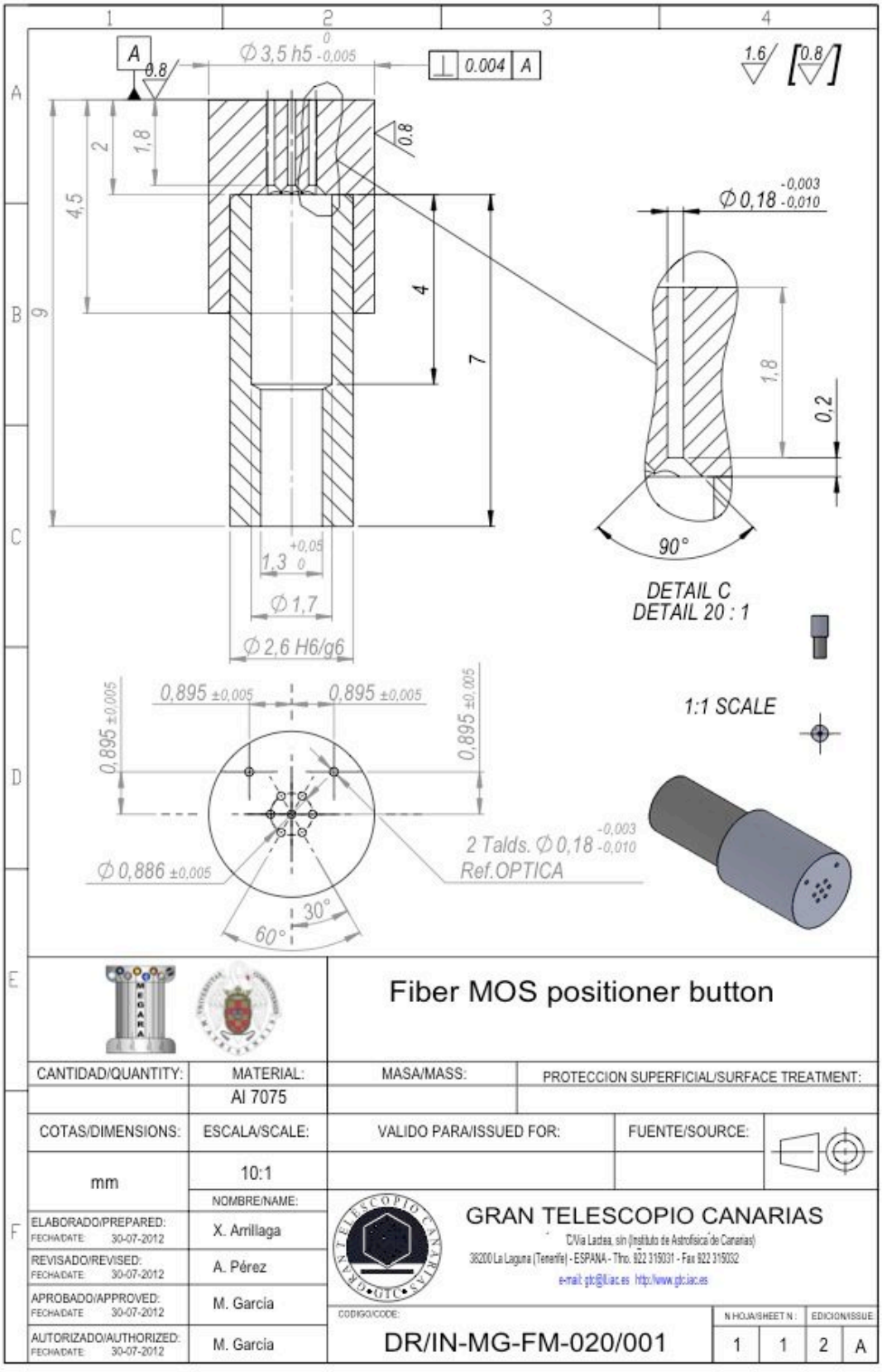

Figure 22: *Positioner prototype button manufacturing drawing.*

A more detailed description about the Fiber MOS and the test carried out during this subsystem design is included in R.30 and R.4.

The prototype of one of the positioners was completed during the Preliminary Design phase and was presented during the Preliminary Design Review. This unit is shown in Figure 23 (before the optical fiber bundle was attached on December 2011). The results of the tests performed on this prototype are included in R.4.

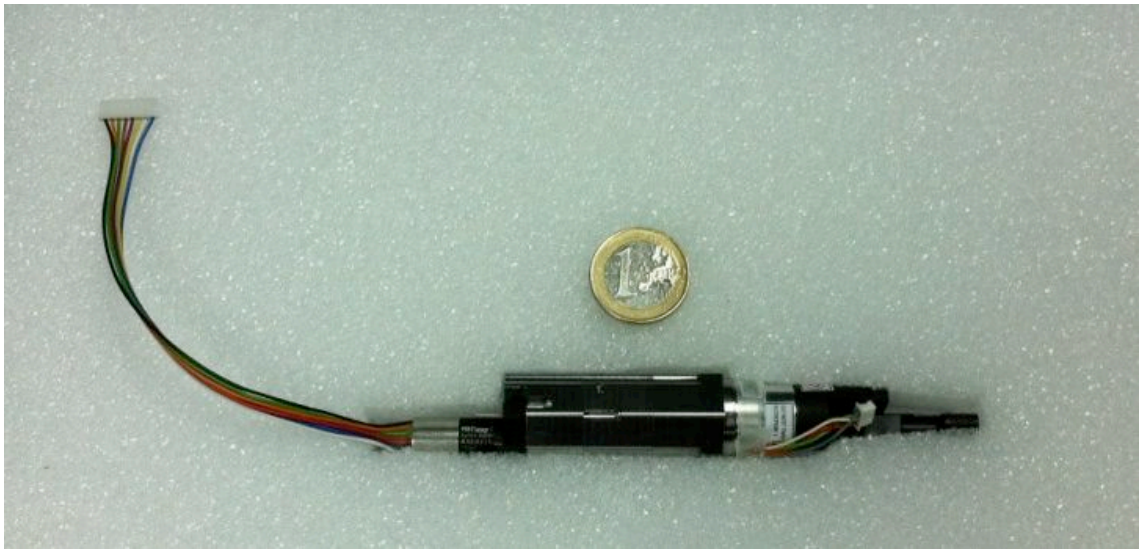

Figure 23: *Fiber MOS positioner prototype (December 2011).*

5.1.7 Folded Cassegrain Rotator Adapter

The F-C Rotator Adapter provides the MEGARA interface to the F-C Rotator at the GTC. The adapter shall support to the Field Lens, the IFU mechanical frames and the Fiber MOS.

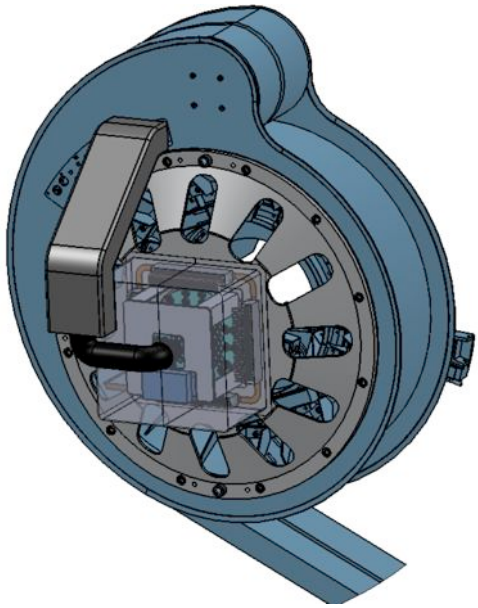

Figure 24: *Rotator Adapter view.*

A specific mechanical frame for attaching the fibers shall be designed and manufactured by taking into account the final arrangement of the IFUs and microlens design described in R.3, which shall incorporate the attachment and alignment system of the central LCB and SCB IFUs.

The interface between the Folded-Cassegrain Rotator Adaptor and the Fiber MOS plate of robotic positioners is defined in R.30. The frame must be aligned in the Folded Cassegrain focal station and the repeatability of the assembly and disassembly on the instrument flange must be guaranteed. The guiding of the MEGARA instrument will be fixed to the rotator by means of eccentrics. The eccentric systems will work on the foreseen pins of the instrument flange.

The total weight of the elements that shall be attached to the Folded Cassegrain Rotator, which includes not only the Folded Cassegrain Rotator Adapter but also the fiber and feeding cables, is estimated in 370 kg with the centre of gravity at Z= 180 mm.

Electronic boxes that contain the positioner controllers shall be hanged of the adapter as well as an additional box that shall contain the positioners power supply. These boxes are shown in Figure 24.

Figure 25 shows the data set of this subsystem.

The F-C rotator adapter detailed description is included in R.30.

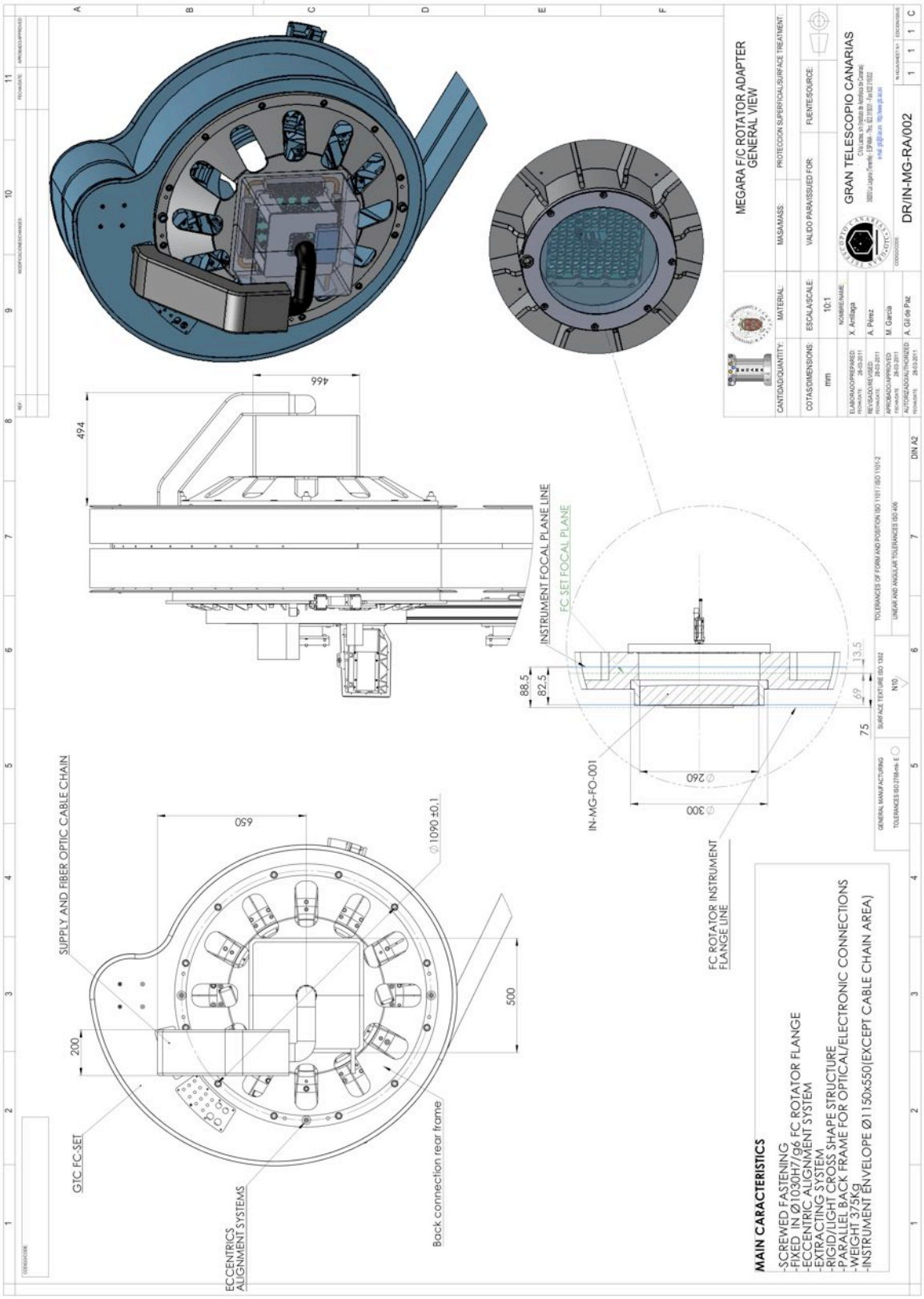

Figure 25: *F/C Adapter Subsystem Datasheet.*

5.1.8 Pseudo-slit frame

The fibers will be arranged in a pseudo-slit configuration (the pseudo-slit frame) and placed in front of each spectrograph at the pseudo-slit position. The pseudo-slit frame for all configuration modes shall be identical to allow a standard interface at the pseudo-slit position.

The focal plane at the pseudo-slit position is smoothly curved with a ROC of 1075mm and a size (tangential to the curve) of 119mm. For all LCB, SCB and MOS modes the fibers are mounted at the pseudo-slit, buffered side by side, forming a regularly spaced linear array. The fiber outer diameter allows achieving approximately the requested gap between consecutive fibers. This assembly in-line is acceptable since the scientific requirements of having 2 projected pixels on detector between adjacent fibers to avoid cross-talking is equivalent to have a pitch of 178 μm, so that having 170μm pitch is fully acceptable.

As the polishing of the fiber mounted in a curved surface is not advisable, the decision was to split the pseudo-slit frame in several flat frames (where fibers are attached), called boxes, arranged to follow the curvature of the pseudo-slit. Figure 26 describes the geometry of the proposed boxes for providing the pseudo slit frames.

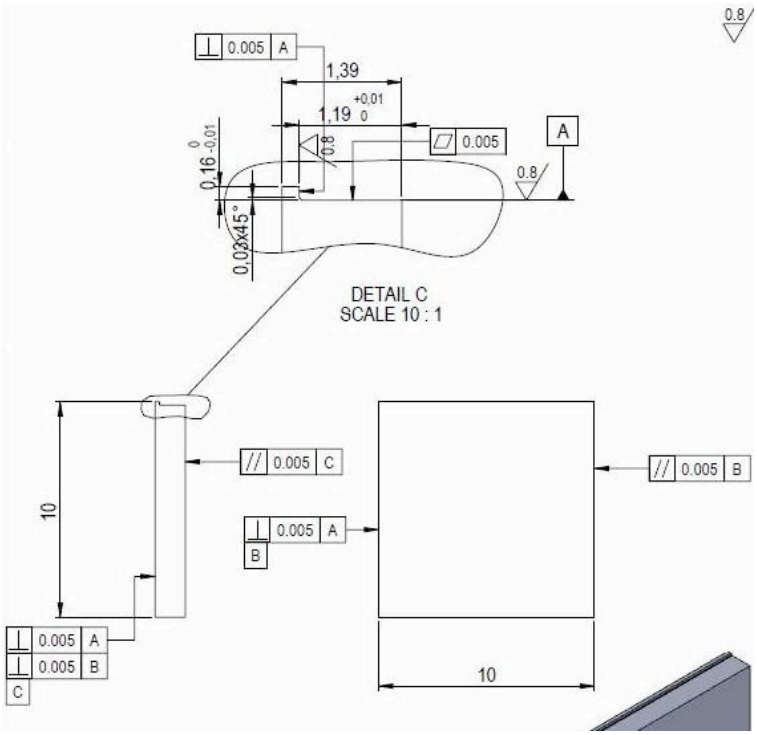

Figure 26: *Pseudo-slit box.*

In order to follow the pseudo-slit curvature the number of fibers in each box (and, therefore, the longitudinal dimensions, D) shall be different in each box. More information about the pseudo-slit plate design and optical evaluation of boxes geometry can be found in R.3.

5.1.9 Pseudo-slit and on-sky fiber positions

In this section we describe the relation between the on-sky positions of the fibers and their positions on the pseudo-slit. As main general criteria we aim (1) to use the central part of the pseudo-slit (which, on average, delivers the best image quality) to fibers located in the central parts of the FOV of either the LCB or SCB IFUs, (2) to have all 7 fibers from each MOS positioner (and sky bundle) placed together on the pseudo-slit so to minimize inter-positioner cross-talk (with the central spaxel placed in the middle of the seven fibers in the pseudo-slit), (3) to place the 7 fibers from each sub-unit close in the pseudo-slit and always in the same pseudo-slit box, (4) to evenly distribute the sky-bundes along the LCB pseudo-slit, (5) to take advantage of the focal-plane cover when null-cross-talk observations are to be performed (in the case of the LCB and MOS alone), and (6) to simplify the mounting procedure of the fibers on each pseudo-slit. Below we summarize the resulting distribution of the LCB, MOS and SCB fibers on-sky and in the pseudo-slit after applying these criteria.

In Table 4 we show the boxes and sub-units of 7 fibers associated to them in which the three pseudo-slits have been divided.

5.1.9.1 LCB fiber positioning

In the case of LCB we have arranged the 567 fibers coming from the IFU microlens array plus the 56 fibers from the 8 sky bundles in a total of 81 sub-units of 7 fibers distributed in 17 boxes on the pseudo slit. In Figure 27 we show how the 73 sub-units of the LCB IFU have been distributed on the sky. We also show the order of each individual fiber on the pseudo-slit from bottom to top (fiber #312 will be located at the very center of the pseudo-slit). Note that, except for the central column of 7-spaxel (7-fiber) sub-units, the rest of the sub-units are placed alternatively between the left and right sides of the field in order to take advantage of the Focal Plane Cover when used. Consecutive sub-units are mounted one next to the other in their boxes and their fibers interlaced on the pseudo-slit (again, except for the central column of sub-units).

Figure 28 shows the results of the MEGARA Simulator for the fiber arrangement described above in the case of the default mode of use of the instrument (no Focal Plane Cover; right panel) and with the left side of the Cover placed in front of the focal plane (left panel). This figure shows only the central part of the corresponding simulated full CCD frames, i.e. the central part of the pseudo-slit. We show here both fibers that are interlaced (e.g. those coming from sub-units 38+39 and 42+43, which are adjacent on the pseudo-slit) and fibers that not, i.e. fibers coming from the central column of sub-units plus sky bundles (see DR/IN-MG-FB-101/002)

5.1.9.2 MOS fiber positioning

Table 4 shows that the MOS is the most demanding mode in terms of the use of the pseudo-slit with the fibers spanning the range between -55.56 to 56.85 mm in their positions along the pseudo-slit. As a consequence of this the image quality performance of the outermost MOS

positioners (in the pseudo-slit) might be not as optimal as for the rest (see DR/IN-MG-FB-201/002).

	LCB		MOS		SCB	
Box	**Number of fibers**	**Arrangement**	**Number of fibers**	**Arrangement**	**Number of fibers**	**Arrangement**
8b	-	-	7	1x7 MOS	-	-
7b	21	3x7 IFU	21	3x7 MOS	-	-
6b	21	2x7 IFU + 1x7 sky	21	3x7 MOS	-	-
5b	21	2x7 IFU + 1x7 sky	21	3x7 MOS	7	1x7 IFU
4b	28	4x7 IFU	28	4x7 MOS	28	4x7 IFU
3b	28	4x7 IFU	28	4x7 MOS	28	4x7 IFU
2b	35	4x7 IFU + 1x7 sky	35	5x7 MOS	35	5x7 IFU
1b	42	6x7 IFU	42	6x7 MOS	42	6x7 IFU
0	231	31x7 IFU + 2x7 sky	231	33x7 MOS	231	33x7 IFU
1a	42	6x7 IFU	42	6x7 MOS	42	6x7 IFU
2a	35	4x7 IFU + 1x7 sky	35	5x7 MOS	35	5x7 IFU
3a	28	4x7 IFU	28	4x7 MOS	28	4x7 IFU
4a	28	4x7 IFU	28	4x7 MOS	28	4x7 IFU
5a	21	2x7 IFU + 1x7 sky	21	3x7 MOS	7	1x7 IFU
6a	21	2x7 IFU + 1x7 sky	21	3x7 MOS	-	-
7a	21	3x7 IFU	21	3x7 MOS	-	-
8a	-	-	14	2x7 MOS	-	-

Table 4: *Summary of the arrangement of the fibers in the pseudo-slits. We include the list of boxes defined (column 1), the level of occupancy (columns 2, 4, 6) of the different boxes of all three MEGARA pseudo-slits (namely, LCB, MOS, SCB) and of the number of sub-units of 7 fibers in each box (columns 3, 5, 7). In the case of the LCB we also identify the boxes hosting 7-fiber sky bundles. The location of these sky bundles can be seen in the corresponding manufacturing drawing. Boxes 1b through 8b are located in the bottom part of the corresponding pseudo-slit while those with labels 1a through 8a are at the top.*

The MOS positioners that make use of the most extreme positions in the pseudo-slit are those with identification numbers 1, 91, and 92, which are located either at the corners of the FOV or in the interface region of the Focal Plane Cover. In the case of the MOS, the 7 fibers from each minibundle will be placed together on the pseudoslit (not interlaced, in order to minimize inter-

positioner cross-talk when the Focal Plane cover is in its default -open- position) but adjacent positioners will be located in different halfs of the field, for null-cross-talk observations.

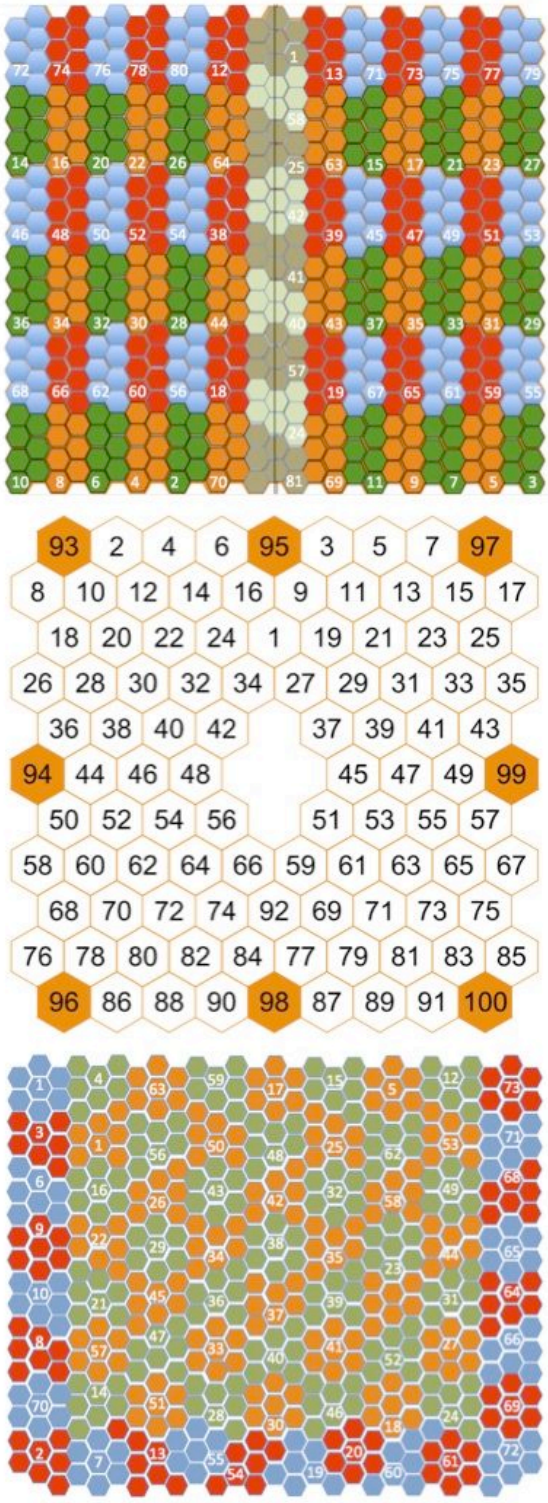

Figure 27: *Distribution in the focal plane of all 7-spaxel (7-fiber) sub-units for the LCB (top) and MOS (center) and SCB (bottom). In the case of the MOS, sky bundles are shown in orange.*

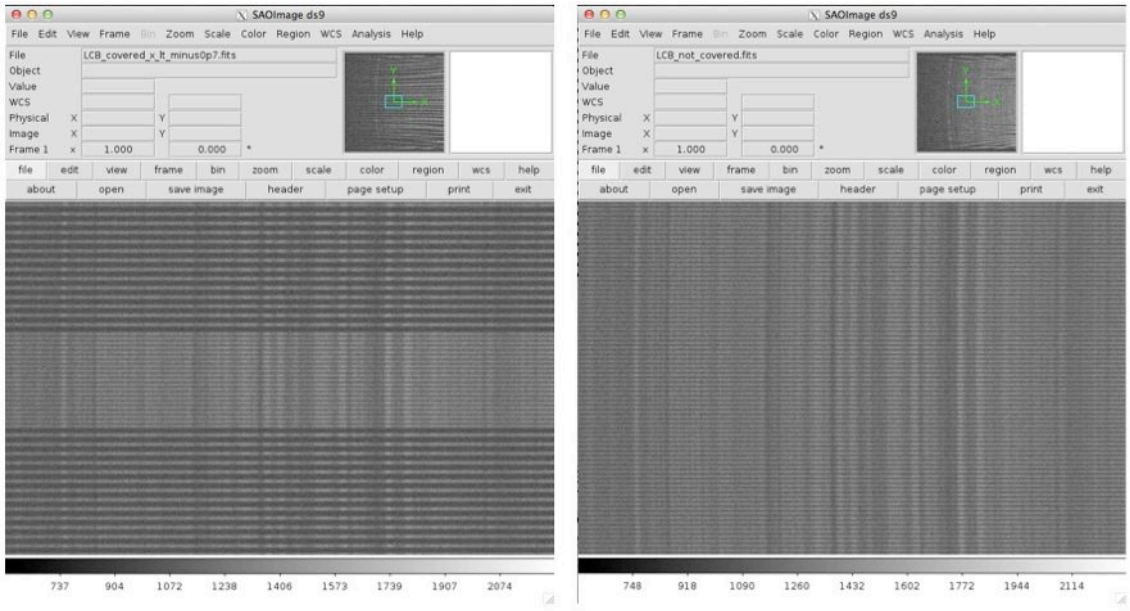

Figure 28: *Simulated MEGARA CCD frames with the fibers placed in their final positions of the pseudo-slit. Left: Simulated CCD frame when the left side of the focal plane is covered (using the Focal Plane Cover). Right: The Focal Plane Cover is placed in its default position (open). Note: Only central the part of the frame is shown in each case (see full frame at the top right corner of each panel). The dispersion direction is aligned with the rows while the spatial one (i.e. the pseudo-slit) is along the columns.*

5.1.9.3 SCB fiber positioning

Finally, with respect to the positioning of the fibers of the SCB we do not consider the case of using the Focal Plane Cover since, due to the improved image quality of the SCB and larger distance bewteen adjacent fiber cores on the pseudo-slit relative to the fiber core size, the expected level of cross-talk is already rather low. The application of the other criteria defined above made us place the 7-spaxel sub-units near the center of the FOV in the central parts of the SCB pseudo-slit. Note, however, that the SCB makes use only of the central 88.7 mm of the pseudo-slit, which further ensures an optimal image quality when using this mode.

In the case the SCB, the focal plane has been divided in sub-units following a non-regular pattern in order to ensure that the spaxels from the same sub-unit are contiguous on the FOV (see Figure 27). This criterion simplifies the transition between individual fibers and 7-fiber sub-units at the back of the microlens array.

5.2 Spectrograph

MEGARA Spectrograph has a fully refractive optical system. The spectrograph is composed by a pseudo-slit, where fibers are placed simulating a long slit 119mm length and with a ROC of 1075mm. The pseudo-slits will be moved using x-y mechanism that will allow exchanging the pseudo-slit in use between that of LCB, SCB or MOS modes, and also will be used as a focusing mechanism that will be configured in the z-axis for each of these modes and VPH.

Following the light path we find then the collimator, which is composed by 5 lenses (1 singlet and two doublets). The first lens of the collimator is the only aspherical surface of the instrument, which also one of the smallest lenses in the system (140mm diameter; blank diameter 160mm). A slit shutter is placed right beyond the first collimator lens. The shutter has three positions: open, closed and the position where the order sorting filter is placed in the optical path. This latter position will be selected to reject the blue end of the spectrum during the observation with the reddest disperser elements. The pupil has 160mm free diameter and it is the location for the VPH-gratings. Once the beam passes through the grating it goes to the camera (composed by two doublets and 3 singlets, being the last lens also the cryostat window) that focuses the light onto the detector.

In the following subsections we briefly describe the design of the spectrograph optical components, the spectrograph mechanics, the cryostat and the Data Acquisition System (DAS), and provide either detailed design (in the case of the MEGARA Optics) or preliminary design (for the rest of these subsystems) reference documents where these are described in more detail.

5.2.1 Optical design

This section summarizes the main properties of the different spectrograph subsystems with optical functionality, which includes the pseudo-slit, the collimator, the pupil elements and the camera.

The pseudo-slit is composed by a long slit 119mm length and with a ROC of 1075mm, where the 100μm-core fibers (that could be coming from the LCB or the MOS) shall be mounted buffer side by side achieving a 170 μm pitch. In the case of the 70μm-fiber-based SCB we received the confirmation that these fibers can be manufactured with a 170μm external coating. This fact will allows to mount also the 70μm-core fibers side by side on the SCB pseudo-slit.

A singlet and two doublets compose the collimator as shown in Figure 29. The Collimator is f/3 and the focal length is 484.4 mm.

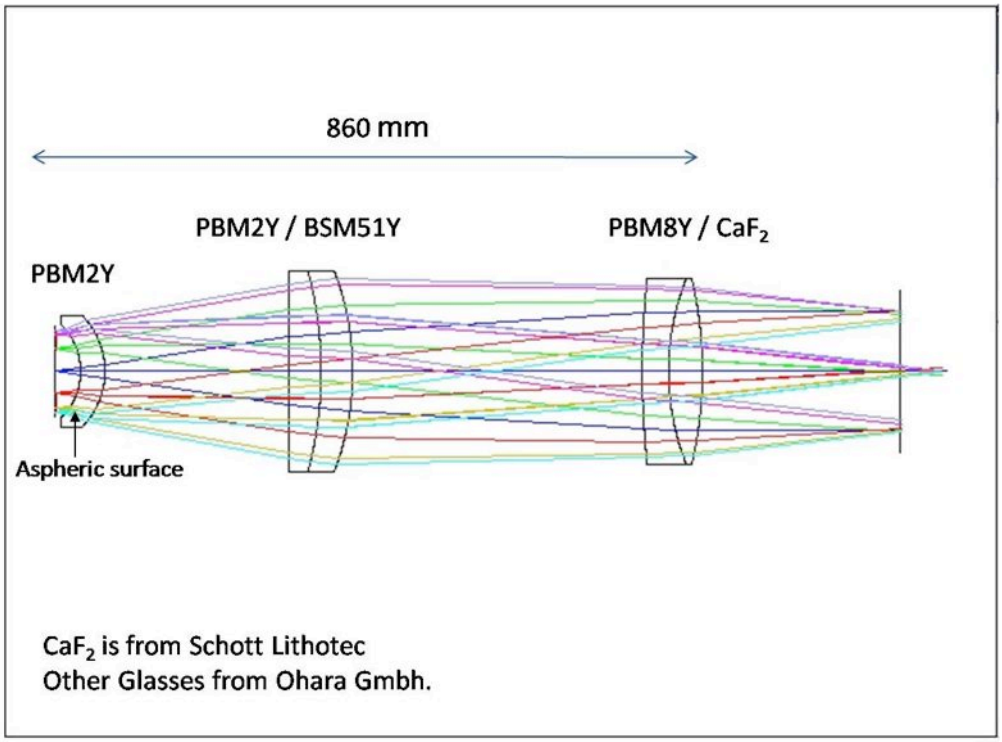

Figure 29: *Collimator layout. The collimator is composed by one PBM2Y singlet (aspherical) and two doublets. The first doublet will be mounted on a linear stage, acting as focusing mechanism to optimize image quality in each grating configuration.*

Specifications of the collimator optical elements are summarized in Table 4.

Collimator Optical Elements (an asterisk, *, indicates that the lens is cemented in a doublet)					
Element	Material	R_1 (mm)	R_2 (mm)	Central Thickness (mm)	Blank ∅ (mm)
COLL-S1	PBM2Y	-91.0 (x)	-113.3	35.0	160.0
COLL-D2*	PBM2Y	flat	-728.1	35.0	277.0
COLL-D3*	BSM51Y	-728.1	-398.8	35.0	277.0
COLL-D4*	PBM8Y	1259.9	344.5	25.0	265.0
COLL-D5*	CaF2	344.5	-542.5	45.0	255.0

Table 5: *Collimator lenses parameters. COLL-D2/D3 and COLL D4/D5 are cemented in doublets. A value of 30μm of RTV141 has been included in the design for the doublets. (x) High-order aspheric.*

The only aspheric that we are using in the optical design is the COLL-S1 element. This is a high order aspheric, which characteristics are shown in Figure 30.

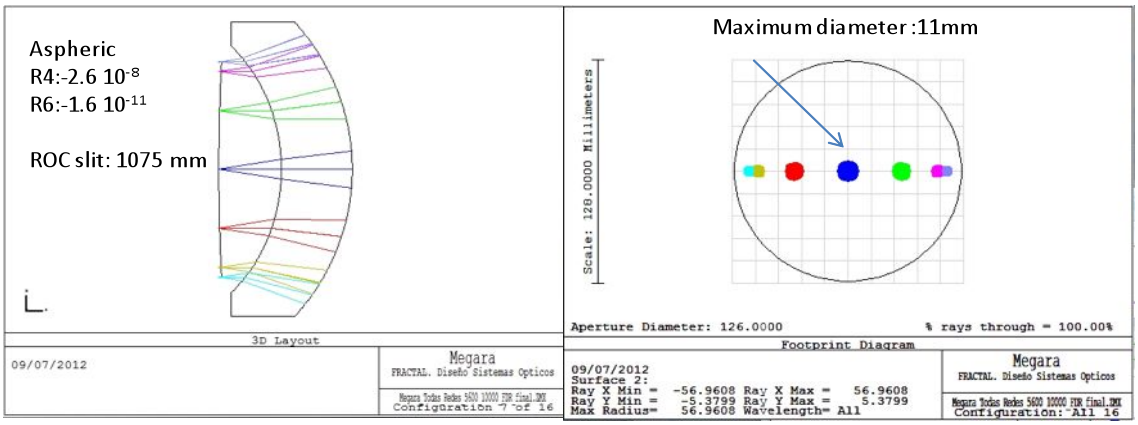

Figure 30: *Collimator S1 element. This is a high order aspheric. Optical parameters are shown on the left. The footprint diagram is on the right.*

The pupil size is 160 mm. Different types of pupil elements (all of them based on VPH-type gratings) can be accommodated in the pupil position. The spectral resolutions of MEGARA in terms of R_{EED80} ($\lambda/\Delta\lambda_{EED80}$) are 5,500, 10,000 and 17,000 (respectively for LR, MR and HR VPHs) in the case of the LCB and MOS. When expressed in terms of the FWHM of unresolved lines in the extracted (1D) spectra the spectral resolution becomes R_{FWHM}~6,000 (low resolution; LR), R_{FWHM}~12,000 (mid-resolution; MR) and R_{FWHM}~18,700 (high resolution; HR). With regard to the SCB the spectral resolutions reached are R_{FWHM}~7,000, 13,500 and 21,500 respectively for LR, MR and HR VPHs. With regard to the wavelength coverage MEGARA offers full optical coverage with the LR VPHs (R_{FWHM}~6,000) with the MR+HR VPHs (R_{FWHM}~12,000) combined. See below for a description of how this full-optical coverage will be achieved in each case.

The ranges for which the high-resolution VPHs are designed and included in the budget are those defined by the Science Team (centered at Hα 6563Å and the CaT lines at 8500-8700ÅÅ). Note that the MEGARA Detailed Design also includes a MR VPH centered in the Hα region.

The scientific performance of the complete MEGARA gratings is given in Table 6.

VPH Name	Setup	R_{FWHM}	λ_1-λ_2 Å	λc Å	$\Delta\lambda$ (@ λc) Å	Δv km/s	lin res Å/pix
VPH405-LR	LR-U	6028	3653 – 4386	4051	0.672	50	0.17
VPH480-LR	LR-B	6059	4332 – 5196	4800	0.792	49	0.20
VPH570-LR	LR-V	6080	5143 – 6164	5695	0.937	49	0.23
VPH675-LR	LR-R	6099	6094 – 7300	6747	1.106	49	0.28
VPH799-LR	LR-I	6110	7220 – 8646	7991	1.308	49	0.33
VPH890-LR	LR-Z	6117	8043 - 9630	8900	1.455	49	0.36
VPH410-MR	MR-U	12602	3917 - 4277	4104	0.326	24	0.08
VPH443-MR	MR-UB	12370	4225 – 4621	4431	0.358	24	0.09
VPH481-MR	MR-B	12178	4586 – 5024	4814	0.395	25	0.10
VPH521-MR	MR-G	12035	4963 – 5443	5213	0.433	25	0.11
VPH567-MR	MR-V	11916	5393 – 5919	5667	0.476	25	0.11
VPH617-MR	MR-VR	11825	5869 – 6447	6170	0.522	25	0.13
VPH656-MR	MR-R	11768	6241 – 6859	6563	0.558	25	0.14
VPH712-MR	MR-RI	11707	6764 – 7437	7115	0.608	26	0.15
VPH777-MR	MR-I	11654	7382 – 8120	7767	0.666	26	0.17
VPH926-MR	MR-Z	11638	8800 - 9686	9262	0.796	26	0.20
VPH665-HR	HR-R	18700	6445 - 6837	6646	0.355	16	0.09
VPH863-HR	HR-I	18701	8372 - 8882	8634	0.462	16	0.12

Table 6: *MEGARA Baseline gratings: scientific requirements (The resolution, $R_{FWHM}=\lambda/\Delta\lambda_{FWHM}$, is derived from the FWHM ($\Delta\lambda_{FWHM}$) of the 1D spectra and the case of the LCB IFU and MOS modes).*

Table 7 includes the grating physical parameters.

The current calculations have been done to obtain the exact scientific specification in the case of the LR and HR VPHs. For the MR we have selected a common average apex angle (44º) for the

prisms so the spectral resolutions would be only approximately those specified in the scientific requirements for these VPHs. Note that the difference are very small, so the MEGARA Science Team agreed to fix the apex angle for all MR VPHs for the sake of simplicity and to reduce costs and minimize risks during the manufacture.

VPH Name	R_{EED80}	λ Bragg Å	θ Bragg degrees	Record lines/mm	Prism Apex degrees	Optical Aperture mm x mm
VPH405-LR	5480	4051	26.12	2761	Flat	170 x 210
VPH480-LR	5508	4800	26.12	2330	Flat	170 x 210
VPH570-LR	5528	5695	26.12	1964	Flat	170 x 210
VPH675-LR	5545	6747	26.12	1658	Flat	170 x 210
VPH865-LR	5555	7991	26.12	1400	Flat	170 x 210
VPH890-LR	5561	8900	26.12	1257	Flat	170 x 210
VPH410-MR	11456	4104	52.98	4942	44.00	180 x 220
VPH443-MR	11245	4431	52.55	4551	44.00	180 x 220
VPH481-MR	11070	4814	52.16	4167	44.00	180 x 220
VPH521-MR	10941	5213	51.86	3832	44.00	180 x 220
VPH567-MR	10833	5667	51.60	3513	44.00	180 x 220
VPH617-MR	10750	6170	51.39	3217	44.00	180 x 220
VPH656-MR	10698	6563	51.24	3018	44.00	180 x 220
VPH712-MR	10643	7115	51.09	2778	44.00	180 x 220
VPH777-MR	10595	7767	50.95	2540	44.00	180 x 220
VPH926-MR	10580	9262	50.73	2123	44.00	180 x 220
VPH665-HR	17000	6646	70,12	3592	67.86	180 x 210
VPH863-HR	17001	8634	69,73	2761	68.61	180 x 210

Table 7: *MEGARA Baseline gratings: VPH specifications.*

The numbers of the two tables above were calculated with the camera focal length of 245,9mm. The requirement of having both "high" (R_{EED80}~17,000) and "low" (R~5,500) spectral resolutions implies very different values for the optimal angle of incidence on the VPHs. These angles need to vary between 26° and 70° for resolutions between 5,500 and 17,000, respectively

(these angles are the ones incident on the hologram). The need of a specific angle for a specific grating (or viceversa) come from the use of VPHs and the need to use the device in the Bragg angle to optimize performance.

The angle between the collimator and camera is fixed to 68°. This is equivalent to 34º between the collimated beam and the normal to the grating[5]. This angle allows reaching resolving powers of R_{FWHM}=12,000 and 18,700 with the use of prisms on both sides of the VPHs and R_{FWHM}~6,000 using flat windows, for 100μm-core fibers in all cases. In the case of the SCB IFU (70μm-core fibers) the spectrum-extracted resolving powers are R_{FWHM}=13,500 (MR), 21,500 (HR) and 7,000 (LR), respectively.

In the figures below we show the distribution of the VPHs in the resolving power versus wavelength coverage plane for all MEGARA VPHs in the case of the 100μm-core fibers (LCB IFU and MOS modes; Figure 31) and the 70μm-core fibers (SCB IFU mode; Figure 32).

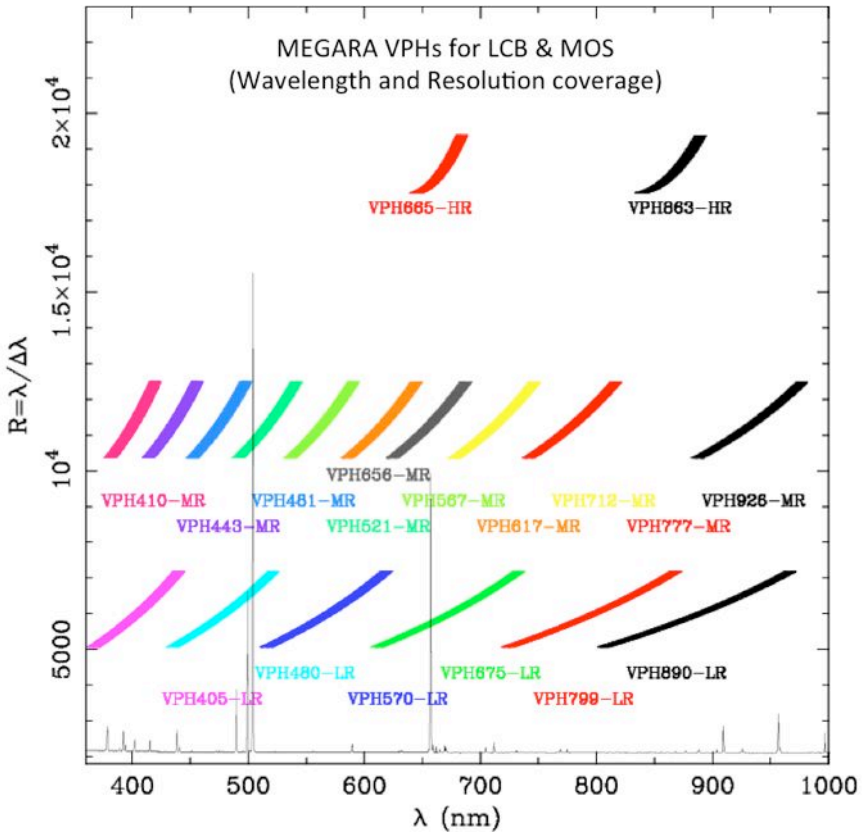

Figure 31: *Coverage of the MEGARA VPHs in resolving power (R_{FWHM}) and wavelength for the LCB IFU and MOS modes (100μm-core fibers). Note that due to the use of VPHs the spectral resolution changes across the detector, which spans an angle of ±7.2º from the pupil, although always within ±20% variation requirement stated in the instrument requirements document (see R.31).*

[5] *An angle of 34º between the collimated beam and the normal to the grating corresponds to a Bragg angle of 26º on the grating for an average refraction index for the VPH-window material of n=1.47 (Fused Silica).*

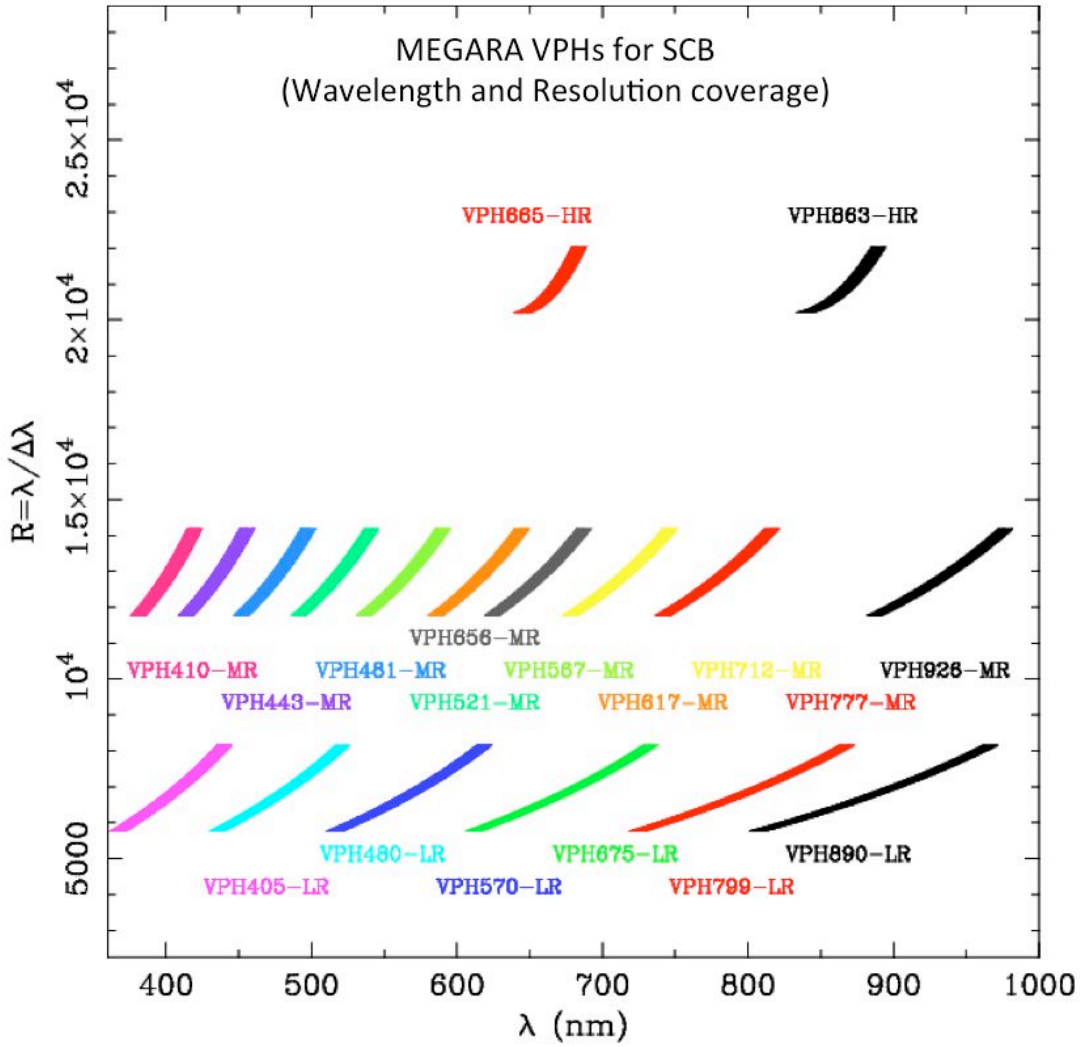

Figure 32: *Coverage of the MEGARA VPHs in resolving power (R_{FWHM}) and wavelength for the SCB IFU mode (100μm-core fibers). Note that due to the use of VPHs the spectral resolution changes across the detector, which spans an angle of ±7.2° from the pupil, although always within ±20% variation requirement stated in the instrument requirements document (see R.31).*

Figure 33 shows the different MEGARA modes (low, medium and high) with the AOI fixed to α = 34º and different pupil elements.

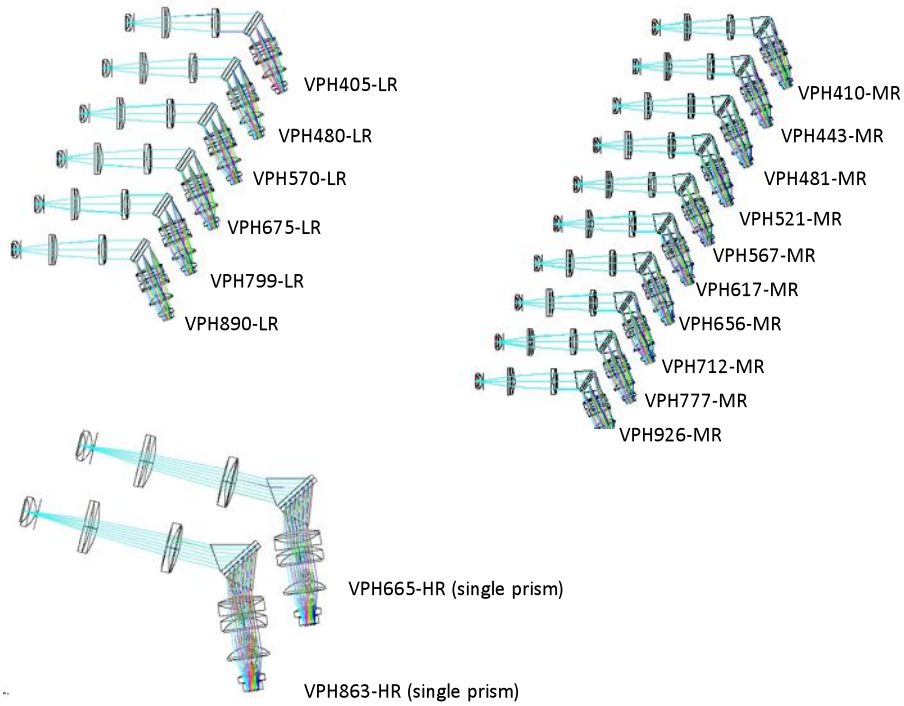

Figure 33: *MEGARA spectrograph: The angle between collimator and camera is fixed to 68°. The low-resolution mode (R_{EED80}=5,500) uses at pupil a VPH grating sandwiched between two flat windows. The different angles on the hologram needed for the different spectral resolutions are obtained by sandwiching the holograms between two prisms (at R_{EED80}=10,000) and by segmenting the pupil in two slices with two prisms placed at each side of the hologram (in the case of R_{EED80}=17,000). Both in the caes of the MR and HR VPHs Fused-Silica flat windows are placed in between the holograms and the prisms.*

In order to cover the entire optical range, different VPHs are needed. With the aim of providing an increased versatility and to reduce the impact on the observatory activities a total of 11 VPHs could be mounted simultaneously in MEGARA.

Here we propose the use of two different configurations for the MEGARA VPH wheel: LR+HR and MR+HR. In the case of the MEGARA LR+HR configuration a total of 6 low-resolution (LR) VPHs allow to cover the entire optical range from 3700 Å to 9500 Å at R_{FWHM}=6,000, 3 mid-resolution (MR) VPHs at R_{FWHM}=12,000 would cover between 25-60% of the entire optical region (depending on the MR VPHs actually mounted on the wheel), and 2 high-resolution (HR) gratings around the Hα and CaT ranges at R_{FWHM}=18,700 (these HR spectral ranges are defined by the MEGARA Science Team and justified as part of the science cases). In the MR+HR configuration all MR and HR VPHs would be mounted simultaneously covering the entire optical spectrum (a ~6000Å-wide range) at resolutions in the range R_{FWHM}=12,000-18,700 for the LCB IFU and MOS modes. This range would be R_{FWHM}=13,500-21,500 when the SCB IFU is used (more details on the computation of the resolving power are given in R.19). The possibility of having mixed configurations that could adapt better to the overall long-term usage of MEGARA by the GTC community are also possible.

In the case of the highest resolution mode, the incident angles are so high that the use of single monolithic prisms implies very large prisms a small amount of vignetting of ~10-19%, depending on wavelength (see Figure 34 and Figure 35). In order to ensure the manufacturability (and availability of blanks) of the prisms these might have to be further reduced and, consequently, the vignetting increased. More details are provided in R.6.

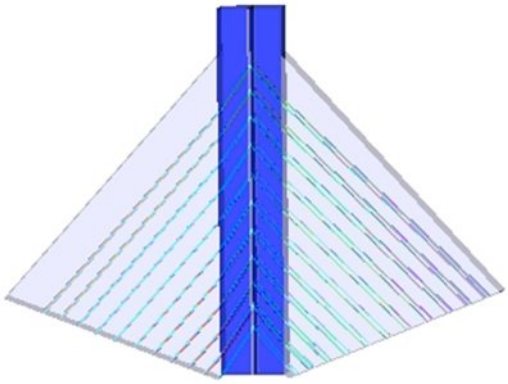

Figure 34: *Prisms for R = 17,000. VPH grating will be sandwiched between two flat windows and then a large prism will be coupled at each side, as in the case of R=10,000. The very large size (250 x 250 x 200) and density of material ρ = 3.61gr/cm3 implies 18725 gr per prism and a total of 41Kg of glass for the complete unit (in addition to the opto-mechanical mount).*

At the Preliminary Design Review we presented a grating design based on the sliced-pupil concept (see R.32). The drawback of this design is that some extra vignetting appears at pupil. Since GRANTECAN has discarded the sliced-pupil design as a valid alternative for the instrument we consider the single-slice VPH gratings as the baseline design for the Optics CDR.

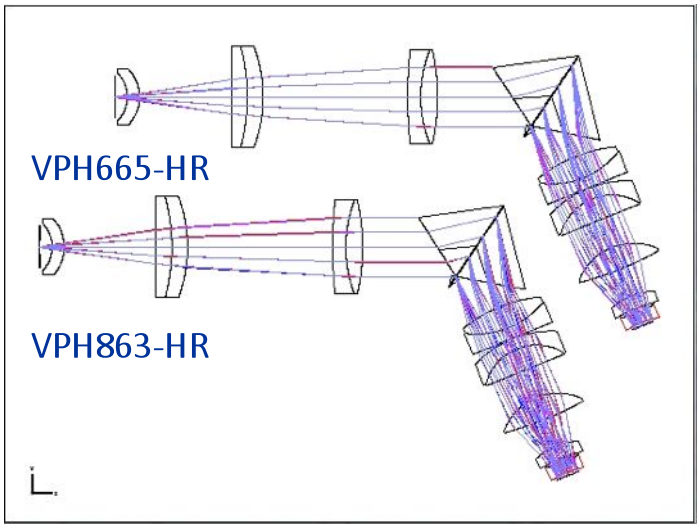

Figure 35: *Design of the R_{EED80}=17,000 (LCB IFU and MOS modes) gratings centered at 6650 Å and 8630 Å using single-slice prisms covering almost the entire pupil.*

The Camera is an f/1.5 and the focal length is 245.9 mm. Two doublets and 3 singlets compose the camera as seen in Figure 36. Image field is 61.4mm x 61.4mm covering 4k x 4k pixels.

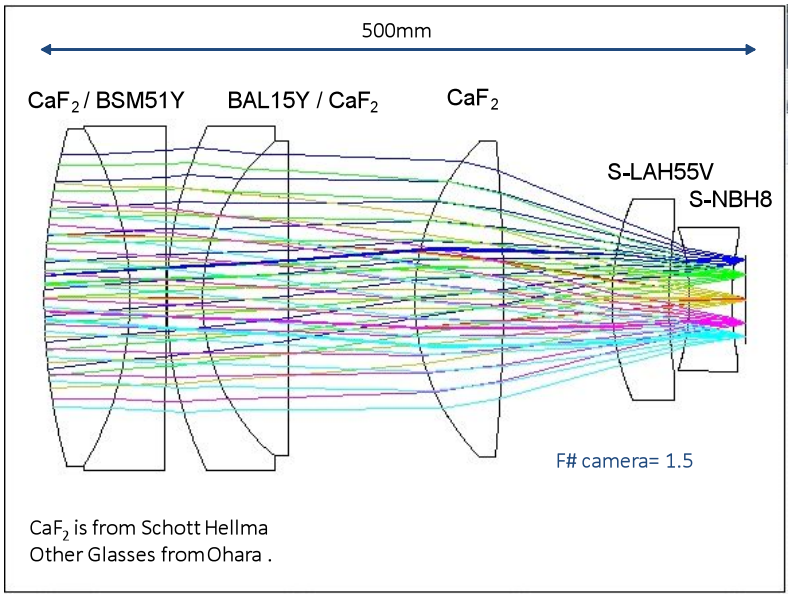

Figure 36: *Camera layout. The camera is composed by two doublets, each of them with one CaF_2 lens and materials as labeled in the figure and three singlets of CaF_2, S-LAH55V and S-NBH8. The last lens is also the cryostat window.*

The characteristics of the camera lenses are summarized in Table 8.

Camera Optical Elements (an asterisk, *, indicates that the lens is cemented in a doublet)					
Element	Material	R1 (mm)	R2 (mm)	Central Thickness (mm)	Blank ∅ Estimation (mm)
CAM D-1*	CaF_2	435.9	-231.7	60.0	210.0
CAM D-2*	BSM51Y	-231.7	Flat	25.0	245.0
CAM D-3*	BAL15Y	269.2	145.1	25.0	245.0
CAM D-4*	CaF_2	145.1	Flat	60.0	225.0
CAM S-5	CaF_2	156	-1143	62.0	225.0
CAM S-6	S-LAH55V	176.4	365.8	40.0	145.0
CAM S-7	S-NBH8	-162.5	219.5	30.0	115.0

Table 8: *Camera lenses parameters. CAM-D1/D2 and CAM-D3/D4 are cemented in doublets. (*) The asterisk indicates that the lens is cemented in a doublet.*

The total expected transmission of the optical system (excluding the pupil elements) is shown in Figure 37.

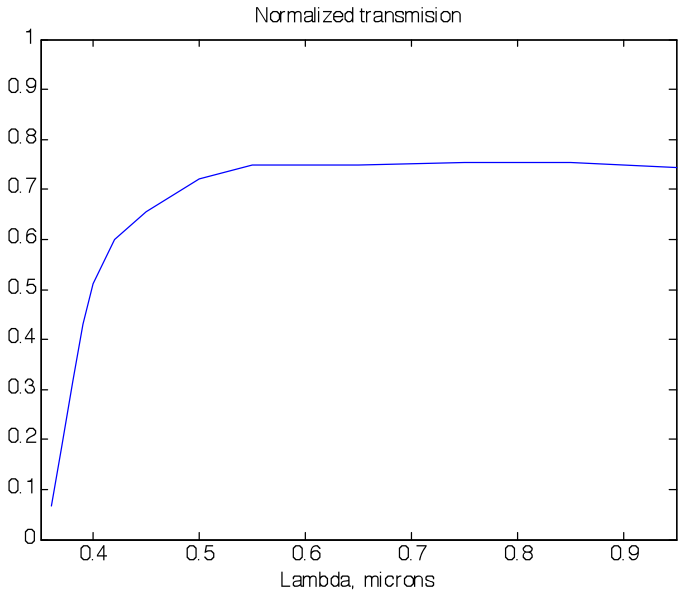

Figure 37: *Predicted transmission of MEGARA Optics (Collimator and Camera)*

Lambda (Å)	Transmission
3600	0.0669
3700	0.1842
3800	0.3168
3900	0.4297
4000	0.5126
4200	0.5994
4500	0.6563
5000	0.7212
5500	0.7489
6500	0.7492
7500	0.7550
8500	0.7545
9500	0.7448

Table 9: *Expected transmission of MEGARA Optics (collimator+camera). First column has the wavelength (in Å) and the second column gives the transmission normalized to unity.*

The detailed description of the spectrograph optical design and its optical evaluation can be found in R.6. In the following lines, we briefly summarize the main characteristics of this design:

1. By fixing the angle between collimator and camera and using the prisms' apex angle that yield the optimal angle of incidence (Bragg angle) for each VPH we optimize efficiency as the change in the angle of incidence (and therefore efficiency) is limited to the range in angles covered by the detector (±7.2°). Figure 38 below shows the change in efficiency for each polarization for VPHs of different spectral resolution, one for R_{EED80}=5,500 on the left and one yielding R_{EED80}=17,000 on the right (LCB IFU and MOS modes).

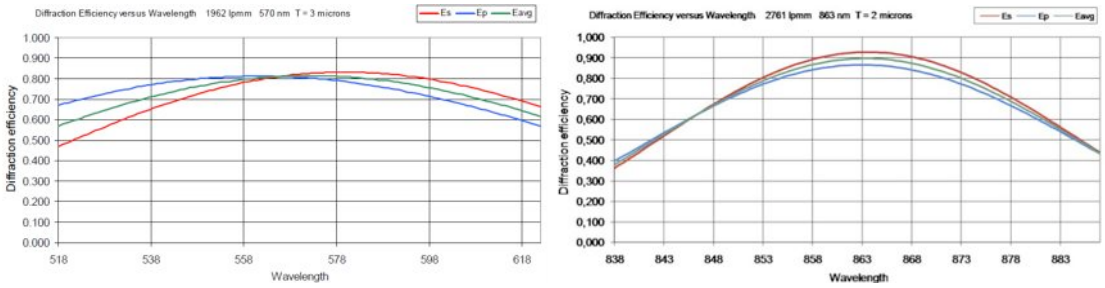

Figure 38: *Efficiency curves as a function of wavelength for VPH570-LR (R_{EED80}=5,500; left) and VPH863-HR (R_{EED80} =17,000; right).*

These figures show that the efficiency never goes below 40% for these two particular cases. In the case of other VPHs, where the dependence of the efficiency with the angle of incidence could be stronger, the efficiency can reach very low values at the edges of the detector (in the wavelength direction). In this case a reduction in the gelatin thickness might be used to partly minimize this effect to the expense of a decrease in the peak efficiency. Figure 33 below shows the new HD-technology efficiency curves for mid-resolution VPH567-MR and VPH926-MR.

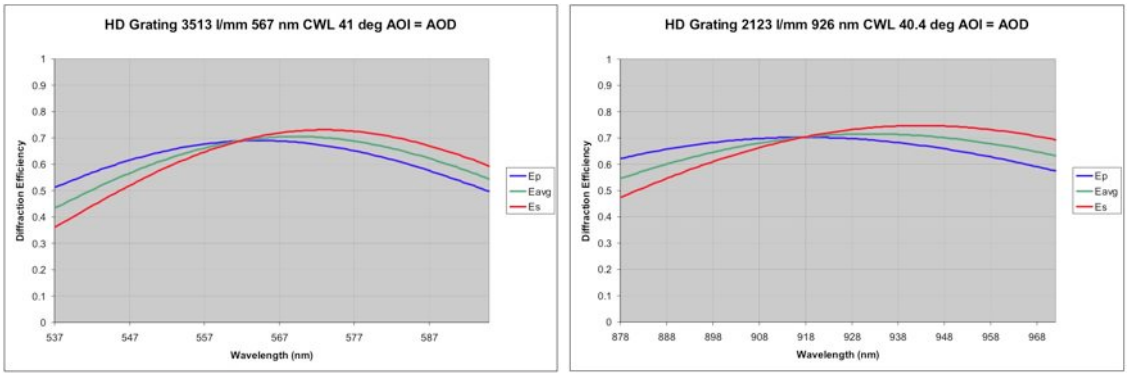

Figure 39: *Efficiency curves for the VPH567-MR (left) and VPH926-MR (right) VPHs.*

In the plots above we show that the HD manufacturing technology patented by Wasatch Photonics allow recovering rather flat and high efficiency curves where the standard Kolgenik method led to very low efficiencies in one of the polarizations (see TEC/MEG/071).

2. The use of different VPHs optimized for each spectral range allows having approximately the same spectral resolution at different wavelengths (within 20% variation), fulfilling the requirements imposed by the MEGARA Science Team.

3. The design provides a small number of different spectral setups (as many as VPHs are used; 11 mounted simultaneously mounted the wheel, 18 designed), which makes the calibration of the instrument a relatively easy task. Calibration exposures should be taken only once per grating.

4. The fact that both collimator and camera are fixed (and located in a table on a platform) makes this instrument extremely stable and its different spectral configurations easily repeatable (since the mechanisms provide the required precision in the pupil). The higher the spectral resolution, the more stability is required.

5. The use of a single angle makes that the pupil is not vignetted in any configuration, so that the size of the VPHs and the needed prisms are fitted as much as possible to the pupil size.

6. Since the camera is fixed, this design allows having the camera and cryostat separated. This is not the baseline at this stage, where the last lens of the camera also acts as window for the cryostat.

7. Figure 40 shows the predicted image quality performance over the evaluated pseudo-slit (110 mm). The blue line (at 24.6µm) establishes the limit for a 100µm fiber core. As it is shown in the figure, the current design leaves enough room for image quality degradation (even in the case of the 70µm fiber core), assuming standard tolerances (see R.6).

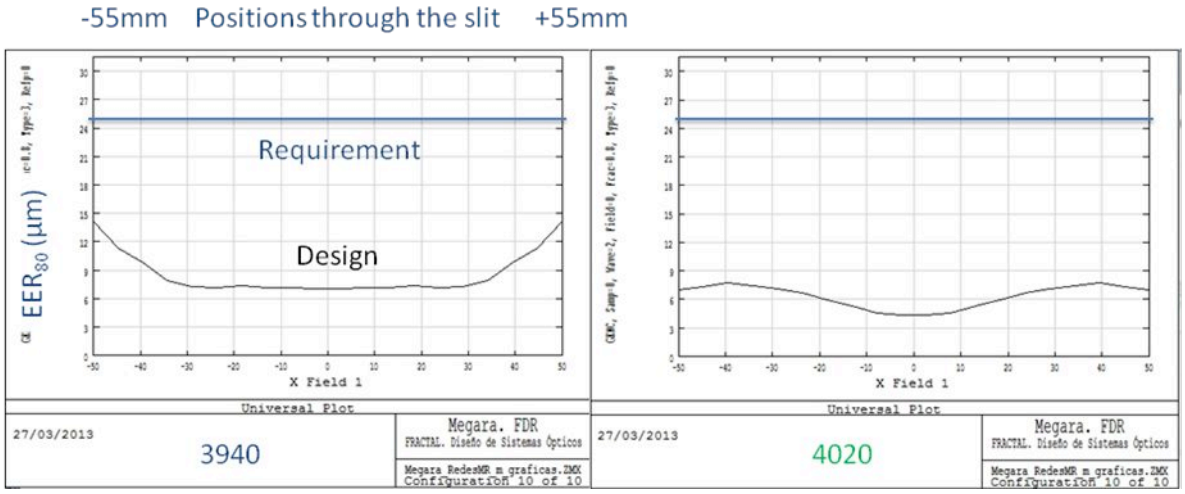

Figure 40: *MEGARA spectrograph performance for VPH410-MR (R_{EED80}=10,000) evaluated at two wavelengths. The plot shows the predicted image quality performance (black line) over the evaluated pseudo-slit (between -55mm and +55mm). The blue line is the target performance (for the projection of a 100µm-core fiber on four 15µm pixels, case of LCB IFU and MOS modes).*

8. This design requires of a large number of VPHs to cover a wide range in wavelengths. Based on the scientific requirements of the MEGARA Science Team a total of 18 VPHs (11 of them mounted simultaneously) would be needed to cover the whole spectrum at R_{EED80}= 5,500 and at R_{EED80}=10,000 when the two windows at R_{EED80}=17,000 are added (resolutions in the LCB and MOS modes). As described above, these VPHs would have an optimum throughput at the working resolutions, preserving the collective power of the GTC.

5.2.2 Mechanical design

The 3D model of the current mechanical design of the MEGARA spectrograph is given in Figure 41.

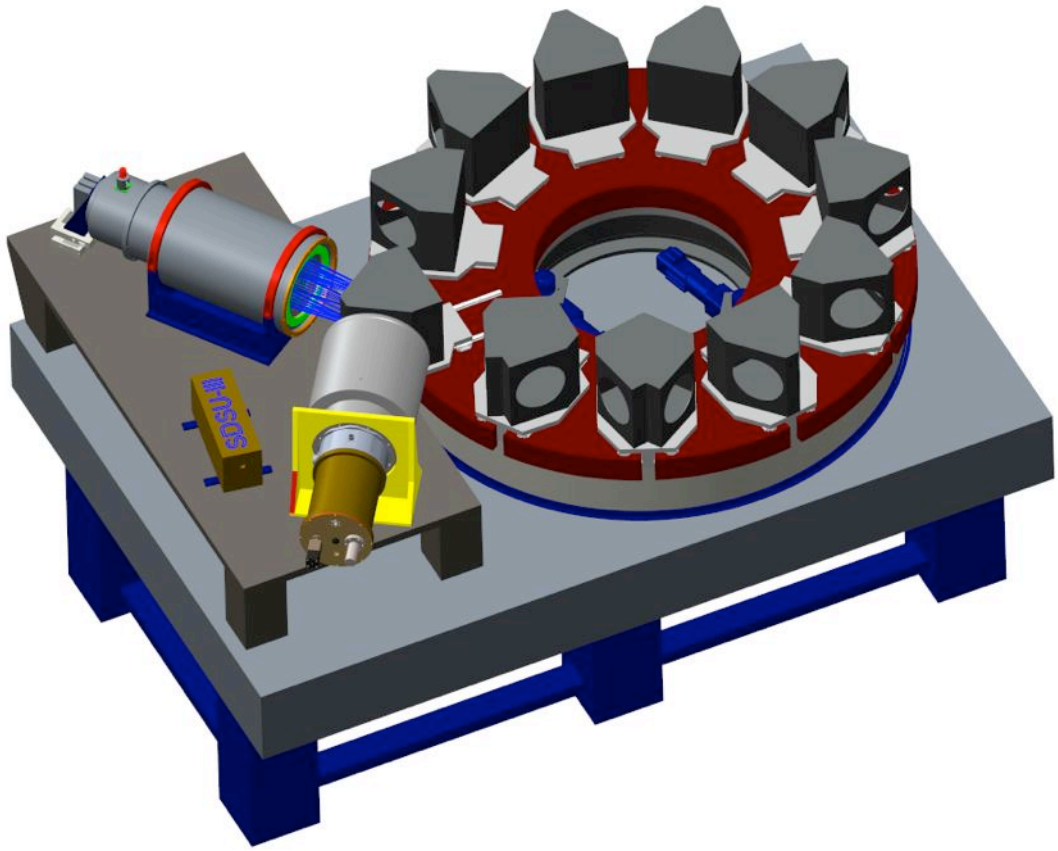

Figure 41: *MEGARA Spectrograph Mechanics: 3D view. Here we show the MEGARA spectrograph in one of the two configurations proposed (MR+HR).*

The main changes in the MEGARA mechanical advanced design compared to that presented at the time of the PDR is the fact that now both Collimator and Camera are integrated in individual barrels (as a consequence of the focus mechanism been moved to the pseudo-slit) and that the wheel is mechanism is driven by two preloaded opposing servo-actuators with pinions (as suggested by GRANTECAN personnel at PDR). Note that the corresponding mechanical Detailed Design will be presented at the time Critical Design Review of the entire instrument.

The focusing mechanism moves the pseudo slit unit mechanism to set the best focus for the specific VPH in use. This is mounted perpendicular to another mechanism that allows selecting the corresponding pseudo-slit (LCB, MOS, or SCB). Both mechanisms provide a minimum incremental motion of 0.1 μm with an absolute precision of 0.5 μm. These numbers satisfy both our pseudo-slit positioning and focusing requirements.

The grating selection mechanism is constituted by the VPH wheel (1880 mm external diameter) and an insertion mechanism. The use of preloaded opposing servo-actuators with pinions makes unnecessary the use of the cone lock, which was presented at the PDR but has been removed for this advanced design.

The mechanical mount of each VPH is screwed to a platform. The platform has a pair of guideways screwed on its downside. These guideways are inserted on their corresponding carriages that are screwed to the wheel. Every VPH can be located in any platform in order to facilitate the operation of the instrument.

Figure 42 and Figure 43 show a 3D view of the wheel and the arrangement of the motor.

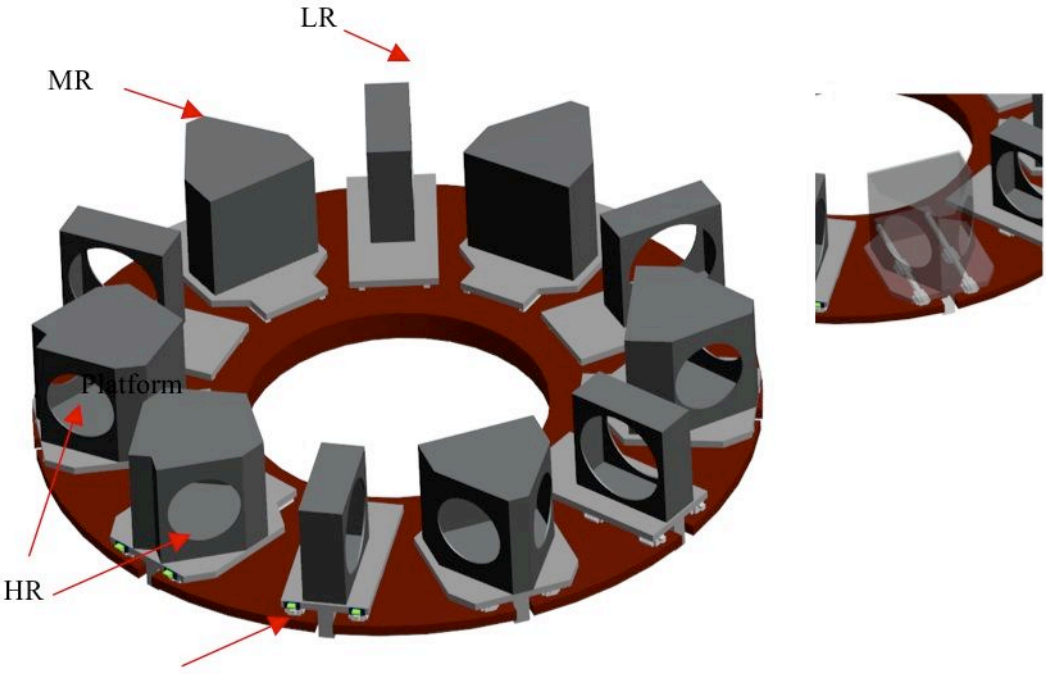

Figure 42: *Detail of the VPHs wheel in MEGARA spectrograph***.**

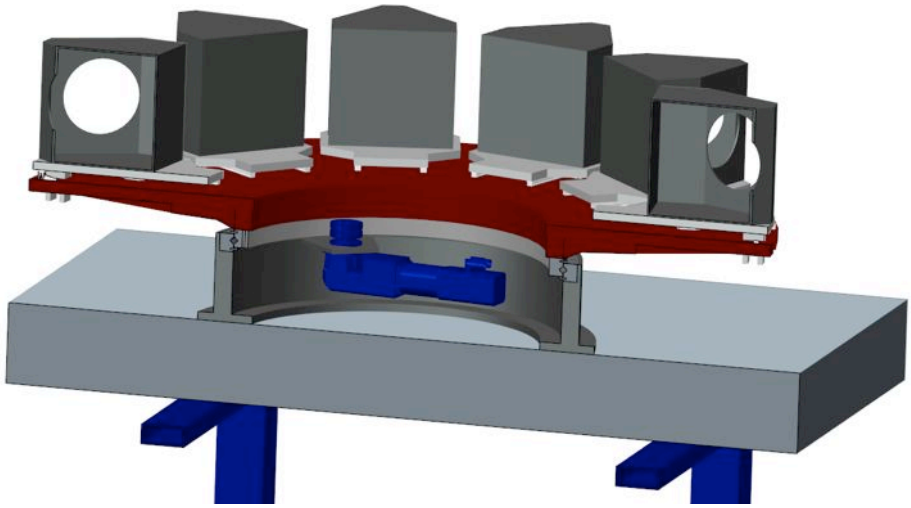

Figure 43: *Cross section of the motor assembly supporting the wheel.*

As shown in Figure 43 the wheel is now moved by a gear and two preloaded opposing servo-actuators with pinions, thereby eliminating backlash. The actuators are complete assemblies made up of a servomotor, a reducer and a brake. Both servomotors shall include an encoder on axis, one motor an absolute encoder and the other one relative encoder. The control electronics (digital) shall control the preload in real time. Finally, it should be noted that the bearings are supplied with the gear machined on their rings as an integral part of the bearings (not shown).

When the wheel is positioned at the VPH of interest, this is translated to the optical path and clamped against hard pads to position it for use. The insertion mechanism consists of a linear guide with an electro-mechanical actuator driven by a stepper motor and with a preloaded ballscrew. This motor shall be equipped with an absolute encoder. The precision of the commercial motors identified yield precisions better than 0.05mm, which allows a fine-tuning of the VPH position and eliminates the need for a hard-stop positioning. Figure 44 shows two different views of the insertion mechanism advanced design.

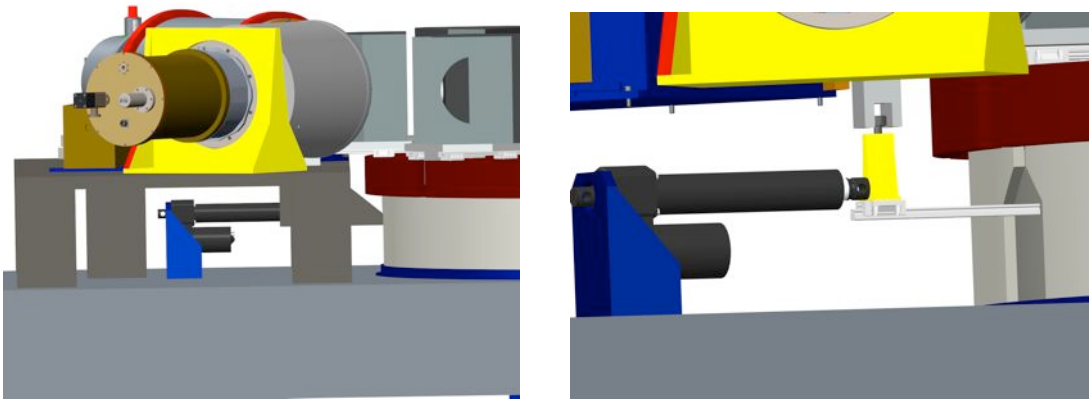

Figure 44: *Left: Lateral view of the MEGARA spectrograph showing the position of the insertion mechanism. Right: Detail of the actuator in direct contact with the bearing support.*

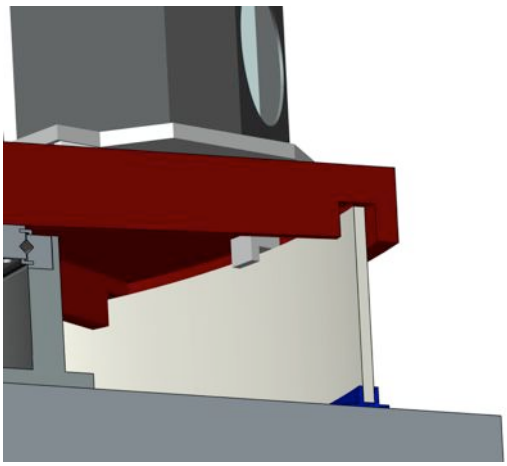

Figure 45: *Detail of the bottom part of the VPH wheel where the location of the DELRIN track is shown.*

Figure 45 above shows the DELRIN track that has been added to the wheel design in order to prevent the VPH platforms to move during the wheel rotation.

Figure 46: *MEGARA shutter mechanical advanced design. The different parts of the shutter assembly are shown at right.*

Finally, in Figure 46 we show the advanced design of the shutter, which is placed right after the first lens of the collimator (the aspheric) and mechanically attached to the collimator barrel.

A detailed description of the Mechanical Detailed Design will be presented at the time of the full-instrument Critical Design Review.

5.2.3 Cryostat

The selected cryogenic device to harbor the CCD detector for the MEGARA spectrograph is a liquid nitrogen open-cycle cryostat. The main characteristics are summarized in Table 10.

Specification	Value	Remark
Cryostat provider	INAOE, Mexico	
Type	Bath dewar	Filled with LN2 99.998%
Version	Open-cycle INAOE astronomical instrumentation lab.	77K Cold-plate. LN2 cryogenic reservoir. OFHC strap to cool-down CCD.
Shape	Cylindrical	CCD head cylindrical with flat faces for mountings and connectors
Largest diameter	255 mm	CCD head 255 mm
Largest length	270.8 mm	With CCD head (TBC): 345.8 mm
Material composition	- Highly polished aluminum on vacuum vessel - Aluminum radiation shield -Stainless steel LN2 tank - Stainless steel front head lid for vacuum window and optics	
Mass	21 kg	Without LN2
LN2 tank volume	6.96 liter	6 liters usable (~92% filled)
Operation position	Horizontal (by requirements; see MEGARA conceptual design)	
Estimated LN2 hold time	44 hours	90 mm diameter window and ~150K CCD operating temperature
Vacuum requirement	$\leq 4 \cdot 10^{-6}$ mbar	Atmospheric to high vacuum pressure sensor included with cryostat
Vacuum flanges	2 ¾ and 1 1/3 CFF	Uses commercial CFF flanges, fittings and valves.
Hermetic connector for CCD signals reading	Detoronics 61-pin	Flange mounting type with custom made wiring.
Hermetic connector for CCD thermometers and heater	Detoronics 10-pin	Flange mounting type with custom made wiring.
Hermetic connector for cryostat main body thermometer and heater	Detoronics 10-pin	Flange mounting type with custom made wiring.
Sorption pump	Active charcoal (TBC)	
Sorption pump re-activator	10.0 Ω heating resistor (TBC) PT-100 temperature sensor	Connected to hermetic connector
CCD Temperature control	Heater and PT-100 temperature sensor	Cabling to CCD head wall hermetic connector

Table 10: *Main characteristics of MEGARA open-cycle cryogenic system*

The LN2 open-cycle cryostat is a custom made product, which has been designed by the INAOE astronomical instrumentation group. The proposed cryostat offers modular stages for easy assembly and testing whilst also allowing future modifications to accommodate the required CCDs, electronics and optics. This system offers the cheapest option for MEGARA.

Cryostat mounting is horizontal and it is designed to be kept static, as well as all the MEGARA components. The complete cryostat assembly consists of two main parts: the dewar back and the CCD Head.

The dewar back (or main body) serves as vacuum jacket and contains the liquid nitrogen tank; it also has on the rear part the liquid nitrogen fill tube, an electrical port for temperature monitor and two vacuum ports. Aluminum has been selected as the primary material for the vacuum jackets described in this document; aluminum alloys offer a good structural choice, easy manufacturability (compared with stainless steel), reduce costs of fabrication and weight but it also offers a very low degassing rate compared to stainless steel for untreated materials and the hydrogen permeation rate is also lower than steel. LN2 tank will be made of stainless steel (TBC) (which has low thermal conductivity). The filling tube has a bellow system, which helps to reduce thermal loading on the cryogens. Cold plate will be made of gold plated OFHC copper to increase thermal conductivity.

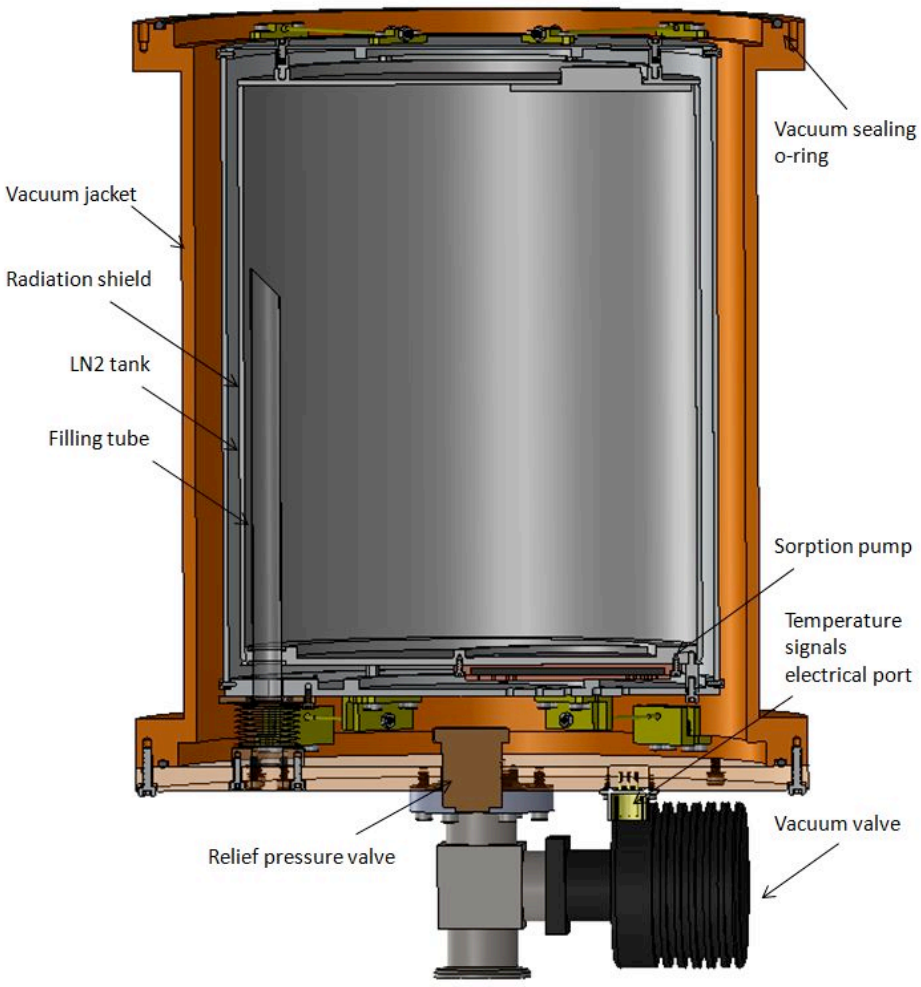

Figure 47: *Cryostat dewar back view.*

The CCD Head is assembled on top of the main body and will contain the CCD detector and its associated electronics; it will contain two electrical ports to read-out the signals from the CCD. CCD supports will be made of low thermal conductivity materials (G10, nylon or Teflon). The CCD detector will be thermally connected to the LN2 tank through a high purity free oxygen copper strap, which can be adjusted to give the desired operating temperature for the detector. A lid on the front part will contain the last lens of the MEGARA spectrograph, which will also serve as a vacuum window. The CCD head mechanical module is intended to be disassembled completely from the cryostat main body for easy handling and integration and verification of CCD components. The CCD and its mountings will be surrounded by an aluminum radiation shield that will help to improve the hold-time of the cryostat.

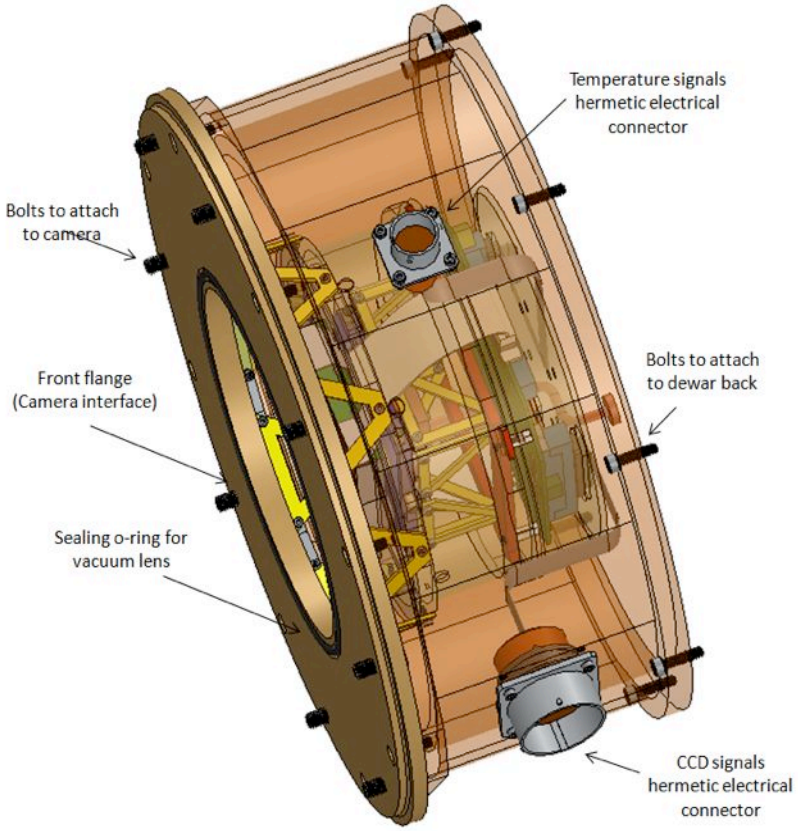

Figure 48: *Cryostat CCD-head.*

The cryostat needs to be under vacuum to achieve a stable temperature condition, which will allow having the CCD at the operating temperature of 150 K. Main vacuum components are listed in Table 11.

The cold-plate of the wet LN2 cryostat should be monitored as well as the detector mounting area. This task can be done with the use of commercial thermometers wired with very low thermal conductivity wires, for example Manganin. Thermometers can be read with commercial monitor/controllers. Table 12 shows a list of the necessary components for the temperature and pressure system in the cryostat.

Supplier	Part number	Characteristics
MKS	972B-71030	*Vacuum transducer 972 DualMag*
MKS	PDR900-1	*Vacuum gauge controller*
Detoronics	DT02H-22-61PN	Hermetic connector for CCD signals 61-pin
Detoronics	DT02H-12-10PN	Hermetic connector for CCD thermometry 10-pin
Detoronics	DT02H-12-10PN	Hermetic connector for cryostat thermometry 10-pin

Table 11: *Main accessories for MEGARA vacuum system*

Product	Supplier	Description	Characteristics
Temperature controller	Lakeshore	Lakeshore 336	Reads Diodes, PTC RTC, NTC RTD, thermocouple. IEE488.2,USB,ethernet
Temp. sensor	Lakeshore	PT-103 sensor	-200 °C to 600 °C
Cables	Calif. Fine Wires	Cryo-cabling	Manganin cables

Table 12: *Main accessories for MEGARA cryostat temperature system*

The following considerations were applied to finally select an open-cycle cryostat (instead of a closed-cycle one) for MEGARA. The full trade-off analysis can be found in R.10.

- Feasibility of fabrication and use of proven technologies, risks can be overcome by using good design practices which include simulations and finite element models, as well as experimental tests of critical parts
- Current facilities at GTC can be use without the need of modifications or special requirements; current technicians and telescope staff can operate the cryostat without the need of specialized training
- All the vacuum and thermometry accessories are commercial and standard for this type of purposes thus can be found easily and costs are reduced.
- Cost of LN2 cryostat is similar to a closed-cycle system for the first unit, but it can be 15% cheaper for a second unit if more than one spectrograph could be included in a future (although the baseline MEGARA scenario is having only one cryostat). LN2 cryostats are very robust systems with a minimum of maintenance required which reduces long term costs; in the other hand a closed-cycle system needs to be serviced at least every 6 months, and also a spare cold-head is suggested to be purchased, this last argument will increment significantly the price of a system like this.

A detailed description about the MEGARA cryostat can be found in R.9.

5.2.4 Detector and Data Acquisition System

The detector will be an E2V CCD231-84-0-E74 device. This measures 4096 x 4112 x 15μm pixels and has four outputs. There are several variants of this device but we have chosen the Deep-Depletion Silicon version with the Astro Multi-2 AR coating as being the one best suited for the demands of MEGARA. The CCD is capable of delivering < 3e- read noise and has excellent QE across almost the whole visible spectrum.

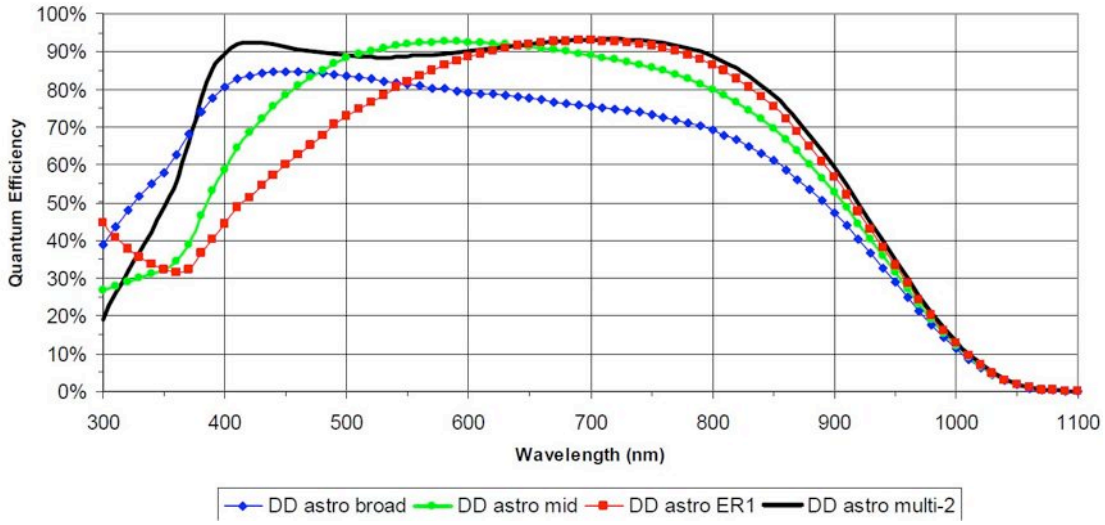

Figure 49: *The QE of the proposed CCD with various AR coats.*

The use of Deep Depletion Silicon means that fringing in the red part of the spectrum is minimized. The CCD will be mounted in an LN2 cryostat and operated at approximately 158K to ensure low-noise operation. The positioning of the CCD within the cryostat is critical since the cryostat window will be active. The assembly of the camera will be greatly facilitated by the CCD package, which is designed for mosaicing applications. It has a thickness of 15 ± 0.01 mm and contains three mounting bolts to ensure tight thermal contact with the base plate. Figure 50 shows the CCD and PCB at the CCD head.

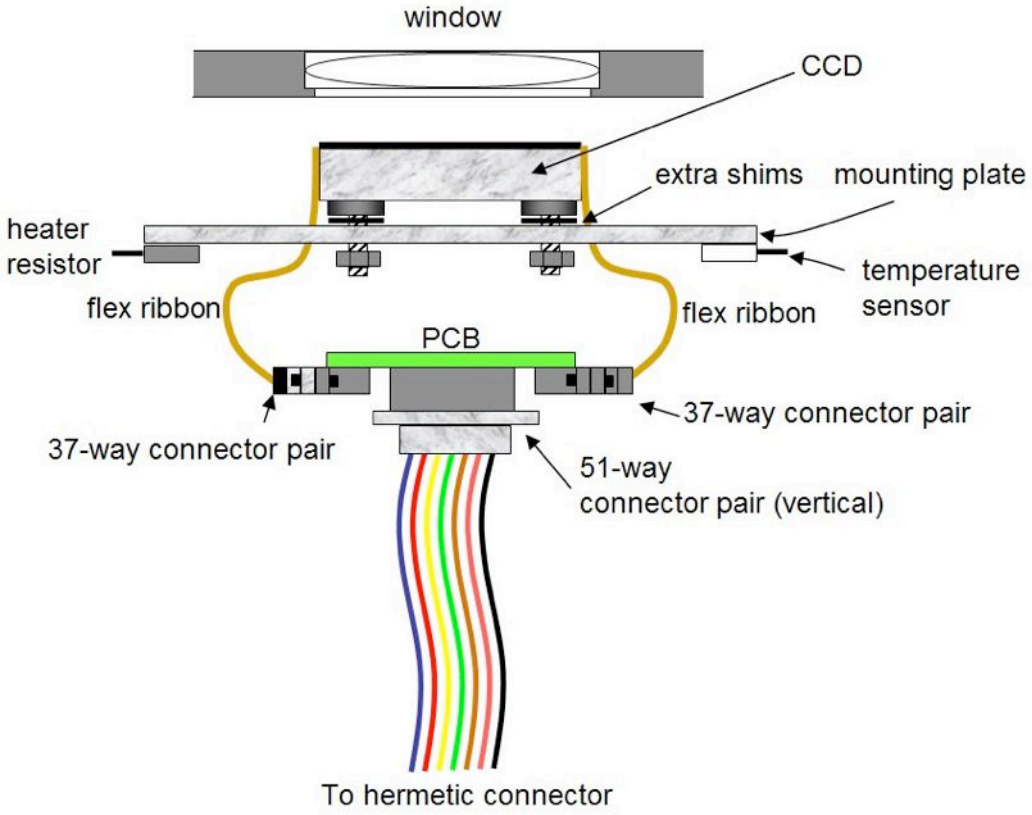

Figure 50: *CCD and PCB at the CCD Head.*

The CCD has two integral flex-ribbon cables mounting 37-way μD connectors. These have very-low thermal conductivity, which aids considerably the thermal design of the camera. The μDs will mate to a static protection PCB mounted parallel to and a short distance behind the CCD within the vacuum space of the cryostat. The PCB will contain zener diodes to prevent potentially damaging voltages from reaching the CCD. The PCB also contains capacitors to decouple the CCD bias signals (important for low-noise and good channel separation), an LED for engineering tests, a Pt100 thermometer and connectors to the thermometer and heater mounted close to the CCD.

The PCB must be mounted within a radiation shield to ensure it does not cool excessively. Additionally it will be mounted on the cold parts of the CCD support structure via insulating pillars. The thermal conduction down the 56 30AWG copper wires that connect the PCB to the outside world will then ensure that it does not cool below -40^{o}C.

Figure 51 shows the CCD connections details.

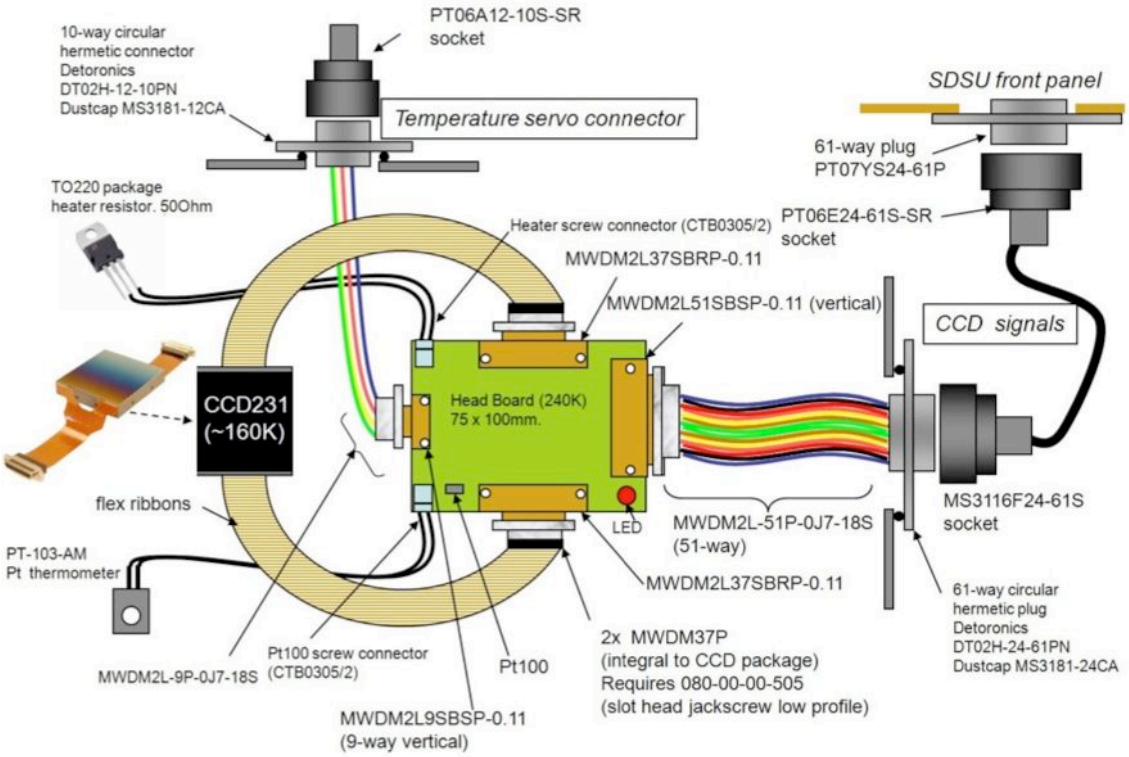

***Figure 51**: Schematic of internal cryostat connections.*

The CCD will be interfaced to an ARC controller mounted close by the cryostat. The controller will contain a single clock card and a single 4-channel video processor card in addition to the DSP processor/timing card. The controllers' external PSU will be mounted close by.

The ARC Controller shall interface with a final controller element, the ARC-65 PMC mezzanine interface card that will be fitted in the control computer VME rack.

The camera temperature will be measured and controlled using a Lakeshore 336 device. This will be rack mounted some 4m from the camera system, connected to it by two cables. One of these will connect to the Pt-100 temperature sensors mounted on CCD base plate and the PCB. It will also carry power to the CCD temperature servo heater. The second cable will connect to a Pt-100 sensor mounted on the LN2 tank and another on the sorbtion pump ("Getter") used to maintain the vacuum once the system is cold. It will also carry power to the activation-heater mounted on the sorbtion pump. The Lakeshore 336 can be programmed using a keypad and the temperature and heater power displayed on the front panel. Data can also be read across an Ethernet interface. More information about temperature sensors is provided in Table 12.

The cryostat pressure will be measured using an MKS972 sensor. This outputs data across an RS232 interface. To make this data available across the network, a Perle IOLAN port server will be used. Temperature and pressure data will be incorporated into image header information for engineering and diagnostic purposes. More information about temperature sensors is provided in Table 12.

A more detailed description about the MEGARA DAS design can be found in R.11.

5.3 Control System

The MEGARA Control System includes the hardware and software components that are required to provide the MEGARA control and the integration of the instrument in the GTC Control System (GCS).

Additionally, the MEGARA project includes the design and development of the MEGARA Science Community Tools, which refers to the software tools that shall be developed by the MEGARA Consortium to facilitate the preparation of the observing programs and the exploitation of the data provided by the instrument to the GTC community.

The MEGARA Control System shall be designed to fulfill, as much as possible the GCS standards (any non-conformity due to the identification of obsolete components or any other reason shall be identified and communicated to GTC for approval before being adopted) and shall be delivered to GTC to be integrated in the GCS. The MEGARA Science Community Tools shall be developed following the hardware and software architecture decided by the MEGARA Consortium and shall be made available to the astronomical community out of the GTC network.

The following subsections summarize first the software and hardware architecture of the MEGARA Control System and then the scope of the MEGARA Science Community Tools.

5.3.1 MEGARA Control System Software

The MEGARA Control System will provide the capabilities to move the different mechanisms of the instrument, to readout the data from the detector controller, the necessary routines for the Inspector Panels and the Sequencer strategies.

The MEGARA Mechanisms Control System shall be composed by a set of devices that represents the different MEGARA components. These components (i.e., focal-plane cover, shutter, focusing, grating exchange mechanisms, Fiber MOS positioners, detector, etc.) shall receive the positioning demands requested by the user in the Observing blocks and provide the data, monitors and alarms that must be generated to the GCS.

Figure 52 shows the different subsystem that compose the MEGARA Control System.

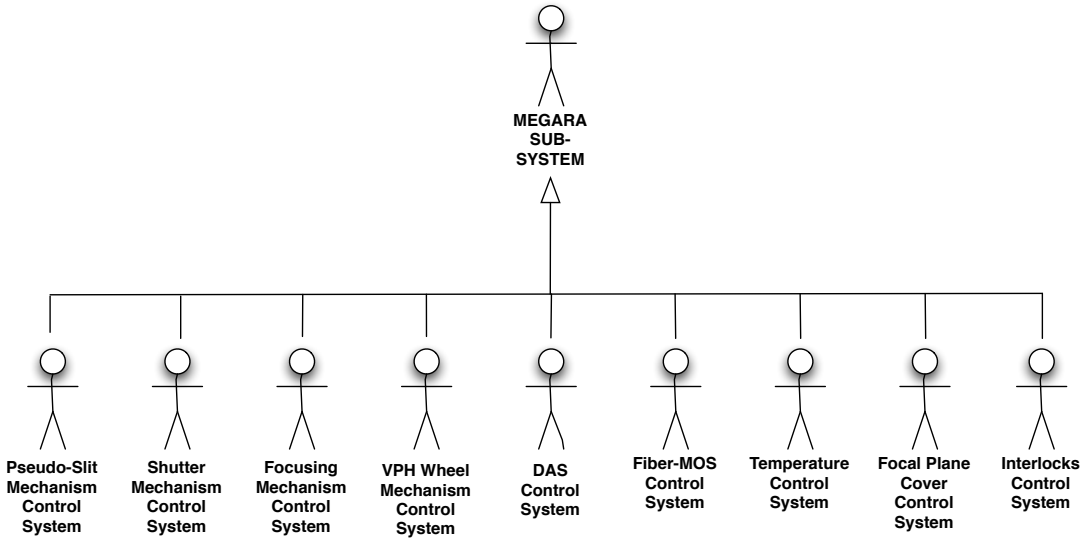

***Figure 52**: MEGARA Control System devices.*

Figure 53 shows the main classes involved in MEGARA Control System.

The MEGARA Inspector Panels (MIP) shall include the instrument specific user interface components. The MIP shall consist of a library that would incorporate the instrument specific GUI panels that will be linked to the Inspector main program.

The MEGARA Control System Software Architecture is described in detail in R.21. In addition, R.22 and R.23 provide the Stakeholders and Use Cases of the MEGARA Mechanisms Control System.

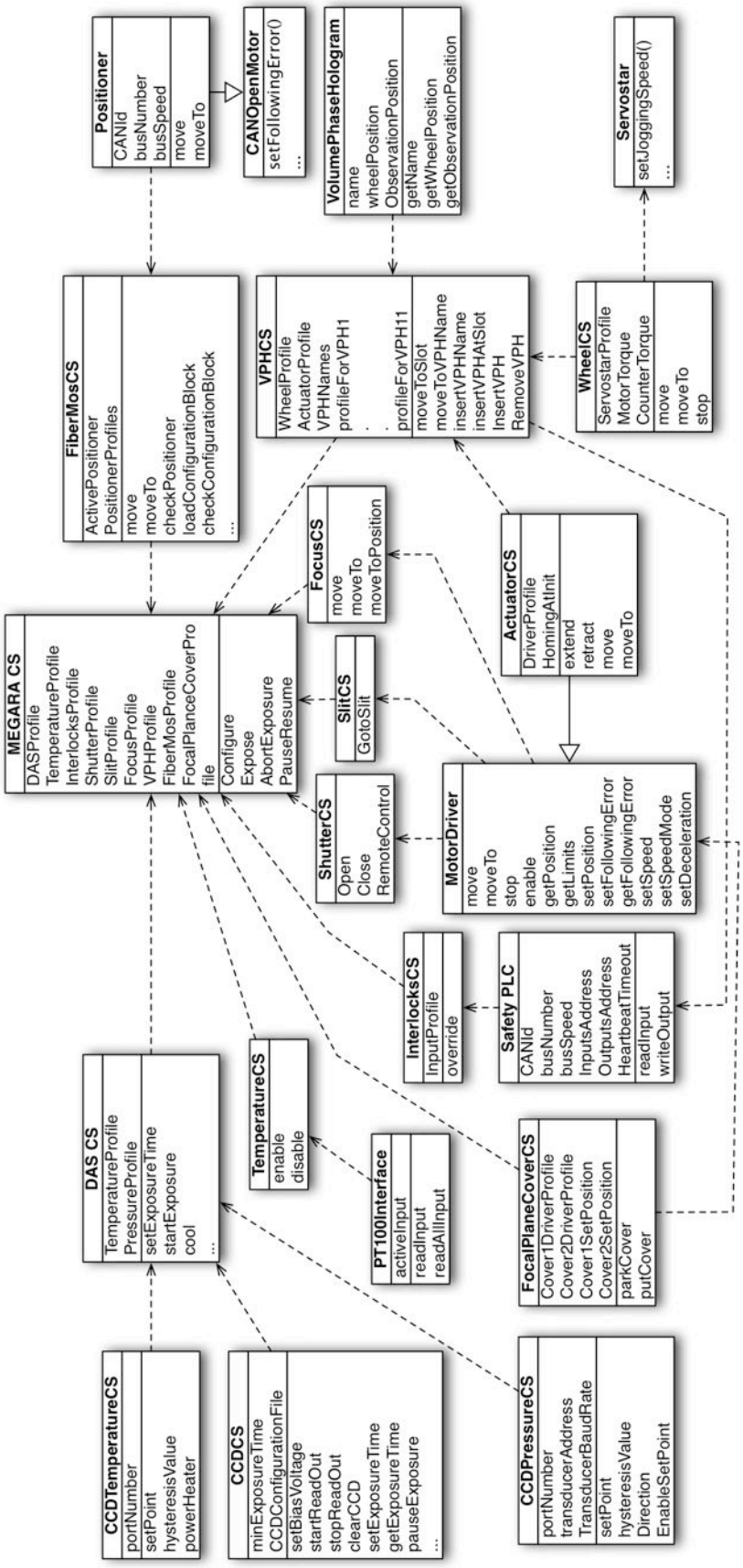

***Figure 53**: MEGARA Control System classes.*

5.3.2 MEGARA Control System Hardware

The MEGARA control system hardware will be divided into two separated parts (physically or logically depending on the final electronic cabinets characteristics). The Control cabinet will gather all the workstation and interface to the GTC control system. The Power Cabinet will gather all the power electronic, mainly DC motor drivers and power supplies. Both cabinets will be equipped with an AC panel that provides a filtered 230 V AC to the cabinets.

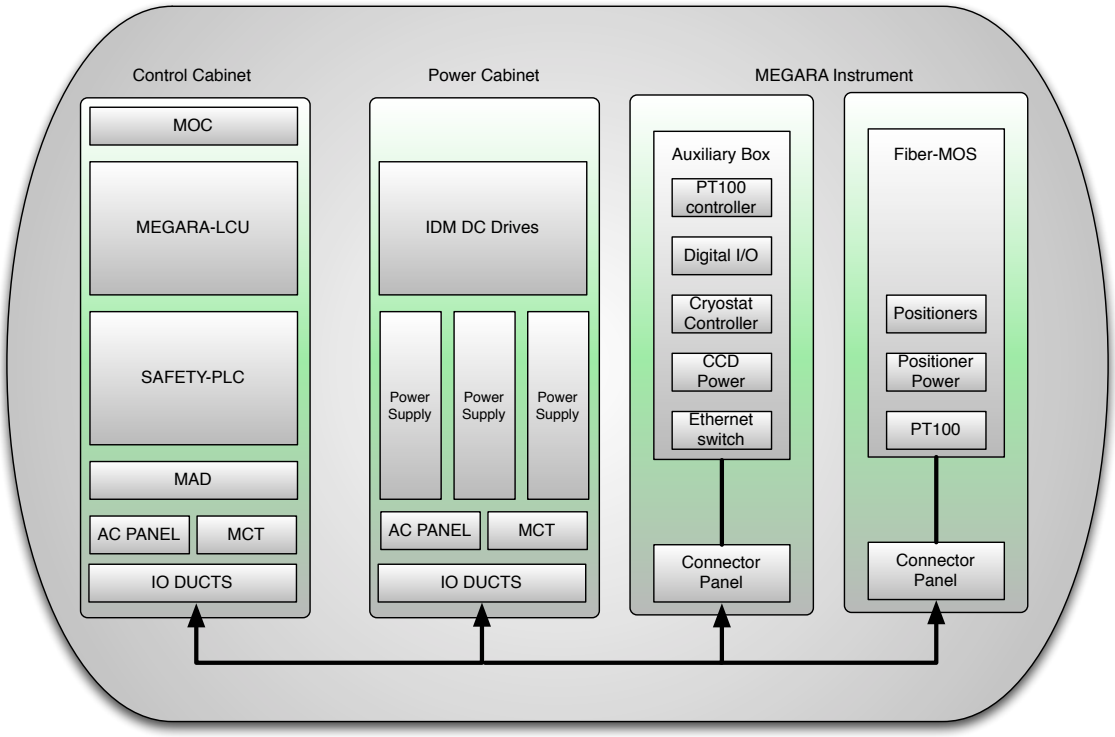

***Figure 54**: MEGARA Control System Hardware overview.*

The Control Cabinet shall contain:

- The MOC, a module used to interface optically the control cabinet with the GCS communication network. Hence, the control cabinets of the GCS are distributed through the Telescope chamber. All the control cabinets communicate with the GCS via optical fiber. The MOC includes all the transceivers required to adapt the different signals and communication protocols to the FO links.
- The MAD, a module used to remotely turn ON / OFF the equipment inside control cabinets. The MAD is controlled via CANopen and includes a CANopen / FO transceiver.
- The AC PANEL, a module that includes the electrical protection for the AC mains power in the Control Cabinets. This module distributes the 230 V AC to the electronic equipment.
- The MCT, a module used to control the temperature of the cabinet. It starts automatically in "FAN Mode" when the door is closed. The System Supervisor turns ON the cooling and controls the temperature via CANopen.

- The SAFETY-PLC: an industrial PLC with failsafe inputs/outputs that handles interlocks signals.
- MEGARA-LCU: a VME rack running VxWorks that hosts the MEGARA Control System (MCS) and DAS control system.

The MEGARA Control System Hardware Architecture is described in detail in R.24.

5.3.3 MEGARA Science Community Tools

The MEGARA Science Community Tools is a set of stand-alone applications that shall be developed by the MEGARA Consortium to facilitate the preparation of the observing programs and the reduction of the data obtained with the instrument.

- The MEGARA Observing Preparation Software Tools (MOPSS) shall assist observers to optimally plan their observations with GTC/MEGARA. The MOPSS is composed by the Exposure Time Calculator, the Image Simulator, and the Fiber MOS Positioning tool.
    - The MEGARA Exposure Time Calculator shall simulate the signal-to-noise (S/N) ratios that will be obtained for the continuum and a spectral line of a target for a given exposure time, MEGARA setup, and night atmospheric conditions.
    - The MEGARA Image Simulator shall simulate data frames of any ideal 3D datacube of a source in the same way it would have been observed by GTC/MEGARA for a given setup. The Simulator shall return a MEGARA frame in fits format with the simulated spectra corresponding to the projection of each spaxel on the detector plane, including the expected sky contribution and the effects inherent to the observation (bias, flat, geometrical distortion, non-linear dispersion, crosstalk, differential atmospheric refraction), as well as its row stacked spectra frame.
    - The Fiber MOS Positioning tool shall determine the optimal assignment of the 92 positioners used in the MOS mode for an input list of source coordinates in the 3.5x3.5 arcmin^2 to cover as many sources as possible, and provide in which order must be the positioners be moved to avoid collisions among adjacent ones (minimizing the time to configure them at the same time).
- The MEGARA Data Reduction Pipeline shall supply the users with data corrected from instrument signatures, which can be used at different stages of data acquisition and analysis. The goal of the MDRP is to supply users with a final data set in physical units, with which they can begin their scientific analysis, without the need of additional data processing. The user shall be able to modify the predefined parameters of the MDRP to customize data processing.

The MEGARA Science Community Tools shall not be integrated with the GTC Control System. A more detailed description of these tools can be found in R.25, R.26, R.27 and R.28.

6. MEGARA SYSTEM ENGINEERING

Systems Engineering provides the methodology for developing a complex system, like MEGARA, in a structured and orderly manner and, therefore, helps to ensure that the whole instrument is correctly developed from the beginning, minimizing risks and anticipating problems that may arise.

The main tasks that are carried out by the System Engineer are summarized as follows:

- Implement the requirements engineering, which aims to: ensure that the initial requirements are correctly interpreting user needs; generate, monitor and maintain a coherent set of specifications at different levels of the system and ensure traceability between subsystem and system requirements and specifications.
- Perform system analysis, resolve requirement conflicts, carry out trade-off, develop and use simulation models, analyze project risks and perform RAMS analysis.
- Define and maintain system configuration (define Product Tree and Interface Table).
- Prepare and execute the Integration and Verification Plan.
- Develop the Operation and Maintenance Plan.

The System Engineering Plan was developed for the complete system life cycle, from conceptual design to the final instrument acceptance in GTC. The activities must be reviewed at the end of each phase in order to add the needed details to the activities (WBS) to be performed in the following phase. The System Engineering activities for the Detailed Design were reviewed at the end of the Preliminary Design Phase.

During the Detailed Design, the System Engineering activities for the manufacturing and AIV phases shall be reviewed in order to be ready to be executed during the next project phases.

System Engineering is also responsible of identifying and assessing any deviations on design, interfaces and performances that could arise at any level and to manage configuration changes and non-conformity proposals.

The MEGARA System Engineering Plan at Detailed Design is described in detail in R.12.

In the following subsection, we briefly summarize the current state of several system engineering activities identifying the reference documents where the information is provided.

6.1 Requirements, Specifications and Interface documents

The following Requirements, Specifications and Interface documents are kept in MEGARA:

- RQ/IN-MG/001 - MEGARA Functional Requirement Documents
- RQ/IN-MG/002 - MEGARA Interface to GTC

- SP/IN-MG/001 - MEGARA System Specification
- INT/IN-MG-FB/IN-MG-S1/001 - MEGARA Fiber Bundles - Spectrograph Interface Document
- INT/IN-MG-FM/IN-MG-FM/001 - MEGARA Fiber MOS Positioner - Fiber MOS Positioner Button Interface Document
- INT/IN-MG-FO-000/IN-MG-RA-000/001 - MEGARA Folded Cassegrain Field Lens - Folded Cassegrain Rotator Frame Interface Document
- INT/IN-MG-RA/IN-MG-FM/001 - MEGARA Fiber MOS Focal frame - Fiber MOS Positioners Interface Document
- INT/IN-MG-RA/IN-MG-RA/001 - MEGARA Rotator Adapter - Focal Frames Interface Document
- INT/IN-MG-S1-000/IN-MG-S1-040/001 - MEGARA Support Structure - Camera-Cryostat Support Structure Interface Document
- INT/IN-MG-S1-000/IN-MG-S1-100/001 - MEGARA Support Structure - Slit Unit Interface Document
- INT/IN-MG-S1-000/IN-MG-S1-300/001 - MEGARA Support Structure - Collimator Interface Document
- INT/IN-MG-S1-000/IN-MG-S1-400/001 - MEGARA Support Structure - Spectral subsystem mechanism Interface Document
- INT/IN-MG-S1-000/IN-MG-S1-700/001 - MEGARA Support Structure - CCD Controller Interface Document
- INT/IN-MG-S1-040/IN-MG-S1-500/001 - MEGARA Camera-Cryostat Support Structure - Camera Interface Document
- INT/IN-MG-S1-200/IN- MG-S1-300/001 - MEGARA Shutter - Collimator Interface Document
- INT/IN-MG-S1-400/IN- MG-S1-400/001 - MEGARA VPH Optics - VPH Opto-mechanics Interface Document
- INT/IN-MG-S1-400/IN-MG-S1-470/001 - MEGARA VPH Opto-mechanics - VPH Grating platforms Interface Document
- INT/IN-MG-S1-500/IN-MG-S1-600/001 - MEGARA Camera - Cryostat Interface Document
- INT/IN-MG-S1-610/IN-MG-S1-630/001 - MEGARA CCD Head - Detector and associated electronics Interface Document

- INT/IN-MG-S1-700/IN-MG-S1-900/001 - MEGARA CCD Controller - Shutter Controller Interface
- INT/IN-MG/IN-MG-CS/001 - MEGARA Control System Interface Document
- INT/IN-MG/IN-MG-FB/001 - MEGARA Fiber Bundles Interface Document

6.2 Product Tree and Interfaces between MEGARA components

The MEGARA Product Tree (graphical view and complete list of components and parts) is included in TEC/MEG/008 (R.13).

The MEGARA Interface table (which includes the complete list of interface documents and drawings) is included in INT/MEG/001.

6.3 System Technical Budgets and RAMS analysis

The following technical budgets are being defined for MEGARA:

- Image quality (included in TEC/MEG/100)
- Spectral resolution and spectral resolution repeatability (TEC/MEG/115)
- Image stability (TEC/MEG/116)
- Transmission (TEC/MEG/055)
- Flux homogeneity (TEC/MEG/117)
- Spectral alignment and spectral alignment repeatability (TEC/MEG/023)
- Mass (TEC/MEG/061)
- Power consumption (TEC/MEG/061)
- Glycol water consumption (TEC/MEG/061)
- Compressed air (TEC/MEG/061)
- Thermal dissipation (TEC/MEG/061)
- Reliability (TEC/MEG/048)

The RAMS (Reliability, Availability, Maintainability and Safety) analyses that are being carried out during for the MEGARA instrument are the following:

- Maintainability Analysis, where it is analyzed the system maintenance feasibility and to minimize and facilitate its maintenance during the operation phase.
- Failure Analysis (FMECA), where the potential failure modes of the system are identified and evaluated.

- Reliability Analysis, where the percentage of time that the system could be unavailable is estimated.
- Spare analysis, where the outputs from the FMECA's and reliability analyses are taken into account in order to provide a spare parts list that include the spare part that must be maintained in the different maintenance levels (i.e., observatory and sea-level base).
- Safety Analysis, where the hazards that could happen to the persons that are involved in the use and maintenance of the system area analyzed.

More information about the RAMS Analysis is provided in TEC/MEG/048.

6.4 Integration and Verification Plan and Integration at GTC

The MEGARA Integration and Verification Plan shall include all the activities that shall be done to finally verify that MEGARA fulfils the top-level requirements and it is ready to be integrated at GTC.

The MEGARA complete verification implies two steps: (a) subsystems must be assembled and verified before being integrated in the whole instrument and, (b), the accepted subsystems must be integrated and the whole system verified at LICA.

- The preparation of the MEGARA Subsystems Acceptance Plan includes first the identification of the subsystems that are going to be verified independently, producing then the general verification schedule and, finally, preparing the detailed description of the activities that must be performed. The different subsystems AIV plans are kept in separate documents. A first version of the following AIV documents is already prepared:
    - TEC/MEG/079 MEGARA Fiber MOS Integration Plan
    - TEC/MEG/077 MEGARA Fiber MOS Acceptance Tests at AVS
    - TEC/MEG/078 MEGARA Fiber MOS Acceptance Tests at LICA
    - TEC/MEG/084 MEGARA Optics: Testing Plan at INAOE and CIO
    - TEC/MEG/063 MEGARA Cryostat Integration Plan
    - TEC/MEG/064 MEGARA Cryostat Acceptance Tests at INAOE
    - TEC/MEG/065 MEGARA Cryostat Acceptance Tests at LICA
    - TEC/MEG/049 MEGARA Detector Characterization: Test bench and prototype system
    - TEC/MEG/062 MEGARA Detector Integration and Assembly Test Plan
    - TEC/MEG/050 MEGARA Detector Characterization Test Plan
    - TEC/MEG/086 MEGARA Spectrograph Mechanism Acceptance Tests

- TEC/MEG/085 MEGARA Spectrograph Mechanism Integration Plan

- The System Acceptance Plan shall include the integration and verification activities of the system as a whole. Verification activities shall include engineering tests and spectroscopy mode tests. The Integration and Verification Plan of the MEGARA instrument is contained in the document MEGARA Integration and Verification Plan (TEC/MEG/045).

Once the whole system is verified MEGARA shall be ready to be delivered and integrated at GTC.

The MEGARA Integration Plan at GTC identifies all the activities that shall be performed to integrate MEGARA at GTC, which can be divided following the instrument decomposition by subsystems location. It means that the activities will be grouped as follows:

- Activities to be performed at the Folded Cassegrain focus to integrate the Folded Cassegrain subsystems.
- Activities to be performed at the Spectrograph location to integrate the Spectrographs.
- Activities to route the fiber bundles from the Folded Cassegrain position to the Spectrograph location.

The Integration Plan of MEGARA at GTC is contained in the document MEGARA Instrument Integration on Site (TEC/MEG/046).